K|RITH

KWAZULU-NATAL RESEARCH INSTITUTE FOR TUBERCULOSIS AND HIV

UNIVERSITY OF KWAZULU-NATAL

A Microfluidics System for Drug Susceptibility Testing in *Mycobacterium smegmatis*

2015

by

Brilliant Bonisile Luthuli

Submitted in fulfilment of the requirement for the degree of Masters in the School of Laboratory Medicine and Medical Sciences

A Microfluidics System for Drug Susceptibility Testing in *Mycobacterium smegmatis*

Brilliant Bonisile Luthuli

A thesis submitted to the College of Health Sciences, University of KwaZulu-Natal, Medical School, for the degree of Master of Biomedical Sciences.

This is a thesis in which a chapter is written as a set of discrete research paper, with an introduction and final discussion. This chapter would have been published in internationally recognized, peer-reviewed journal.

As the candidate's supervisor, I have approved this thesis for submission.

Supervisor:

Signed:--  . Name: **Dr F Balagadde** Date:- March 30, 2016

AUTHOR'S DECLARATION

DECLARATION 1-PLAGIARISM

I, **Brilliant Bonisile Luthuli**, declare as follows:

1. The work described in this thesis has not been submitted to UKZN or other tertiary institution for purpose of obtaining an academic qualification, whether by myself or any other party.
2. That my contribution to the project was as follows:
   I contributed to the design of the project, designed and manufacture the microfluidic chip and also performed all the experiment.

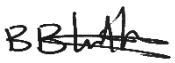

Bonisile Luthuli **Date: November 2015**

Student number: 209528709

DECLARATION 2-PUBLICATION

DETAILS OF CONTRIBUTION TO PUBLICATION that form part and/or include research in this thesis (include a publication that was published and give details of the contributions of each author to the experimental work and writing).

Publication

Luthuli BB, Purdy GE, Balagaddé FK (2015) Confinement-Induced Drug-Tolerance in Mycobacteria Mediated by an Efflux Mechanism. PLoS ONE 10(8): e0136231. doi:10.1371/journal.pone.0136231

Bonisile Luthuli contributed to the design of the project, designed and manufactured the microdialyser chip, as well as its previous iterations. She performed all the experiments and contributed to the writing of the above publication.

ACKNOWLEDGEMENTS

I am sincerely grateful to my advisor Dr Frederick Balagaddé whose guidance, motivation and belief in me has made the journey as a Master's student in research interesting and adventurous. Not only do I think he is the ideal supervisor, he has also been a great mentor. To him I am forever grateful. My gratitude also goes to the members of the Bioengineering Lab at KwaZulu-Natal Research Institute for Tuberculosis and HIV (K-RITH) for their useful input and support. I also thank Yashveer Ramlakhan for his assistance and engineering skills during the early days of my project.

I express my gratitude to K-RITH for the unique opportunity of working with world class scientists. I am also indebted to everyone who wishes me well in everything I do whether in person or in secrete.

A special thanks goes to my family for their undying love toward me from as long as I can remember, particularly, my grandmother for her genuine love, guidance and support. I thank my mother, for her everlasting love for me. I am truly blessed and grateful to have her in my life.

Above all I thank God for this wonderful experience called life.

TABLE OF CONTENTS

LIST OF ABBREVIATIONS

AIDS	Acquired Immuno Deficiency Syndrome
ART	Antiretroviral therapy
ATP	Adenosine Triphosphate
CDC	Centre for Disease Control and Prevention
CFU	Colony Forming Unit
CO_2	Carbon Dioxide
DOTS	Directly observed therapy short course
DST	Drug susceptibility tests
DS-TB	Drug susceptible TB
ELISA	Enzyme linked immunosorbent assay
FDA	Food and Drug Administration
HIV	Human Immunodeficiency Virus
katG	Catalase peroxidase enzyme
KZN	KwaZulu-Natal
LTBI	Latent TB Infection
mAGP	Mycolyl arabinogalactanpeptidoglycan complex
MBC	Minimum Bacterial Concentration
MDR-TB	Multi-Drug Resistance- TB
MGIT	Mycobacterial growth indicator tube
MIC	Minimal inhibitory concentration
mRNA	Messanger RNA
MTB	Mycobacterium tuberculosis
MTBC	Mycobacterium tuberculosis complex
NAD	Nicotinamide Adenine Dinucleotide
PAO	Pyrazinoic acid
PCR	Polymerase chain reaction
PDMS	Polydimethylsoloxane
PMMA	Polymethacrylate
PS	Polystyrene
QRDR	Quinolone Resistance Determining Region
RRDR	Rifampicin resistant determining region
rRNA	Ribosomal RNA
RspA	Ribosomal protein S1
TB	Tuberculosis

XDR-TB	Extensively drug resistant-TB
ZN	Ziehl-Nelsen

ABSTRACT

Tuberculosis remains a major health concern worldwide. The emergence of strains resistant to anti-tuberculosis drugs has further complicated management of this disease. In addition, the prolonged multidrug chemotherapy (6 to 9 months) required to effectively sterilize drug tolerant mycobacteria that persist in human tissues, impedes disease management efforts. Hence, drug susceptibility tests that can easily detect drug resistant strains in a minimal amount of time whilst detecting both genetic and phenotypic resistant mechanisms is one of the priorities of TB control programs. The aim of this project was to develop a culture-based drug susceptibility testing platform for tuberculosis using microfluidics technology. A microfluidic platform has many advantages such as large scale integration, high throughput screening, automation and requires minimal human involvement. Such qualities are ideal for a diagnostic test.

We designed and built the microdialyser which is a physical cell culture system that has micro-sized cell culture chambers that are as small as 200 pL in volume, mimicking the volume of a membrane bound compartment of human macrophage—a cell that harbours TB bacilli. This system provides a unique advantage of performing drug susceptibility testing in a micro-sized environment which resembles an in vivo growth environment. With the miracle of miniaturization, the microdialyser can support 120 microdialyser units to operate independently. Since each microdialyser unit is very small it consume minimal reagents and therefore reduces costs.

Each culture system is monitored in situ to provide automated, real time, non-invasive measurement of cell density. The microdialyser system was used to perform drug susceptibility tests using *M. smegmatis* cells. This system revealed an epigenetic drug-tolerant phenotype of *M. smegmatis* that appears when mycobacteria are cultured in a space-confined bioreactor and disappears in larger growth chambers with respect to rifampicin. We then investigated possible underlying mechanisms that caused the drug tolerance, which eluded detection in conventional culture systems. In view of these results we highly recommend that this system be further validated with *M. tuberculosis* isolates so that it can be employed for routine drug susceptibility testing in clinical settings.

Chapter 1

LITERATURE REVIEW

1.1 Tuberculosis Disease

1.1.1 Features of mycobacteria

The genus *Mycobacterium* is best known for its most pathogenic species—*Mycobacterium tuberculosis*—the causative agent of tuberculosis disease (TB), the world's oldest and deadliest disease. A distinctive feature of pathogenic mycobacteria is their extremely slow growth. Under optimal conditions with sufficient oxygen and nutrients, the doubling time of *M. tuberculosis* can range from 18 to 24 hours depending on the specific factors of the growth environment [1]. This is relatively long generation time for a bacterium. For instance, *M. tuberculosis* grows ~100 times slower than *Clostridium perfringens*, the fastest-growing bacteria on record with an average generation time of ~10 minutes [2]. Interestingly non-pathogenic mycobacterial species generally have considerably faster growth rates. For instance, *Mycobacterium smegmatis*, a non-pathogenic mycobacterial species, has a generation time of 3 to 4 hours [3]. As a result, mycobacteria have been traditionally classified into fast and slow growing species based on whether or not they produce visible growth colonies within 7 days [4,5]. Since non-pathogenic species generally possess faster doubling times, compared to their pathogenic counterparts, the slow growth rate has been associated with pathogenesis in mycobacteria.

M. tuberculosis and *Mycobacterium leprae* are both human pathogens with very slow growth rates (doubling times of ~24 hours and ~14 days respectively) [6]. The mechanisms underlying their slow growth are currently unknown. Limited nutrient uptake has been associated with slow growth rate in pathogenic mycobacteria, however only a minimal increase in cell replication was observed when membrane permeability was increased [7]. Limited RNA synthesis, which resulted in retarded protein synthesis, was found to be a more plausible factor in the slow growth rate of pathogenic mycobacteria. From that point onward mycobacteria were sub-divided into two taxonomic groups: slow growers with a single rRNA operon and fast growers with two operons [8,9]. The correlation between growth rate and the number of rRNA operons per mycobacterial genome provided the best explanation for differences in the growth rate of mycobacterial species[10].

A distinctive feature of all mycobacterial species is a unique cell wall with high lipid content, comprised mostly of mycolic acids, cord factors and wax-D [11]. The mycobacterial cell wall consists of an inner peptidoglycan layer followed by a layer of arabinogalactan; thereafter is a layer of mycolic

acids, forming the mycolyl arabinogalactanpeptidoglycan complex (mAGP). The outer part of the cell wall is composed of free lipids, glycolipids and glycoproteins that are particularly rich in fatty acids such as peptidoglycan, phosphatidylinositol mannose, lipomannan, lipoarabinomannan, cord factors and wax-D.

As is the case in almost all other known bacterial species, the peptidoglycan layer together with arabinogalactan is responsible for shape maintenance and cell wall structural integrity of mycobacteria [12]. Meanwhile the lipid coating comprised of mycolic acids and glycoproteins bestows exclusive characteristics to mycobacteria—such as an impermeable outer membrane, extreme hydrophobicity, acid-fastness, resistance to harsh environments as well as a great variety of antimicrobial agents. These properties are also useful for long-term survival of mycobacteria under otherwise stressful conditions such as in the presence of lysozymes and oxygen radicals encountered in the phagocytic vacuole [13].

Another feature of clinical importance in *M. tuberculosis* is its ability to become dormant by entering into a non-replicative state characterised by low metabolic activity and epigenetic drug resistance (derived from a physiological state and not genetic mutation) [14]. This characteristic presents a major challenge for tuberculosis disease control given that current tools are by and large limited to detection and treatment of metabolically active mycobacteria. Most TB detection and drug susceptibility tools rely mainly on the ability of the *M. tuberculosis* to grow in order to be detected by colony forming units. These techniques are based on estimation of growth for a *M. tuberculosis* strain in the presence or absence of a drug. Liquid culture based techniques aimed for more rapid detection use the metabolic activities of growing bacteria. For instance BACTEC 460 and Mycobacteria Growth Indicator Tube (MGIT) can detect growth dependent changes such as CO_2 and oxygen consumption, respectively. Techniques such as resazurin and tetrazolium bromide rely on *M. tuberculosis* to reduce nitrate to nitrite, [15] while phage-based techniques rely on the ability of mycobacteriophage to multiply in living mycobacterial cells [16]. The application of the above mentioned techniques is limited to actively dividing bacterial cells. Dormant bacilli are also tolerant to killing by antimycobacterial agents. First line TB drug such isoniazid can only target metabolically active bacilli leaving behind dormant bacilli [17,18]. These features have contributed to the success strategy of *M. tuberculosis* as a formidable pathogen for decades or even centuries, by allowing the microbes to withstand unfavourable conditions only to recover when growth-favourable conditions return.

1.1.2 Tuberculosis Disease Impact

1.1.2.1 Global Epidemiology

TB remains one of the deadliest curable infectious diseases the world has ever encountered. It was a hard-learnt lesson when the disease, which had been pacified by antibiotics in both industrialised and developing countries, returned with full force during the early nineties. However, upon return it exerted a devastating impact fuelled by the prevailing HIV/AIDS epidemic. So severe was the devastation that it was immediately declared a global emergence by World Health Organisation in 1993. An estimated 9 million people worldwide developed TB disease in 2013, which is a 26% increase from the 6.6 million cases reported in 1990 according to the World Health Organisation[19,20]. Thirteen percent of the 9 million were HIV-positive. Of the 1.5 million people that died from TB in the same year, 25% (or 360 000) were HIV-positive. Africa as a region accounts for about 80% of the HIV-positive TB cases and TB deaths among people living with HIV [20].

The brunt of the global TB cases were reported from South-East Asia, which accounted for more than half (55%) and Africa with 31%. India and China accounted for 24% and 11% of total cases, respectively. Meanwhile, the Americas (3%), East Pacific Mediterranean (6%) and European (5%) regions accounted for only a small fraction of the global disease burden [21]. The top ten countries worldwide in terms of incidence were mostly in Africa with Swaziland, Lesotho and South Africa which ranked first, second and third, respectively. In these countries, estimates suggest that about 1 person in every 100 (1000 per 100000 population) develops TB disease each year.

TB infection manifests in two phases, as latent TB infection (LTBI) and active TB. TB infection is established when *M. tuberculosis* bacilli lands inside the alveolar macrophages in the lungs, which recruit other cells of the immune system to form a cage around the bacilli called a granuloma. The granuloma plays a role in maintaining the bacilli in a dormant state. By creating a physical enclosure around the mycobacteria and preventing them from disseminating to other areas outside the granuloma. In this state the tubercle bacilli can persist in the human host for years and even for the entire lifetime of the human. In LTBI, the patient does not become contagious and has no related symptoms or illness. Active TB on the other hand, is a symptomatic state of the disease whereby a patient can spread the disease to close contacts via airborne transmission. The typical symptoms of active pulmonary tuberculosis include fever, night sweats, weight loss, cough, and chest pains. In some instances, active TB patients may appear healthy and in others, they may become chronically ill. TB transmission occurs when a healthy person inhales aerosolized droplets containing *M. tuberculosis* bacilli released by a person with active TB when sneezing, laughing or coughing [22]. Although persons with LTBI are not at risk of dying, the risk of advancing to active TB is estimated at 10% during one's life time [23]. In immune-compromised individuals, as in the case with HIV infection, this risk increases to 10% a year [24]. The greatest risk of progression from LTBI to active tuberculosis is reported to occur

in the first two years after infection with tubercle bacilli. This risk is increased in children younger than four years; persons living with HIV, people with diabetes and other chronic conditions; as well as those using immunosuppressant medication [25]. One third of world's population is infected with latent form of TB which can progress at any time to an airborne and transmittable disease.

The vast majority of people suffering with active TB are adults during otherwise economically productive years of their lives (between 15 and 45 years of age), thereby causing large social and economic burdens to their respective countries [26,27]. The disease has a particularly devastating effect on the livelihood of poverty-stricken families because of the relatively high costs associated with proper diagnosis and treatment as well as the opportunity cost associated with disease morbidity, resulting in less money earned to spend on food and nutrition. A majority of developing countries lack the systems required to ensure effective distribution of anti-TB chemotherapy. Such factors motivated the implementation of directly observed therapy short course (DOTS) as a component of World Health Organisation's strategy for global TB control [28].

DOTS is a strategy used to reduce the number of TB cases. In DOTS, healthcare workers observe patients as they take their medicine. Left to their own devices, many people with tuberculosis in resource-poor countries fail to take all their medication which contributes to the proliferation and spread of drug-resistant tuberculosis. DOTS ensures that the patient with TB completes therapy to maximize the cure outcome and to prevent drug resistance from developing in the community [29]. DOTS functions by integrating government commitment, case detection, treatment regimen supply together with directly observed therapy, effective drug supply, and standardized assessment of treatment outcome [28]. A cumulative total of 56 million people were successfully treated for TB between 1995 and 2012, as a result of this programme, which saved approximately 22 million lives [30]. However, as much as DOTS has done appreciably well in other parts of the world, the incidence of TB continues to increase in sub-Saharan Africa, with public health incidence rates surpassing the 1000 cases per 100,000 population mark[20].

1.1.2.2 The State Of Tuberculosis in South Africa

Overall, 450, 000 cases of active TB and 40, 386 TB-related deaths were reported in 2013 in South Africa, making it the country with the third highest TB incidence in the world[31]. Statistics South Africa—an agency responsible for producing timely, accurate and official statistics including deaths, unemployment estimates in the country—ranked TB as the leading cause of death in the country in 2013. This burden is partly attributed to conditions of poverty that favour transmission of the disease. For instance, most of the poor population resides in rural communities and informal crowded settlements, lacking essential facilities such as proper sanitation, clean water supply, medical services and electricity. Long distances to and from healthcare centres present a major barrier to the access of health care and treatment in these communities. A large portion of the population relies on public

transport, including universal shared taxi and buses which are cheaper, for mobility. However, this mode of transportation increases the risk of TB transmission among the passengers given that the passengers are forced to sit in close proximity to each other and in many instances, such as in cold or rainy weather, they are operated with the windows closed and poor air circulation[32]. In crowded clinics during winter seasons, with closed windows and poor ventilation, patients seeking medical help may become infected with TB while waiting to receive medical attention in waiting rooms. Inadequate education and high level of unemployment in these communities drive people to commit petty crimes and end up in jail. Prisoners are often mixed together in confined settings that are ideal for the spread of TB. Prisons act as a reservoir for TB, pumping the disease into the community through staff, visitors and former inmates [33]. However, the incidence and mortality patterns vary remarkably across the country, most likely because of substantial regional differences in the prevalence and distribution of health care systems and infrastructure.

The high prevalence of HIV infection has played a decisive role in increasing and maintaining the high burden of TB in the country. In 2007 South Africa contained only 0.7% of world's population, but shockingly had 17% of global burden of HIV [34]. Currently, 60% of active TB cases are also co-infected with HIV and 65% of those are from the KwaZulu-Natal province. TB infection in South Africa is highly concentrated in KwaZulu-Natal with 31% active TB cases followed by Eastern Cape (14%), Western Cape (14%) and Gauteng (13%) [35]. With the exception of urban areas, most communities in these provinces are normally served by a single community clinic without disease detection facilities. In the rural areas, people often live in homes which are scattered with long walking distances (10km on average) to the nearest healthcare facility. This also results in patients skipping clinic visits and foregoing TB medication. Since the clinics are highly overcrowded and medical staff are stretched too thin, there are scenarios where patients have to return home without receiving medical help after being turned away or told to return on the next day. Low levels of education in the rural communities also play a role in fuelling the TB burden. When confronted with illness, many patients will first exhaust all treatment options with local traditional healers before visiting a clinic or hospital [36]. As a result, several weeks may pass by before a patient with active TB seeks proper medical attention. There is also an unfavourable perception associated with the typically negative attitude of healthcare workers in rural communities which has proved to be an obstacle for patients seeking TB treatment [37].

Despite the comprehensive efforts made to lessen the TB burden such as the implementation of the DOTS strategy, only a treatment success rate of 74% was reported. The World Health Organisation had projected a much higher success rate well above 85%, considering that TB disease is curable with proper medical attention [38]. Nonetheless, TB notifications increased two-fold during the same period. In spite of the successes achieved by DOTS around the globe, the strategy seems to stall in high HIV-

burdened countries [39], such as South Africa, which are characterized by high TB and HIV prevalence rates. In spite of being the wealthiest country in Africa, South Africa is far from meeting the target set by the Stop TB partnership and the Millennium Development Goal of reducing the prevalence and mortality rate of TB in half by 2015 relative to 1990 levels, according to the World Health Organisation TB report of 2014. This was an intermediate target meant to pave the way for a more ambitious goal of eliminating TB (defined by >1 case of TB disease per 1 million population) by 2050. As long as a single TB patient can infect approximately 10 contacts before receiving treatment in a high HIV prevalence setting,[40] it must be anticipated that each TB case will most probably yield another, fueling the epidemic [41]. To comprehensively address the TB burden in South Africa, necessary factors including, health care facilities for TB treatment that are easily accessible with more powerful detection tools are required for better disease diagnosis and control.

1.2 TB Treatment and Drug resistance

In the 1940s streptomycin was discovered as the first antibiotic with a proven ability to kill *M. tuberculosis* [42]. As a result, this drug was solely used in TB treatment until it was discovered that the use of a single agent in TB treatment can yield drug resistance. Ever since then, anti-TB chemotherapy research focused efforts on drug combination regimens capable of overcoming drug resistance [43]. Today there are more than 10 drugs currently approved by the U.S Food and drug agency (FDA) for treating TB. These anti-TB drugs are categorised into two classes: First- and second-line drugs. First line drugs—including isoniazid, rifampicin, pyrazinamide and ethambutol—have high potent activity against TB and form a core of TB treatment regimen. Second line drugs—including fluoroquonolones and aminoglycosides—on the other hand are reserved for multi-drug resistance —which is resistance to rifampicin and isoniazid. However, the second line drugs are in general more costly, less effective and more toxic than first line drugs [44].

1.2.1 Drug Susceptible TB Treatment

Drug susceptible TB is treated by the first line drugs which form the core of the TB treatment regimen. These include isoniazid (IHN), rifampicin (RIF), pyrazinamide (PZA) and ethambutol (EMB).

Isoniazid (INH)

Isoniazid (isonicotic acid hydrazide) is one of the most effective and commonly used anti-TB drugs. It has been a key drug in TB treatment since its introduction in 1952 [45]. Isoniazid is bactericidal, albeit only on actively growing tubercle bacilli, and is not active against non-replicating bacilli or under anaerobic conditions. INH enters the mycobacterial cells by passive diffusion. INH itself is non-toxic to the mycobacterial cell but acts as a pro-drug that is activated by the *M. tuberculosis* catalase-peroxidase enzyme KatG [46]. KatG oxidatively activates INH to a range of carbon, nitrogen and

oxygen radicals. These free radicals contribute to mycobacterial cell killing by damaging a variety of cellular components such as lipids, proteins and nucleic acids. However, the primary target of INH is NADH-dependent enoyl acyl carrier protein reductase, InhA, involved in fatty acid elongation in mycolic acid synthesis.

Amongst the free radicals derived upon KatG mediated INH activation is(isonicotinic acyl radical), a highly reactive species that reacts with NAD bound within the active site of InhA forming an INH-NAD adduct a tight binding inhibitor, causing NADH dissociation from InhA and therefore rendering the enzyme non-functional [47,48].

Genetic studies characterised INH susceptible strains by a functional *katG* gene and at the same time, deletion of the *katG* gene resulted in transformation of INH susceptible strains to INH resistant strains. INH resistant clinical isolates of *M. tuberculosis* often lose catalase and peroxidase enzymes encoded by *katG* gene in high level resistant strains (MIC > 5 μg/ml). Depending on the type of mutation, and the degree to which function of the KatG enzyme is preserved, the MIC of isoniazid may range from 0.2 to 256 μg/mL.

INH resistance may also arise from mutations in the *inhA* gene or its promoter reducing affinity of isonicotinic acyl radical for NADH. Overexpression of InhA may also result in INH resistance. Mutations in *InhA* gene also cause resistance to the structurally related second line drug ethionamide. However these mutations usually confer low level resistance with MIC ranging from 0.2 to 1 μg/mL.

Several mutations that confer resistance to INH outside the inhA and katG regions (genes) have been reported. These include the mutation in the ndh region which codes for NADH dehydrogenase which has also been observed in ethiomide resistant strains. Mutations in this gene cause changes in the NADH dehydrogenase structure which hinders INH-NAD adduct from binding to the inhA active site. A mutation in ahpC, a gene that codes for alkayl hydroperoxidase reductase was also found to confer resistance to INH. However, these mutations only confer resistance in less than a quarter of clinical isolates that are INH resistant.

Resistance to isoniazid is predominantly associated with mutations in *katG*. Although the frequency of isoniazid associated mutations varies with geographic region, population and genotype [49]. About 75% of INH resistance originates from *katG gene* mutations. Therefore most drug susceptibility test methods for INH resistance focuses on detection of mutations in the *katG gene*. This implies that 25% of INH resistance may be overlooked.

Rifampicin (RIF)

Rifampicin is a semi-synthetic drug that has demonstrated an excellent sterilizing activity against tubercle bacilli since its introduction in 1972 [50]. Rifampicin acts by binding to the β subunit of DNA

dependent RNA polymerase (RpoB)—the enzyme responsible for RNA transcription—resulting in inhibition of mycobacterial messenger RNA elongation and thereby killing the organism [51]. A key feature of rifampicin is its potency against both actively growing and slow growing bacilli [52]. This feature is a major factor of the drug's ability to shorten TB treatment from 12-18 months to 9 months. Rifampicin has a few adverse reactions, which include pigmentation of body secretions such as urine, tears and sweat to orange-red and gastro intestinal upset [53]. Due to its efficient activity, rifampicin together with isoniazid are considered the backbone of TB treatment.

Rifampicin mono-resistance in *M. tuberculosis* is very rare. Rifampicin resistance generally serves as a marker for dual resistance to both isoniazid and rifampicin which is multi-drug resistance (MDR-TB). The great majority of *M. tuberculosis* clinical isolates resistant to rifampicin show mutations in *rpoB* gene that encodes the *B*-subunit of RNA polymerase. Mutations in this gene result in conformational changes in the enzyme structure and thereby present a low affinity for the drug which leads to resistance [54]. The vast majority of RIF resistance is caused by mutations found in the 81 base pair region of *rpoB* gene also known as rifampicin resistance-determining region (RRDR). Mutations in this region have been found in about 96 % of rifampicin-resistant *M. tuberculosis* isolates. Mutations at positions 531, 526 and 516 are among the most frequent mutations in RIF-resistant strains [55]. Present-day, detection of mutations that cause rifampicin resistance serves as a rapid screening for MDR-TB as RIF resistance has been found to be highly correlated with MDR-TB [56,57]. Some studies have reported RIF resistance with no mutation in the 81 base pair region of the *rpoB* gene suggesting unknown mutations and phenotypic factors as contributors to rifampicin resistance. Therefore, phenotypic methods remain an important component for drug susceptibility testing [58].

Pyrazinamide (PZA)

Pyrazinamide is a structural analogue of nicotinamide an active form of vitamin B3 that plays a role in energy production due to its role as a precursor of NAD, an important molecule involved in energy production. PZA is an important first-line anti-TB drug discovered in 1952. Its routine use in TB treatment reduced treatment duration time from the previous 9-12 months to the current 6 months which is now known as short course therapy. Its potent sterilizing activity and treatment-shortening potential is attributed to its unique ability to target a population of persistent bacilli residing within acidic pH environment inside macrophage compartments that is not killed by other drugs. Unlike other anti-TB drugs, PZA has high sterilizing activity *in vivo* but no activity against bacilli under normal neutral conditions. This requirement of acidic condition for the activity of the drug makes PZA *in vitro* drug susceptibility testing more difficult since the growth of the bacilli is impaired in acidic pH.

PZA is a pro-drug that requires modification within the mycobacterial cells to its active form, pyrazinoic acid (POA) by an enzyme pyrazinamidase (PZase). PZA enters the cells by passive diffusion. POA produced within the cells reaches the cells surface and excreted through a weak efflux pump. Small protonated POA molecules are capable of diffusing back across the membrane accumulating inside the cells, resulting in a collapsed proton gradient, reduced membrane potential and affecting membrane transport. Intracellularly, POA has been found to target ribosomal protein S1 (RspA). POA directly binds to RspA which result in the inhibition of trans-translation, a process involved in rescuing stall ribosomes during mRNA decoding, tagging truncated protein for degradation [59]. PZA resistance is brought about by mutation in *pncA*—the gene encoding PZase [60]. The majority of *pncA* mutations include point mutations, deletions, and insertions in a 561 base pair region of the open reading frame or in the 81-base pair region of its putative promoter [61]. The majority of PZA resistant clinical strains have *pncA* gene mutations and a small percentage of resistant strains contain no mutations in *pncA* or its promoter suggesting alternative mechanisms of resistance such as limited uptake and enhanced efflux. Mutations in the *rspA* gene encoding RspA, the target of POA can also confer PZA resistance. In research studies they have shown that, conformational changes induced by mutations or sequence variation in the C-terminus of RspA abolished POA binding activity [62].

Ethambutol (EMB)

Ethambutol (EMB) was reported to have anti-TB activity in 1961 and is now part of the modern-day short course therapy for drug susceptible TB alongside INH, RIF and PZA. Similar to INH, EMB acts against actively growing bacilli and has minimal effect on non-replicating bacilli. Arabinosyltransferase—an enzyme involved in arabinogalactan synthesis—is the target of EMB in *M. tuberculosis*. EMB disrupts biosynthesis of the cell wall component arabinogalactan. Arabinosyltransferase enzyme is responsible for the polymerization of arabinose into arabinan of arabinogalactan. Overproduction of arabinosyltransferase leads to EMB resistance [63-66].

EMB resistance in *M. tuberculosis* is usually associated with mutations in the *embCAB* operon. *EmbB* gene encoding arabinosyltransferase is organised into an operon with *embC* and *embA* in this order *embCAB*. These three genes share 65% amino acid identity and they all presumed to encode transmembrane proteins [67]. Mutations in *embB* and *embC*, are responsible for EMB resistance particularly mutations in the *embB306* codon, which have been used as a maker for EMB resistance in genomic drug susceptibility tests. However mutations in *embB306* locus appear in only 60% of EMB resistant clinical strains. In addition, this mutation has also been observed in EMB susceptible clinical isolates. The exact role of the *embB306* mutation in EMB resistance is not clearly understood, since about 35% of EMB resistant strains do not possess mutations in the *embB* region suggesting presence of yet unknown underlying mechanisms of EMB resistance [68].

1.2.2 Standard TB Treatment Regimen

Centers for Disease Control and Prevention (CDC) recommends that all health providers who attempt to treat TB must be knowledgeable to prescribe the standard treatment regimen and have the means to assess adherence to the regimen until treatment completion given that treatment failure may result in drug resistance and disease relapse [69]. Newly diagnosed TB patients must receive a multi-drug regimen for a duration of 6 months. The standard treatment regimen is made up of an intensive phase lasting 2 months followed by a continuation phase that lasts for 4 months. During the intensive phase four drugs are recommended including isoniazid, rifampicin, pyrazinamide and ethambutol. This phase is reported to kill 99% of bacilli rendering patients non-infectious within approximately 10-14 days with subsided symptoms. However some patients may not respond to treatment the same, and some patients can take two months to convert from sputum positive to sputum negative. In the continuation phase that takes place during the four remaining months, only 2 drugs—rifampicin and isoniazid—are used. These drugs have a high sterilizing effect on eradicating all remaining bacilli.

Although a 6 month regimen is the preferred option, an alternative continuation phase where ethambutol substitutes rifampicin can be used for 6 months thereby extending treatment duration time to 8 months. The shorter duration of continuation phase with rifampicin and isoniazid is more likely to fail especially in patients co-infected with HIV and that is where the 8 months regimen become useful [70]. The 8 month regimen may also be used in cases where treatment adherence cannot be assessed throughout the continuation phase. The recommended TB regimen in South Africa is INH, PZA, RIF and EMB in a fixed dose combination given 7 days a week for the first 2 months. If a patient is clinically improving and converted to smear negative at the end of the second month, they receive a fixed dose combination of INH and RIF given 7 days a week for 4 months [71].

In cases where a TB patient returns after disease relapse or treatment failure after receiving the first treatment course i.e. patient sputum sample remains smear positive after 5 months or more, it is recommended that the patient sample undergoes drug susceptibility testing for at least isoniazid and rifampicin before getting access to MDR-TB treatment. Upon confirmation of MDR-TB, a standard MDR-TB regimen or individually customized regimen is then administered. MDR-TB regimen varies according to the drug susceptibility results. The standard MDR-TB regimen in case of rifampicin and isoniazid resistance is 8 months of pyrazinamide, kanamycin, ofloxacin, prothiomide and cycloserine followed by 12 months of ofloxacin, prothiomide and cycloserine. In MDR-TB treatment, the intensive phase is defined by the duration of treatment with an injectable agent. The injectable agent should be continued at least 4 months after the patient first became smear-or culture-negative. The continuation period is recommended to last for a minimum of 18 months after culture conversion from a sputum sample. Extension of therapy to 24 months may be indicated in chronic cases with extensive pulmonary damage [72].

In cases where DST results take long, the standard MDR-TB regimen in South Africa comprises of at least 5 drugs: EMB, PZA, KAN, moxifloxacin, ETH and terizidone. The current SA guidelines recommend at least 6 months of injectable drugs, with treatment duration time up to 18 months after culture conversion [73]. South Africa wallows in a status quo of persistently unsatisfactory clinical outcomes with less than 45% MDR-TB treatment cases reported successful [20].

1.2.3 Drug Resistant Tuberculosis

Drug resistant TB is caused by decreased susceptibility of the *M. tuberculosis* strain to one or more anti-TB drugs. The emergence of drug resistant TB strains has posed a major threat in global TB disease control. Drug resistant TB result from a spontaneous mutation of a gene encoding an anti-TB drug target or inappropriate programmatic or individual use of TB treatment. Patients who have never received TB treatment could develop drug resistance due to transmission of the drug resistant strain. Such resistance is referred to as "primary resistance''. On the other hand, resistance that result during the course of TB treatment due to poor adherence is called an "acquired resistance". Drug resistant TB was first observed shortly after administration of streptomycin to TB patients in late 1940s suggesting that the use of a single agent can easily confer drug resistance.

MDR-TB is a disease caused by *M. tuberculosis* strains that are resistant to the two most potent first-line anti-TB drugs, isoniazid and rifampicin. MDR-TB possesses a major problem on efforts made to combat TB disease globally. MDR-TB is difficult to treat compared to drug susceptible tuberculosis. It develops mainly from inappropriate use of drug-susceptible treatment options. A patient who develops active TB with MDR-TB may spread this form of TB to other people. Globally, it was estimated that 5% of TB reported cases had MDR-TB in 2013, of which 3.5% were treatment naïve and 20.5% previously treated TB cases. Drug resistance surveillance showed that an estimated 480 000 people developed MDR-TB in 2013 and 210 00 people died [74].

According to the World Health Organization reports, in 2013 the highest percentage of MDR-TB cases were in Europe and Asia. Among new cases, the highest MDR-TB estimates reported in Belarus (35.2%) and Republic of Maldova (23.7%). Previously treated cases of MDR-TB were highest in Belarus 54.5% and Kazakhstan 55%. MDR-TB cases in Africa remain under reported. New cases of MDR-TB were highest in DR Congo 2.6%, Ethiopia 1.6% and South Africa 1.8%. Low level of reported drug resistance in Africa may not be an accurate portrayal of reality due to lack of resources. Many countries in the African region have not completed a drug resistant survey to investigate levels of MDR-TB. Out of the 36 high TB burdened countries, only 26 have managed to generate drug resistance data through special surveys, where only half of them conducted surveys, between 2010 and 2013. Currently 3 countries have not finished survey since mid-1900s Democratic Republic of Congo (DRC), Zimbabwe and Kenya.

Investigating drug resistance in Africa remains a challenge where routine DSTs are not accessible to all TB patients due to lack of laboratory capacity. As a result, this affects treatment outcome. This is evident by the lowest treatment outcome of MDR-TB cases in the African region of less than 50% compared to the Eastern Mediterranean region which scored the highest mark of 64%. TB is a curable and manageable disease, which the European region has shown, however with only the right resources in place. Thorough assessment of TB drug resistance is of urgent need in Africa.

In 2012, news of the massive deployment of GeneXpert—a new rapid diagnosis and drug-susceptibility testing system for TB—was received with high hopes by everyone concerned with detrimental impact TB has caused. This meant that more patients would have a same day diagnosis followed by treatment on the very same day. The benefits of GeneXpert primarily include a short turnaround time of 2 hours for detection of TB and drug resistance against rifampicin. However, these benefits did not translate to reduced severity of the overall TB related illness due to the high cost of the GeneXpert machine, which is too expensive for most stakeholders. Most rural clinics cannot afford the price. GeneXpert is also neither suitable nor practical at the present time especially in low and middle income countries. For a more in-depth discussion on GeneXpert see section 1.3.3.2.

South Africa had an estimated burden of approximately 26 000 notified MDR-TB cases, situated on the 5th place among highly MDR-TB burden countries[75]. However, only 40% of diagnosed cases received MDR treatment in 2013, most likely because of resource constraints, creating an even major dilemma, fuelling extensively drug resistance TB.

Poor management of MDR-TB has emerged to a newer form of resistance, extensively drug-resistant TB (XDR-TB). In XDR-TB, the *M. tuberculosis* strain is also resistant to rifampicin and isoniazid in addition to one of the fluoroquonolones and any of the second-line injectable drugs. XDR-TB detection relies on the capacity of available laboratory to reliably perform and detect *in vitro* resistance to rifampicin and isoniazid together with fluoroquinolone and second-line injectable drugs. Automated culture systems are recommended for second-line DST, which allows identification of XDR-TB from 4 to 9 weeks. However, liquid culture systems are labour intensive, expensive, time consuming and require specialised equipment and a well-serviced biosafety level 3 facilities, which most resource limited countries cannot afford. As a result, in 2012 only 5% of new bacteriologically confirmed DSTs were performed for first line TB drugs worldwide. Furthermore, DSTs for fluoroquinolones and second-line injectable drugs was performed for only 23% of patients with TB who were confirmed to have MDR-TB [76]. From 2006 when the first cases of XDR-TB were announced, 100 countries in 2013 have reported at least one case of XDR-TB [74]. According to the World Health Organisation out of 1269 XDR-TB patients reported in 2013, only 22% completed treatment successfully while 35% died, 10% failed treatment and 33% were lost to follow up.

However, this report does not represent global magnitude since only 40 countries were able to report XDR-TB outcome.

In South Africa 10% of MDR-TB cases are XDR, only 15% were successfully treated while 40% died and 36% were lost to follow up [20]. Most XDR-TB cases in South Africa were detected in KwaZulu-Natal (1298), Western Cape (230) and Eastern Cape (488) [77]. In KZN 80% of patients with active TB are co-infected with HIV. This high mortality of XDR-TB patients in South Africa was partly associated with elevated levels due to HIV co-infection (270, 000) in TB patients [20]. High HIV infection had shown to worsen XDR-TB cases when 52 out of 53 XDR-TB patients who were HIV infected died during the Tugela Ferry outbreak in KwaZulu-Natal. It was also reported that 55% of those XDR-TB patients had never received any TB treatment before showing that they were infected with already drug resistant strains of TB [78]. Some studies have reported no significant difference in mortality rates between HIV positive patient on active ART from HIV negative patients, suggesting that antiretroviral treatment contribute towards a better outcome to those co-infected with HIV and XDR-TB [79].

XDR-TB treatment is far more expensive, less efficacious and more toxic compared to treatment of drug susceptible TB. Clinical outcomes remain poor in South Africa, with a poor treatment success rate of less than 20% in XDR-TB patients compared to current success rate of less than 45% in MDR-TB which is also poor [73]. XDR-TB is very difficult to treat and associated with high mortality rate. Recent studies have demonstrated higher treatment success rates where six anti-TB drugs were used in intensive phase instead of four [80]. XDR-TB treatment regimens are usually individualized based on drug-susceptibility testing and treatment may incorporate drugs on group 5 such as clofazimine and delamanid that are not yet approved in case four of the approved second line anti-TB drugs are less effective, although data on efficacy and safety of group 5 drugs is still limited [81,82].

1.2.4 Drug-resistant TB Treatment

First line therapy often fails to cure TB in the case of drug resistance. MDR-TB, defined as resistance to at least two first line drugs; INH and RIF, is currently one of the greatest concerns in TB control worldwide. Treatment of MDR-TB requires the use of second line drugs that are generally more difficult to acquire, more expensive and more toxic compared to first line drugs. The World Health Organization classified the existing anti-TB agents into 5 groups based on drug efficacy, potency, class and frequency of use against TB (Table 1). All TB regimens are designed from these groups according to whether the strain of *M. tuberculosis* is DS-TB, MDR-TB or XDR-TB. The following drugs are classified as second line drugs for the treatment of drug resistant TB:

Table 1: World Health Organisation recommended grouping of anti-TB agents

Group Number	Group Name	Anti-TB agent	WHO Abbreviation	Research Abbreviation
1	First line oral agents	Isoniazid	H	INH
		Rifampicin	R	RIF
		Ethambutol	E	EMB
		Pyrazinamide	Z	PZA
2	Injectable anti-TB drugs	Kanamycin	Km	KAN
		Amikacin	Am	AMK
		capreomycin	Cm	CAP
3	Fluoroquinolones	Levofloxacin	Lfx	LEV
		Moxifloxacin	Mfx	MXF
4	Oral bacteriostatic second line anti-TB drugs	Ethionamide	Eto	ETH
		Prothiomide	Pto	PRO
		Cycloserine	Cs	CYL
		Para-aminosalicyclic acid	PAS	PAS
		Para-aminosalicyclate sodium	PAS-Na	
5	Anti-TB drugs with limited data on efficacy and or long term safety in the treatment of drug-resistant TB	Bedaquiline	Bdq	BDQ
		Delamanid	D	DLM
		Linezolid	Lzd	LZD
		Clofazimine	Cfz	CFZ
		Amoxicillin/clavulanate	Amx/Clv	AMC
		High-dose isoniazid	High dose H	

Aminoglycosides

Aminoglycosides including Kanamycin (KAN), Amikacin (AMK) and capreomycin (CAP)—a macrocyclic polypeptide isolated from *Streptomyces capreolus*—are important injectable drugs in the treatment of multidrug resistance TB. Although they descend from two different classes of antibiotics, they all apply their antimicrobial activity at the protein translation level. KAN and AMK are closely related drugs that have similar mechanism of action with CAP, which is associated with changes in ribosomal RNA. These drugs inhibit protein synthesis of *M. tuberculosis* and therefore target actively dividing bacilli. KAN, AMK and CAP bind to ribosomes of *M. tuberculosis* and prevent elongation of the peptide chain during protein synthesis. Resistance to KAN and AMK is associated with mutations in the *rrs gene* encoding the 16S rRNA. High levels of cross resistance between these two

aminoglycosides have been observed where CAP becomes more valuable. Resistance to capreomycin has been associated with a mutation in the gene *tlyA* encoding 2'-O-methyltransferase, an enzyme involved in addition of methyl groups to rRNA of 16S. However, some studies have reported capreomycin resistant isolates lacking mutations in the *tlyA* gene [83].

Fluoroquinolones (FQ)

Fluoroquinolones are synthetic antibiotics with a broad spectrum of activity, commonly used in treatment of various bacterial infections for instance in the gastrointestinal, respiratory and urinary tract. They have shown excellent activity against *M. tuberculosis* both *in vitro* and *in vivo.* Fluoroquinolones drugs that have been used to treat multi-drug resistant TB are ofloxacin, moxifloxacin, levofloxacin and gatifloxacin. Ciprofloxacin was recently found to have a weaker efficacy against TB compared to its counterparts and is no longer recommended as part of TB treatment [84]. Severe side effects from some fluoroquinolones which may result in sudden death have impelled the World Health Organisation to recommend that only levofloxacin and moxifloxacin which have high potency and fewer side effects be used to treat MDR-TB patients [84]. Fluoroquinolones inhibit bacterial DNA gyrase thereby preventing DNA replication.

DNA gyrase is a topoisomerase which consists of two sub units A and B, encoded by *gyrA* and *gyrB*, respectively. Most FQ resistance occurs from *M. tuberculosis* strains with mutations in a small region of *gyrA* gene called the quinolone resistance determining region (QRDR) and less frequently in gyrB gene.

Thioamides

Thioamides consist of ethioamide and prothioamides which are derivatives of isonicotinic acid as is INH. Thioamides are pro-drugs that require activation by mycobacteria upon cell entry. Although ethioamide have structural similarities to INH and a similar target which is the inhibition of InhA in order to halt cell wall synthesis, they seem to have a different activator, flavin monooxygenase encoded by *ethA* gene [85,86]. Thioamides have similar efficacy against *M. tuberculosis* and they can be used interchangeably. Mutations in *EthA* gene and *InhA* were found in ethioamide resistant clinical isolates [87].

P-aminosalicyclic acid (PAS)

P-aminosalicyclic acid is one of the first anti-TB drugs, discovered in 1944. As old as it has been, its mechanism of action is still unknown. Recent studies have shown that PAS is a pro-drug that is activated to its active metabolite by an unknown enzyme. Activated PAS then targets dihydrofolate synthase, a key enzyme in folate synthesis. Overexpression of *drfA* gene confers PAS-resistance in *M. tuberculosis* strains [88].

Cycloserine (CYL)

D-cycloserine is a key antibiotic currently used in second-line treatment for extensively drug resistant TB. Cycloserine is a structural analogue of an amino acid D-alanine which can be found in bacterial cell walls. It acts as a competitive inhibitor of alanine:alanine ligase, an enzyme that combines alanine amino acids into an alanylalanine peptide, an important component in peptidoglycan synthesis and thereby interrupting mycobacterial cell wall formation [89]. The key advantage of cycloserine is the absence of cross resistance with other drugs. Overexpression of alanine racemase and alanine:alanine ligase, enzymes involved in alanine metabolism and peptidoglycan biosynthesis respectively result in D-cycloserine resistance [90].

Group 5 anti-TB drugs

These drugs are not yet well studied for use in drug resistant TB, but may only be used to support regimens for patients with MDR-TB or XDR-TB that are resistant to other routinely drugs.

Amoxicillin/clavulanate

Amoxicillin/clavulanate is a β-lactam antibiotic. β-lactams antibiotics were initially developed to treat infection caused by gram-positive bacteria in 1940s. β-lactams targets the cell wall synthesis by binding to the transpeptidases which catalyzes peptidoglycan cross linking [91]. Although the broad spectrum of β-lactamase activity in *M. tuberculosis* limits the antibiotics potential of B-lactam in TB treatment, addition of clavulanate have shown to inhibit b-lactamase activity thereby enhancing B-lactam activity [92]. The combination of B-lactam and B-lactamase result in increased efficacy against TB for instance in amoxicillin/clavulanate. Amoxicillin/clavulanate is an antibiotic used as a last resort in drug resistant TB treatment due to its unclear efficacy and safety. Although it is inexpensive, amoxicillin/clavulanate has been subjected to quality concerns and its interaction with TB and HIV medication is still unclear.

Bedaquiline (BDQ)

Bedaquiline also known as diarylquinoline or TMC207 was approved by the Food and Drug Administration (FDA) in late 2012 for treatment of drug resistant TB. This compound shown high activity against both sensitive and resistant strains of mycobacteria [93]. This was the first time in over 40 years that this agency had approved a new TB drug with a different mode of action. Bedaquiline is a first in the new class of drugs aimed to treat the drug resistant strain of TB. Bedaquiline targets mycobacterial ATP synthase, a critical enzyme in ATP synthesis of *M. tuberculosis*. Binding of bedaquiline to the oligomeric and proteolipid subunit-c of mycobacterial ATP synthase leads to inhibition of ATP synthesis, which later result in bacterial death. It is effective against replicating and dormant organisms since dormant organisms also require ATP to survive. However, the drug's safety

remains questionable, given the potential risks including serious side effects, elevated risk of death, demonstrated in a phase II trial, where about 11.4% of patients taking bedaquiline died during clinical trials compared with 2.5% of those taking placebos. As the drug carries some significant risks, it is mandated to be used only in patients who do not have other treatment options [94].

Clofazimine (CFZ)

Clofazimine is a lipophilic riminophenazine antibiotic that was primarily used for treatment of multibacillary leprosy in 1962. Clofazimine was shown to be active against *M. tuberculosis in vitro* including MDR-TB strains, it was however considered ineffective in treatment of pulmonary TB. Early studies demonstrated inconsistent therapeutic activity of clofazimine in various animal models including rabbits and guinea pigs. Over the years with the emergence of MDR-TB and XDT-TB, a renewed interest in clofazimine as an anti-TB drug was triggered. Even though it has been recommended for use in patients with drug resistant TB, it is not approved or well-studied for treatment of TB. Clofazimine is recommended for use in combination with other drugs in the second-line treatment of drug resistant TB. Pigmentation of skin to reddish-brown in colour is one of the unpleasant side effects which gradually subsides upon treatment cessation [95].

Delamanid

Delamanid is a novel drug that was approved by European Medicines Agency late in 2013 for the treatment of drug resistant TB on condition that it is used as part of an appropriate combination regimen in adult patients whose currently approved regimen cannot be used due to resistance or intolerability. However, delamanid is not yet widely available for patients outside the European Union or clinical trials. Delamanis is a dihydro-nitroimidaoxazole derivative and a pro-drug that is activated by a mycobacterial enzyme, deazoflavin dependent nitroreductase to its active metabolite that plays a role in the inhibition of the mycolic acid synthesis. Studies have shown that delamanid has high potency, least risks of drug-drug interaction with antiretroviral drugs which makes it an important option in treating drug resistance in patients infected with HIV [96,97].

Linezolid

Linezolid is an antibiotic used in drug-resistant treatment when limited options exist. Although not approved for TB treatment, linezolid demonstrated high efficacy against XDR-TB on clinical trials. However it is often not given to patients with XDR-TB due to its lack of availability and prohibitive cost [97]. Linezolid had been shown to cause severe side effects including anaemia/thrombocytopenia—a lack of blood platelets which causes slow blood clotting after injury which may result in constant bleeding. Despite these severe side effects, studies have reported cures among patients with MDR-TB treated with linezolid.

Linezolid falls within a group of compounds called oxazolidinones which bind to the 50S subunit of the prokaryotic ribosome, preventing the binding of 30S subunit to form a complex with mRNA initiation factor and formylmethionyl-tRNA, blocking the assembly of a functional initiation complex for protein synthesis preventing mRNA translation. The advantage that comes with incorporation of linezolid in drug resistant treatment regimen, is that this drug has a unique target that does not overlap with existing drugs [98].

1.3 Currently Available TB Diagnostics and Drug Susceptibility Testing Tools

Diagnosis of tuberculosis is confirmed by identification acid-fast bacilli by smear or by isolation of *M. tuberculosis* in cultures or identification of its genomic material by molecular tests.

Drug resistant tests are not routinely carried out in most cases and it is only after treatment failure that drug resistant tests are performed [99]. This fuels the spread of drug resistance which is difficult to manage. Focussing on rapid and easily accessible diagnostics and drug susceptibility testing is of paramount importance to enable early detection and prescription of appropriate anti-TB drugs. This is bound to minimize the spread of TB and drug resistant TB strains. XDR-TB is currently associated with high mortality rate and therefore posing a major challenge that threatens public health.

1.3.1 Miscellaneous Tests

1.3.1.1 Sputum Smear Microscopy

Sputum smear microscopy is primarily the mostly used method for diagnosis of pulmonary TB predominantly in low and middle income countries [100]. Two techniques are used for TB diagnostics with sputum smear microscopy; fluorescent microscopy which uses acid-fast fluorochrome dye (auramine –rhodamine) and conventional microscopy uses carbol fuchsin Zeihl-Nelsen (ZN) or Kinyuon staining. Zeihl-Nelsen staining is a widely used technique for the identification of acid-fast bacilli. In this process a thin smear of the sputum specimen is deposited on a glass slide, exposed to hot carbol fuchsin dye for 3 minutes, rinsed, decolourized with a dilute acid-alcohol solution and stained with methylene blue solution and rinsed with water. Mycobacteria absorb the carbol fuchsin dye but withstand decolourization by the acid-alcohol, as a result of the high lipid content in their cell walls which explains the name acid-fast bacilli [101]. The conventional light microscope is then used, where the bacilli appear dark red to dark purple against the blue background. When the sputum is stained with fluorochrome dye rhodamine-auramine stain in which case a fluorescent microscope is used, the bacilli fluoresces yellow to white against the dark background. Auramine is more sensitive than Ziehl-Nelsen stain but less specific and more expensive [101,102].

Sputum smear microscopy is useful in low income settings which are highly burdened by TB, because it is rapid, simple to perform and cost effective [102]. In areas with very high TB prevalence, sputum microscopy is highly specific. It also correlates with infectiousness identified by high bacterial

load—the number of bacilli in the smear and the probability of their being identified by microscopy [103]. The sputum microscope results are reported and graded according to each patients' bacillary concentration reflecting the extent of lesion in a particular patient which is directly proportional to the infectiousness of the case (Table 2). Although this technique is the most widely used rapid diagnostic test, it has some limitations. The threshold of detection is immensely compromised when the bacterial load is less than 10000 organisms per mL sputum sample. This explains the sensitivity of 60% which drops drastically in paediatric TB and patients co-infected with HIV and TB to 30%.

Table 2: Grading of AFB smear as per WHO recommendation

No. of acid-fast bacilli (AFB)	Fields	Report
No AFB	In 100 immersion fields	Negative
1-9 AFB	In 100 immersion fields	Positive scanty (report exact number)
10-99 AFB	In 100 immersion fields	1+ positive
1-10 AFB	Per fields (examine 50 fields)	2+ positive
More than 10 AFB	Per fields (examine 20 fields)	3+ positive

Limited resources and large number of samples, all combined together often reduce the observation time per slide to less than 60 seconds which contributes to the reduction of sensitivity of the test [100]. Sputum microscopy cannot distinguish between dead, alive bacilli or and mycobacterial species and cannot differentiate between drug susceptible and resistant strains. Overall, sputum smear microscopy still plays a pivotal role in resource limited communities and high TB burdened area until a more reliable, affordable and fast diagnostic test is available, until then, sputum microscopy seems to be here to stay.

1.3.1.2 Chest X-ray

Chest radiography is often used for evaluation where there is compatible symptoms but negative laboratory tests results [102]. Chest X-ray assists a clinician to determine the presence of TB in the lung in a form of lesion. Patients with active TB often have upper lobe cavitary infiltrates [101]. However, an X-ray might present some abnormalities in lower or mid-lung field in TB patients. However, there have been instances where a chest X-ray may appear normal even in the case of TB infection; this is often observed in patients co-infected with HIV and TB. Poor film quality and non-expert readers have been reported to compromise this test [104].

1.3.2 Phenotypic Methods

1.3.2.1 Culture Based Method

Conventional culture methods for drug susceptibility testing (DST) are based on inoculation of *M. tuberculosis* culture on solid media. For many years, DST on solid egg and agar based media were

used as a standard technology and is still being used in many countries worldwide. The standard method using egg-based Lowenstein-Jensen (LJ) medium includes the proportional method, the absolute concentration method and the resistance ratio method which have been well standardized with clinical samples. Substantial amount of data from many countries report the proportional method to be the most commonly used [105]. The proportional method enables a precise estimation of the proportion of *M. tuberculosis* mutant strains resistant to a given anti-TB drug. This is determined by comparing quantity of growth in a drug-containing and drug-free control medium from countable colonies (50-100). The proportion of bacilli resistant to a given drug is expressed as the resistant portion of a percentage of the total population used. If over 1% of *M. tuberculosis* mutant population can grow the strain is rendered resistant [106,107].

The absolute method uses a standardized inoculum grown in drug-containing media and drug-free media. Several concentrations of each drug are tested, and resistance is expressed in terms of the lowest concentration of drug that inhibits growth called minimal inhibitory concentration (MIC). This method is greatly affected by the initial number of organisms [107,108].

The resistance ratio method compares growth of the unknown tubercle bacilli strains with the drug susceptible standard laboratory reference strain (H37Rv) in the same set of tests. Resistance is expressed as the ratio of the MIC of the test strain divided by the MIC of the standard strain. An isolate with a ratio of eight or more is considered resistant to the given drug [107,108].

When performed on egg-based media, the final results' reading is done after 42 days of incubation. When agar-based media is used, results are obtained after 21 days of incubation. This delay is additional to the time required to first grow isolates in drug free medium from sputum sample in case an indirect method is used which can take 3 weeks. In contrast to the indirect method, is the direct method where the concentrated sputum specimen is directly inoculated to a set of drugs containing and drug-free media. The direct method has more advantage in that the results become available sooner and better represent the patient's original bacterial population. However, this is determined by the initial bacterial load from the sputum sample [108,109].

Conventional culture method remains the gold standard because it has been standardised for DST of many drugs, require no specialised equipment, inexpensive and more reliable than the sputum smear microscopy. The greatest limitation of the conventional culture tests is the long turnaround time, with 3 weeks to a month of incubation until the results can be obtained. Meanwhile the patient needs to start their drug treatment. In addition, when using egg-based media, a large number of tubes are inoculated for each test and incubated for 42 days, requiring large amount of incubator space. Careful quality control of all batches produced with drug susceptible or resistant for reliable results is of paramount importance and this is labour intensive.

New phenotypic methods have been developed aimed at rapid detection of growth using metabolic activities of dividing mycobacteria to determine mycobacterial growth and drug susceptibility. More recent methods include BACTEC MGIT-960 TB system which is based on liquid medium. MGIT is an automated, continuously monitoring system based on fluorometric technology for detection of oxygen consumption by bacteria growing inside the MGIT tubes. Each MGIT tube contains a fluorescent sensor which is oxygen quenched, embedded at the bottom of the tube. The consumption of oxygen by growing mycobacteria causes the fluorochrome to fluoresce under UV light. DSTs are performed on prepared kits of anti-TB drugs, mycobacteria are then inoculated on two tubes, one containing the testing drug. Detection of fluorescence in drug-containing tubes determines that a given strain is resistant. The test is completed within 10 days [110].

The limitation of the MGIT is the richness of medium used where non-mycobacterial species and other fast growing mycobacteria can overgrow present *M. tuberculosis* and therefore yield false positive results. This system is too expensive for laboratories in resource limited settings due to the cost associated with acquiring of MGIT-960 system components, the price list are $63,900 for the 960 instrument, $824 for a carton of 100 culture tubes and $92.70 for the supplement kits (100 tests, growth and antibiotics supplements) [111].

1.3.2.2 Phage-based Test

The use of bacteriophage for bacterial detection was first reported over a century ago where an assay to detect Salmonella using phage Felix 01 was described in 1954. Mycobacteriophage are phage that infect species of the mycobacterium genus. Over 200 different mycobacteriophage have been described infecting a broad range of mycobacterial hosts isolated from soil, surface water, stool and resection specimens of patients with TB or sarcoidors [112,113].

The FASTplaque TB (Biotec, Ipswich, Suffolk, UK) is the only commercially available phage-based kits for detection of mycobacteria on the market. FASTplaqueTB is a phage amplification assay which detect the presence of mycobacteria by the formation of plaques at the end of the assay and offers a phenotypic test with a turnaround time of 4 days [114].

Initially the samples containing the target cell is mixed with a high titre of the bacteriophage. The samples are then incubated to allow time for cell infection to occur and for phage to enter the cell, at this point any exogeneous phage that did not enter the appropriate host cells are destroyed by the addition of a virucide. A virucide is a chemical that inactivates the phage but have no effect on the viability of the host cells. The internalised phage is then detected when the progeny get released at the end of the lytic cycle by the formation of plaques (the area of no growth) in a bacterial lawn. The FASTplaqueTB uses a D29 mycobacteria phage with a broad host range and can also infect fast growing, non-pathogenic *M. smegmatis* used as a fast growing host to produce lawns of bacteria to detect newly released phage. A similar assay is also available for the detection of antibiotic sensitivity

as FASTplaqueResponse which can be used on direct patient sample or indirect isolates. In this assay phage growth is inhibited in the presence of the antibiotic [115].

This assay is simple to perform, affordable and require no expensive equipment. However, it does require a functional microbiology laboratory and cannot be used in remote areas. The specificity of this assay is an issue since the test utilizes a broad host range phage D29 to allow slow growing and fast growing mycobacteria to be infected. In addition the test is reported cumbersome with high variability. This makes it difficult to determine whether the cell detected is TB or non-tuberculous and therefore resulting in false positive results, without the use of an additional test such as PCR amplification to confirm signature sequence or culture methods [116].

1.3.3 Genotypic Methods

Genotypic methods are DNA based assays that targets characterised resistant associated mutations to identify drug resistance in *M. tuberculosis*. Mutations conferring drug resistance have been described for most first line and second line anti-TB drugs. There are number of genotypic assays that have been developed and available for the detection of resistance determining mutations in *M. tuberculosis*.

1.3.3.1 Line Probe Assay (LPA)

In 2008, the World Health Organization authorized the use of line probe assays for the rapid detection of MDR-TB. Line probe assay involves DNA extraction, amplification of a predefined gene region associated with resistance, and reverse hybridization of the PCR products with standard immobilized probes for gene mutations associated with resistance [117]. At present there are three commercially available line probe assays for the detection of first-line drug resistance of *M. tuberculosis*. While *rpoB* gene mutations responsible for rifampicin resistance are detected by all three assays; the INNO-LipA (Innogenetics, Belgium) detects RIF resistant mutation in the *rpoB* region only, Genotype MTBDR additionally detects *KatG* mutations, and second-generation Genotype MTBDRplus (Hain LifeScience GmbH, Germany) detects mutations conferring resistance in *rpoB*, *katG* and *inhA* genes [118].

Hain Lifesciences released the GenoType MTBDRsl test in 2009, designed to test for resistance to second-line anti-TB drugs (fluoroquinolones, ethambutol, aminoglycosides and cyclic peptides), which can be used in combination with the MTBDRplus test to identify XDR-TB. The major advantage of LPA is that they can be performed directly on smear-positive sputum samples, giving rapid (approximately 5 h) drug susceptibility results without the need for culture. Many laboratories are now using LPAs as the primary method for DST on cultured isolates of *M. tuberculosis*, replacing phenotypic DST. The disadvantages of LPAs are that they are labour intensive, still limited to detection of resistance caused by known mutations; require highly trained personnel and dedicated laboratory space and equipment.

1.3.3.2 Gene Expert

In 2010, the World Health Organization authorized the use of GeneXpert MTB/Rif TB assay (Cepheid, CA) as the initial diagnostic test for TB in individuals that are suspected of MDR-TB or HIV-TB co-infection. GeneXpert uses real-time PCR with molecular beacons, probes for hybridization to different target segments within a region of the gene of interest. When nucleotide concordance between the probe and target of interest matches, the beacon emits fluorescent signals. The absence of a signalling suggests a mutation in the target segment region [119].

The GeneXpert machine is a fully automated closed system that performs both sample preparation and real-time PCR, producing results in less than 2 hours. GeneXpert is capable of detecting the mycobacterium tuberculosis complex (MTBC) while simultaneously detecting RIF resistance by targeting the RRDR of the *rpoB* gene. Analytical sensitivity and specificity was 100 % according to a study using RIF resistant and sensitive *M. tuberculosis* isolates and non-tuberculosis bacteria [120]. The assay is designed for direct genotypic DST from unprocessed sputum or sediment from a concentrated specimen. Sample reagent is poured into the tube, incubated for 15 min and pipetted into Xpert machine for processing.

Major advantages of the Xpert machine is rapid turnaround time of less than 2 hours, hands-free processing, therefore no highly trained staff is required to run the machine or interpret the results, near-patient technology and high throughput [121,122]. The major limitations include the cost of equipment, the price for GeneXpert machine is approximately US$ 17 000 and the Xpert MTB/RIF tests cost approximately US$ 17 per cartridge which is quite costly [123]. It only can be used in equipped laboratories, and unlikely to be used in rural health centres, due to poor infrastructure and limited resources. GeneXpert is also limited to only detect drug resistance of one drug, rifampicin, it cannot detect resistance-incurring mutations outside of specified target region, and the detection of silent mutations which are falsely interpreted as conferring resistance. However, some studies have reported that most isolates resistant to RIF are also resistant to INH in about 90% of the time, suggesting that the presence of *rpoB* mutation can be used as a surrogate marker for MDR-TB.

1.3.3.3 DNA Sequencing

DNA sequencing is considered the gold standard with the capacity to both identify *M. tuberculosis* isolates and evaluate for drug resistance. Conventional DNA sequencing utilizes a chain-termination method to sequence DNA fragments. It first binds a primer to a denatured single stranded DNA followed by DNA extension which begins at the primer site using DNA polymerase. This is terminated because a dye-labelled dideoxynucleotide interrupts phosphodiester bond between two subsequent nucleotides. This cycle results in DNA fragments of various lengths, which can be separated by electrophoresis and subsequently sequence. The limitations in using this highly accurate method are the high costs associated with it which hinder its use in resource limited setting which are

also highly burdened with TB. In addition, a highly trained personnel is required for results interpretation.

There is a pressing need for a phenotypic test that can produce results with the speed and reliability of the best nucleic acid test but without the limitation of the specific already known DNA sequence mutations that confers drug resistance.

1.4 Phenotypic and Genotypic DST

Traditionally, phenotypic drug susceptibility is determined by either broth or agar dilution which rely on evaluation of bacterial growth in the presence of various concentration of antibiotic. This method allows for determination of MIC of the antibiotic, a lowest concentration that prevents bacterial growth. These tests take long (weeks to months) in slow growing mycobacteria such as *M. tuberculosis*. This may have serious implications; the patient may spread active drug resistant TB endangering many lives whilst waiting to start appropriate treatment.

While various genotypic markers have been identified for drug resistant TB strains, phenotypic methods still predominates genotypic detection methods for antibiotic resistant gene. Measurements of bacterial phenotypic response to antibiotics remains gold standard due to diverse resistance mechanisms and continuous evolution of pathogenic bacteria. The genotypic methods are useful for screening, but may fail in case a newly acquired drug resistance is independent of target gene expression. Gene Xpert for instance is not only expensive, it is also limited to detecting mutations that confer resistance to rifampicin from a predefined region. Genotypic methods are still limited when it comes to detecting epigenetic mechanism that may result in drug tolerance for instance efflux mediated drug tolerance. Efflux pumps are membrane proteins that can extrude a variety of toxic agents such as antimicrobials and chemotherapeutic agents. Substantial proportion of drug-resistant isolates have no identifiable mutations in known resistance associated genes, and it appears that resistance in some of these isolates may result from increased efflux activity. Multiple studies have reported increased efflux pump expression in *M. tuberculosis* clinical isolates. This phenomenon may have serious clinical implication such as prescription of the standard TB regimen to patients with unrecognizable drug-resistant TB. This is likely to happen in areas where access to mycobacterial culture are limited. As a result culture-based drug susceptibility test methods remain the gold standard in clinical microbiology laboratories. Current conventional phenotypic methods employed for drug susceptibility testing have a slow turnaround time as they require long incubation hours and bulky supporting instrumentation. An ideal test would be phenotypic so as to be robust to genetic variations and applicable to emerging disease evolution, while also delivering antibiotic susceptibility information as rapidly as possible to inform the patient's treatment regimen.

Chapter 2

MICROFLUIDICS

2.1 Introduction to Microfluidics

Since its inception in the early 90s, microfluidics technology has undergone tremendous progress. Microfluidics technology is the science of systems that deals with the flow of liquids in micro-sized channels [124]. The microfluidics technology involves designing and manufacturing devices with size dimensions ranging from micrometres to millimetres. A microfluidic device contains a set of micro-channels engraved into materials such as silicon, glass or polymer. These devices enable manipulating fluids in picoliter to microliter volumes in channels with dimensions of tens of micrometres. In a microfluidic chip, the micro-channels serve to achieve a specific function such as mixing, pumping, flowing liquids inside the channels. These micro-channels are connected to the outside by input- and output ports incorporated into a microfluidic chip to allow introduction and removal of fluids and reagents from the chip with external systems such as pressure controller or push syringes.

Different substrate materials have been used for fabrication of microfluidics devices, such as ceramic, Teflon, steel and silicon. The fabrication methods for these different platforms may vary due to the differences in properties of the substrates. Most fabrication processes are based on photolithography, initially developed in IC (integrated circuit) technology. Although silicon is now rarely being used as a substrate for microfluidic devices due to its complicated and costly fabrication process, in the early developmental days of microfluidics technology, silicon was a widely used substrate material for fabricating microfluidics devices for various applications. Silicon contributed vastly to the rapid evolution of microfluidic technology. The fabrication process for silicon-based devices involved lengthy processes such as substrate cleaning, photolithography, metal deposition and wet/dry etching. Moreover, the silicon substrate is relatively expensive and optically opaque therefore limited in optical detection. To overcome these short comings, silicon was later replaced with glass and polymeric materials which on the other hand were less expensive and optically transparent. Polymer materials including polymethacrylate (PMMA), polystyrene (PS), polycarbonate (PC), and polydimethylsiloxane (PDMS) were then adopted. Due to their low cost, ease of fabrication and physical properties, polymers are now the primary materials used in microfluidic research.

The most widely used polymer in fabrication of microfluidic devices is Poly Dimethyl Siloxane (PDMS), an optically transparent, soft elastomer. PDMS has numerous advantages such as biocompatibility, flexibility in moulding, elasticity and simpler fabrication process (soft lithography). Soft lithography is the technique of replicating structures from a master mold onto an elastomeric

PDMS substrate. Microfluidic chip fabrication using PDMS is a relatively simple process that require a special facility called the cleanroom. This process allows rapid building of prototype followed by testing their application in minimal time frames. The microfluidic chips uses miniaturised micro-chemical membrane valves also made up of PDMS which efficiently control the movement of fluids within the channels. Multi-layer bonding of PDMS, microfluidic actuators including on-off valves, switching valves and pumps can be fabricated on-chip. To achieve this, the polymer membrane in between the channels is engineered to be relatively thin—for instance 30 μm. Once the pressure is applied to the upper channel, the membrane deflects downward and closes the lower channel [125,126]. The valves also allow creation of multiple channels which can be used to form different compartments. This process is simple, and the microfluidics device is completed within few hours.

Microfluidics technology is currently explored by various fields and has found many applications in the biomedical field, biological applications and drug screening in pharmaceutical industries such as gene/protein manipulation and analysis, cell-based systems, biosensors and drug discovery and delivery. Some studies have created microfluidic devices for nucleic acid purification, where a single chip was used to sequentially process nanoliter volumes to isolate variable number of bacterial and mammalian cells, lyse them and purify their DNA and mRNA without pre and post sample preparation [127]. Recent development advances in microfluidic technologies have also miniaturized the flow cytometer to perform simple, rapid and affordable CD4 T-lymphocytes counts especially for HIV. In a different study Kitamori developed a micro-ELISA system for rapid and sensitive diagnosis. The permeability of polymer to gases makes it suitable for work with living cells [128].

The microfluidics technology has a number of features suitable for cell-based assays: the micro-scale dimension mimicking the microstructure and native environment of the in vivo systems; it requires small samples therefore low reagent consumption. The polymer used such as polydimethylsiloxane is permeable to oxygen and the microfluidics technology can combine multiple steps such as cell culture, cell sampling, fluidic control, cell lysis, mixing and detection on a single device.

Pathogenic bacteria normally reside in microstructures within human tissues. In order for conventional culture methods to detect bacteria they require small number of bacteria growing into a colony forming unit which usually takes days to months. Advances in microfluidics technology have allowed the use of microfluidic devices to trap and immobilize bacterial cells within micro-channels without altering the cell properties whilst simultaneously exchanging media and observing cell behaviour in real time.

The recent developments of transparent microfluidic devices have enabled long term cell culturing. A number of studies have developed microfluidic devices for bacterial cell growth and one particular study focussed on culturing *Saccharomyces cerevisae* for 8 generations starting from single cells. In a

different study by Balagadde et al., a microchemostat bioreactor enabled long-term culture monitoring using *E.coli* [129]. Recently, Aldridge et al. used a microfluidic device to demonstrate differences in elongation rate and size within a clonal population of mycobacteria, and established that the resulting sub-populations of cells are differentially susceptible to antibiotics [130].

2.2 Benefits of Microfluidics

Microfluidics has the potential to transform management of clinical diseases and the development of new diagnostics at the point of care, for rapid drug susceptibility testing. Developing culture-based drug susceptibility tests using microfluidics has numerous advantages such as effective sample usage since it requires small sample and reagent quantities, high detection sensitivity, and reduced analysis times. At the same time microfluidic devices are easily scalable to perform multiple tests on multiple samples. The large surface to volume ratio of PDMS microfluidic systems enables the rapid detection of the bacterial growth [131]. Direct observation of bacteria dividing from one to two cells allows faster detection of the effect of antimicrobial agents on bacterial growth. Sufficient concentration of oxygen is also required for rapid growth of mycobacteria in microenvironments. High surface to volume ratio of microfluidic micro channels allows abundant oxygen in micro channels. This approach has the potential to shorten the waiting time for DST results, which in turn may encourage prescription of the most appropriate medication to patients and allow patient personalised medicine and treatment. This can reduce the risk of the emergence of drug resistant TB strains.

2.3 Statement of Problem

The emergence of drug resistant TB is becoming a major threat to global health. Drug resistant TB keeps advancing as a result of inappropriate use of anti-TB multi-drug chemotherapy. Physician errors such as improper drug administration and patients' poor compliance are among the major contributing factors to drug resistant TB [132]. Reports have continually showed lower number of drug resistant TB among newly diagnosed cases 2.3%, relative to higher proportion of MDR-TB from retreatment cases 71.4%, suggesting improper use of anti-TB drugs. In South Africa approximately 1.8% new TB cases and 6.7% treated cases are multi-drug resistant [74]. Studies have shown that the majority of new drug resistant TB (DR-TB) cases diagnosed in SA are due to transmission of already resistant strains [133]. Limited access to reliable diagnostic tools is one of the hurdles South Africa has to overcome. To combat this dilemma rapid and reliable drug susceptibility testing tools are required for guidance of treatment and surveillance of drug resistance. Early detection of the bacilli will prevent further spread of drug resistant TB strains in the communities and prevent administration of inappropriate treatment regimen. Microfluidics provides a platform with the potential to produce high throughput, rapid and reliable drug susceptibility methods which are cost effective.

2.4 Knowledge Gaps

After reviewing the literature, it was evident that although DST tests are currently being performed, they still occur at a smaller scale and are cumbersome thereby making it difficult to be outsourced or available to every patient in need of these tools. Cheaper diagnostic tools seem to be cumbersome and take time for results to be available for instance culture methods. As a result these methods are good at detecting resistance but are not efficient. Genotypic methods are fast at detecting resistance however not everyone can afford them and they are also more dependent of already known mutations that cause drug resistance. With that being said these tools might miss drug resistance in case it is presented by an unknown mutation. Therefore an ideal drug susceptibility tool is that which produces fast, accurate result in less time possible. A search of existing literature does not yield any evidence for microfluidics applications for DST in clinical TB practice. However, the literature reveals promising microfluidics devices aimed at development of diagnostic tools that yields highly accurate drug susceptibility results for multiple anti-tuberculosis antibiotics [134,135].

2.5 A Microfluidics Chip for Culturing Tuberculosis

This project was aimed at developing a culture-based drug susceptibility test for tuberculosis using microfluidics that is reliable and fast with less human involvement.

2.6 Objectives

1. To create a microfluidic chip that will grow mycobacterial cells and expose them to different antimicrobial agents.
2. To create a chip that will perform drug susceptibility tests whilst mimicking the microenvironment in terms of size similar to mycobacteria growing inside the membrane bound compartment of a macrophage.
3. To create a drug susceptibility test that can distinguish between bacteriostatic and bactericidal antimicrobial agent.

2.7 Brief Thesis Overview

The aim of this project was to develop a drug susceptibility test using microfluidics. We designed and fabricated the microdialyser chip. Chapter 1 consists of the literature review. Chapter 2 describes the microdialyser chip design and fabrication according to Microfluidics Large Scale Integration (MLSI). Initially the motivation of this design of the microdialyser design is explained and therefore the reason for the modifications of the microdialyser chip design. Chapter 3 shows how we validated the functionality of the microdialyser units using calorimetric assays. We then used the microdialyser units to culture mycobacteria under different growth conditions. This was followed by treating mycobacterial cells with a series of antibiotics where we observed epigenetic drug tolerance which led us to modify the microdialyser chip by introducing bioreactors with variable sizes. We also describe the investigation of the mechanism underlying this phenotypic drug resistance in mycobacteria

growing in a space confined environment which was found to be efflux mediated. Chapter 4 consists of the concluding remarks of this thesis.

2.8 The Microdialyser Chip

2.8.1 Introduction

Mycobacterium tuberculosis resides intracellularly, inside the membrane bound compartment of macrophages within ~5 pL volume. Mycobacteria growing inside macrophages have been reported to be more resistant to antibiotics compared to mycobacteria growing extracellularly in liquid medium. In particular, the study conducted by Hartkoorn et al found that a higher concentration of rifampicin was required to kill intracellular bacilli (148 ng/ml) compared to extracellular bacilli (1.27 ng/ml) [136]. In a different study by Adams et al they revealed that mycobacterial cells exposed to macrophages for 96 hours became more tolerant to antibiotics (more than 200 fold for isoniazid, 20.6 fold for rifampicin and 4.8 fold for moxifloxacin compared to those exposed to macrophages for only 2 hours) [137]. To mimic the size of the membrane bound compartment of macrophages we designed a microdialyser chip with miniaturized reactor volume of 200 pL.

The main objective of this project was to develop a microfluidic-based platform that will grow *M. tuberculosis* isolates in multiple reactors and perform drug susceptibility tests with reduced human involvement. The drug susceptibility testing assay would include trapping growing microbes in microfluidic reactors and perform drug susceptibility screening for rapid measurements. Trapped mycobacteria would be exposed to different drugs or drug combinations at different concentrations to test for drug resistance and also find most effective drug combinations for each isolate. The growth rate was documented using automated optical micrography.

With further research and development, this platform could be developed for investigating hundreds of patient sputum samples at the same time, which would minimize human contact with potentially infectious doses of *M. tuberculosis*. This approach could also be used to screen potential multiple drug compound combination mixtures for determining the most effective drug combination suitable for each specific TB patient. The availability of such a high throughput MTB drug resistance diagnostic and monitoring option could dramatically improve patients' outcomes by preventing clinical disease progression and the transmission of drug resistant TB. This approach would be particularly more affordable in hospitals and medical centres where a high demand for microscopic observation drug susceptibility (MODS) testing also requires highly trained personnel to spend a considerable amount of time on each patient sample.

2.8.2 Design and Fabrication

Using the microfluidic plumbing technology of pneumatically activated Quake valves, mixers and pumps developed previously, we created a miniaturized, culture-based drug susceptibility testing on a chip (figure 9). The chip was fabricated out of silicone elastomer polydimethylsiloxane (PDMS)

(General Electric RTV 615) using multi-layer soft lithography described in the supporting information. The chip can support up to 120 microdialyser units that can run in parallel on each chip.

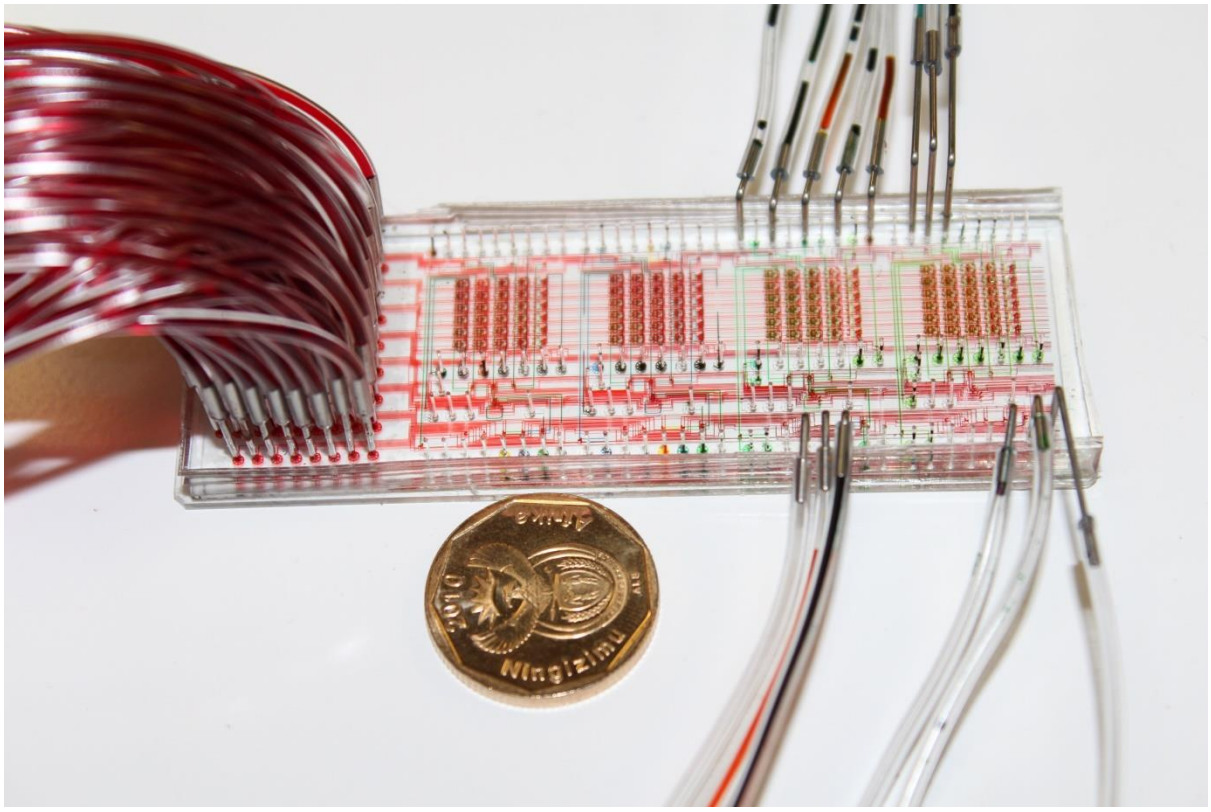

Figure 9: A microdialyser chip with 120 microdialyser units that operate independently. Various inputs have been loaded with food dyes to visualize channels and other subelements of the chip, the tubes filled with red dye shows the 71 control lines. The coin is 10 mm in diameter.

The microdialyser device was designed to trap approximately 5-10 mycobacterial cells in each microfluidic compartment and periodically expose these cells to different drug cocktails. This device consists of four identical modules (figure 11). Each module consists of 8 input ports for different drug stock solutions and a formulator ring for combinatorial drug mixing. The formulator is a fluidic loop that is 10 μm high, 100 μm wide and ~0.02 μL volume, with an integrated peristaltic pump and a series of microchemical valves for injection of fluids into the ring and expulsion of fluids into designated reactors. There are 30 microdialyser units per module. Each microdialyser unit consists of two chambers: a micro-sized cell culture chamber or growth chamber that is ~200 pL in volume connected via a link valve to an adjacent conditioning chamber that stores fresh medium 800 pL (figure 1, chapter 3).

To expel waste products such as used reagents and mycobacterial cell suspension the microdialyser has 15 output ports that operate as outlets. In order for the microdialyser chip to operate at its full capacity, it requires microchemical valves that regulate the flow of fluids inside the channels. The

microchemical valves have different operational duties including mixing of solutions, separation of fluids and trapping organisms in their respective channels. The microchemical valves can constrict and relax only when activated by the computer controlled control lines which can be pressurized— allows for closing and opening these microchemical valves. The microdialyser chip consists of 71 control lines (figure 10).

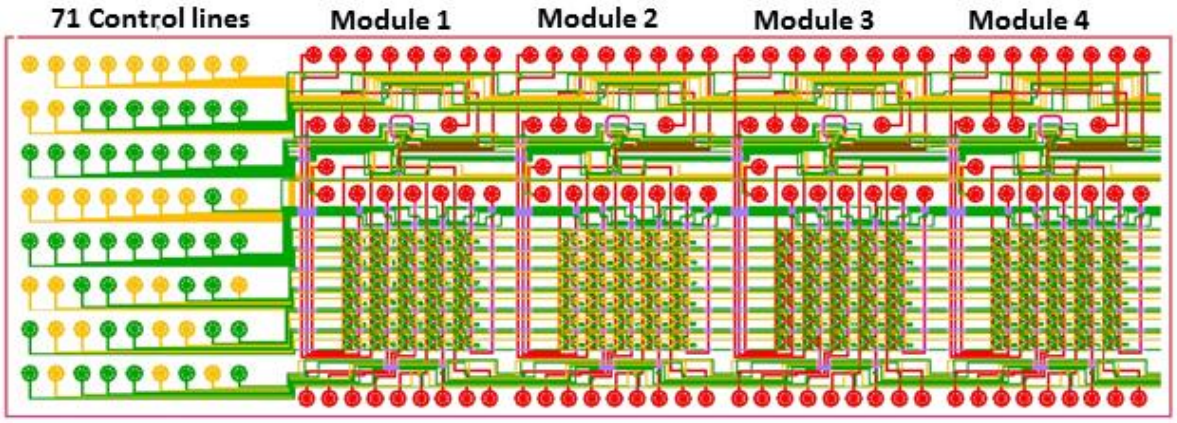

Figure 10: A schematic of the microdialyser chip design with 4 modules. The chip can support 120 microdialyser units that operate independently. The reagents flow channels are shown in red and the control lines are illustrated by yellow and green lines.

2.8.3 Characterization of Diffusive Mixing in a Micro-reactor of the Microdialyser

To characterize the performance of the microdialyser chip we performed calorimetric assays using food dyes. The microdialyser would operate by trapping mycobacteria in miniaturized bioreactors where they will be exposed to different drug cocktails by passive diffusion between the conditioning chamber and the growth chamber. The microdialyser uses a microdialysis scheme to periodically introduce fresh nutrients and remove waste from a captive population of mycobacteria through diffusive exchange, mimicking the passive bi-directional exchange of pro and anti-mycobacterial factors across the macrophage membrane. The 200 pL mycobacterial growth chamber of the microdialyser is connected via a link valve to an adjacent chamber that stores fresh medium. Periodically, the link valve is opened for 60 seconds to allow small molecules to freely diffuse between the two chambers down their concentration gradient: fresh nutrients diffuse into the growth chamber while mycobacterial metabolic waste products diffuse into the conditioning chamber. The relative large size and non-motility deter the mycobacterial cells from exiting the growth chamber when the link valve is opened. Thereafter the conditioning chamber is filled with fresh medium and awaits the next microdialysis step. To investigate the time required for solution in the growth chamber to match that in the conditioning chamber, we calibrated the diffusive exchange functionality of the microdialyser using colorimetric assays. We used food dyes to determine the time it takes to convert

the concentration in the growth chamber to that of the conditioning chamber. We found that on average, the microdialyser replaced the growth chamber fluid within 6 microdialysis steps (figure 1, Chapter 3).

2.8.4 Modification of Microdialyser Chip

The microdialyser chip was modified later to allow various sized microdialyser units. In this design, all the components were kept the same such as the eight inputs port, 15 output ports, the formulator, the number of the control lines and the number of micro-sized reactors remained the same (reactor 11A). However, only six 200pL volume reactors were kept, the rest of the 200pL microdialyser units were replaced by eight 1700pL growth chambers, eight 1200pL growth chambers and eight 500pL growth chambers (figure 11B). Colorimetric assays ascertained that diffusive mixing pattern of the microdialysis scheme was similar across all growth chamber sizes (figure 12).

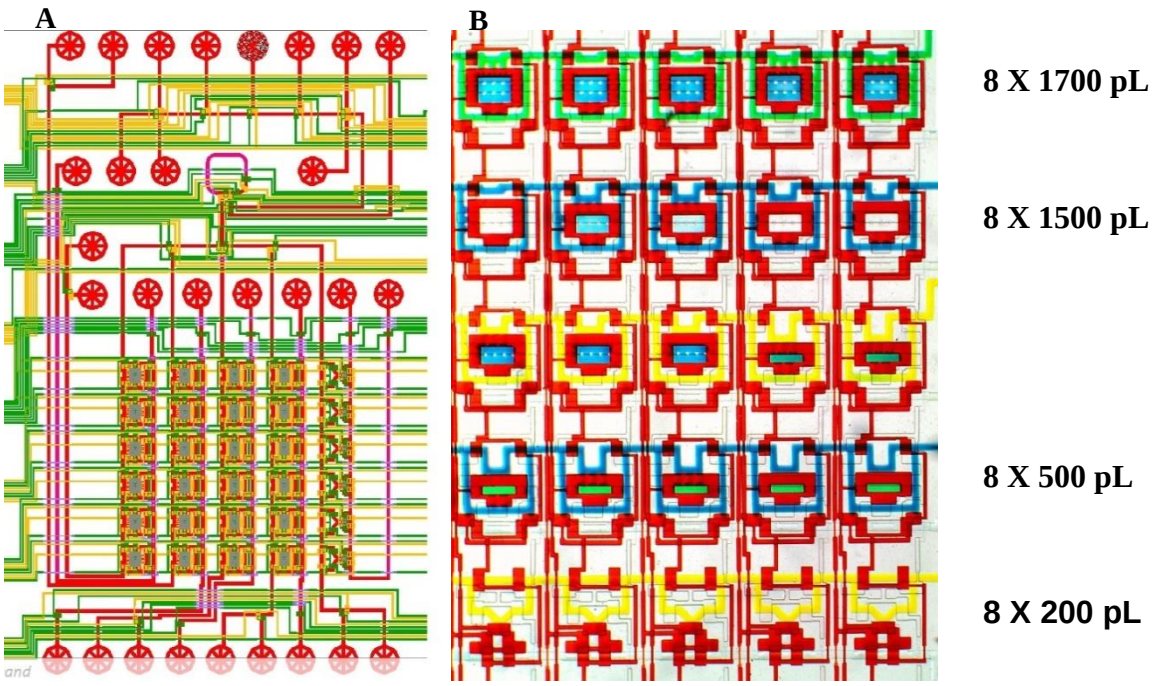

Figure 11: A modified microdialyser chip. A) A schematic of a modified microdialyser design showing one module. Illustrating maintained chip architecture with all other subelements in the modified chip kept the same as in the original design except variations in reactors sizes. B) A pictogram illustrating different reactor sizes ranging from eight 1700 pL, 1200 pL, 500 pL and six 200 pL volume growth chambers. Reactors were loaded with food dyes to visualize different reactor sizes.

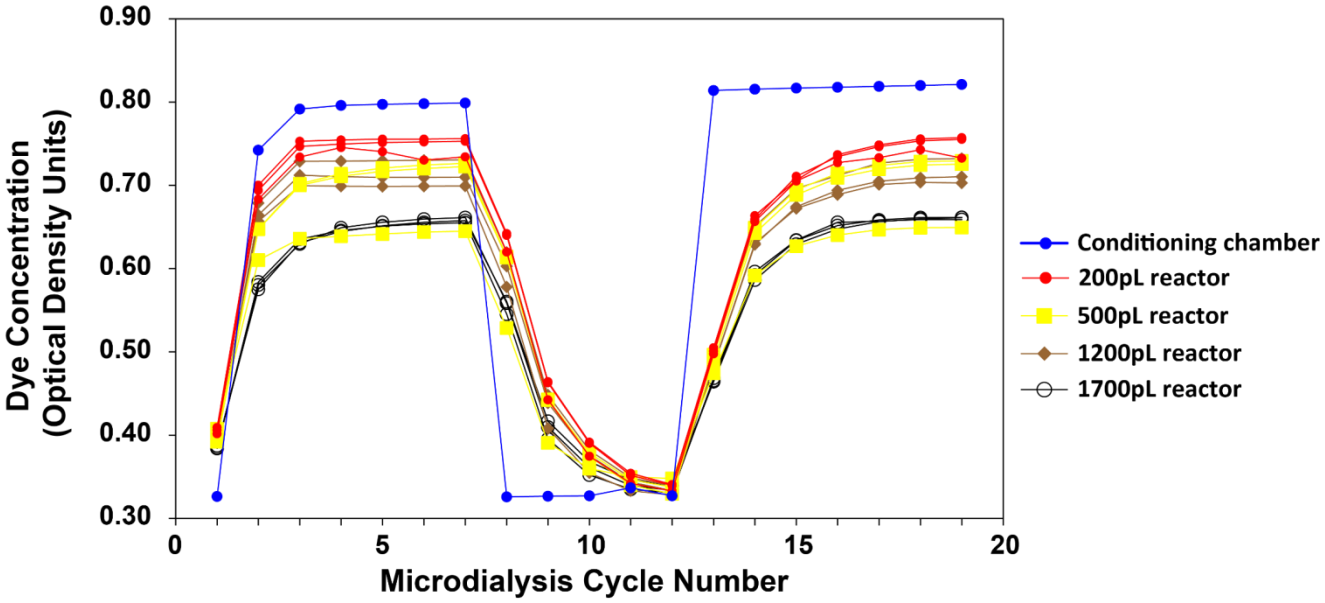

Figure 12: Functional illustration of diffusive exchange in the multi-volume microdialyser showing the dye concentration in the various growth chamber volumes and the conditioning chamber. The formulation in the conditioning chambers is cycled between DYE (cycles 2-7 and 13-19) and WATER (cycles 1; 8-12). The dye concentration in the various growth chambers is determined by the formulation in the conditioning chamber. The chamber-to-chamber variations in dye concentration are attributable to minor height differences in the growth chambers.

During microscopic counting 6 images were captured for each 1700 pL and 1200 pL growth chamber, 3 images for each 500 pL growth chamber and 1 for each 200 pL growth chamber to cover the whole surface area of each reactor. We then developed image-processing algorithms in Matlab to determine the number of cells in each reactor picture set, from which the total cell density was determined. This new microdialyser design has now an additional capability for investigations aimed at addressing mycobacterial growth under variable sized compartments.

2.9 Macrophage Membrane Biology

Macrophages are mononuclear phagocytes which appear throughout the body, which can be found in high numbers in connective tissues, the submucosa of the intestinal tract, the lung, the liver, the spleen and along specific blood vessels. On their cell surface, macrophages express several cell-receptors, which can discriminate numerous bacterial components as bacterial carbohydrates such as, mannose

receptor, glucan receptor, bacterial lipids such as LPS receptors and structure typically found on pathogen surfaces such as Toll-like receptors.

Macrophages engulf and kill invading microorganisms and are crucial for eliciting immune responses. They produce pro-inflammatory cytokines such as IL-1β and TNF-α. Tubercle bacilli are encountered and engulfed by alveolar macrophages, which reside in the lung.

The binding of a bacterium to a macrophage receptor stimulates the engulfment of the pathogen into intra-macrophage vesicles, a process known as phagocytosis. Once the pathogen has been surrounded by the membrane of the phagocyte, it is then internalised into an intracellular vesicle called phagosome. The pH inside the phagosome is then lowered to foster destruction of the pathogen. In addition, phagosomes typically fuse with lysosomes—intra-macrophage organelles containing degradative enzymes enclosed in a membrane— which degrade the pathogen using lysozyme enzymes. Mycobacteria have been reported to withstand the harsh conditions encountered inside the macrophages (phagosomes) because of their thick cell wall. As a result, this has led to a manipulation of the host cells by mycobacteria for their own survival whereby mycobacterial cells replicate within the macrophage instead of dying.

The macrophage is surrounded by a plasma membrane and in a simplified model, the macrophage can be considered to be a tiny growth chamber for mycobacteria with a volume that is approximately 5 pL. Although our smallest growth chamber of 200 pL is ~40 times bigger than the macrophage growth chamber, it is a close approximation of the macrophage volume compared to traditional cell culturing system with volumes exceeding 1 mL and thus at least 200,000,000 times bigger than the macrophage growth chamber.

The microdialyser 200 pL growth chamber to a macrophage growth compartment are both tiny growth chambers and both induce epigenetic drug tolerance to mycobacteria. We thus considered the plausibility that the mycobacterial drug tolerance phenotype observed in our growth chamber is of the same quality as the drug tolerance phenotype observed in intra-macrophage mycobacteria. For a more in-depth discussion on drug tolerance refer to Chapter 3. Included on section 2.3, page 29.

Chapter 3

CONFINEMENT-INDUCED DRUG-TOLERANCE IN MYCOBACTERIA MEDIATED BY AN EFFLUX MECHANISM

The next chapter consists of a manuscript a published on PloS one journal, the publication is available at the following link: http://journals.plos.org/plosone/article?id=10.1371/journal.pone.0136231

Luthuli BB, Purdy GE, Balagaddé FK (2015) Confinement-Induced Drug-Tolerance in Mycobacteria Mediated by an Efflux Mechanism. PLoS ONE 10(8): e0136231. doi:10.1371/journal.pone.0136231

This manuscript describes how the microdialyser chip was utilised for culturing mycobacterial cells in different conditions including different antimicrobial agents. We tested a number of hypothesis to determine the mechanism underlying drug tolerant phenomenon observed in mycobacteria growing in miniaturised bioreactors.

PLOS | ONE

RESEARCH ARTICLE

Confinement-Induced Drug-Tolerance in Mycobacteria Mediated by an Efflux Mechanism

Brilliant B. Luthuli[1], Georgiana E. Purdy[2], Frederick K. Balagaddé[1]*

1 KwaZulu-Natal Research Institute for Tuberculosis and HIV, Nelson R. Mandela School of Medicine, University of KwaZulu-Natal, Durban, 4001, South Africa, **2** Dept. of Molecular Microbiology and Immunology, Oregon Health and Sciences University, 3181 S. W. Sam Jackson Park Rd., Mail Code L220, Portland, OR, 97239, United States of America

* frederick.balagadde@k-rith.org

Citation: Luthuli BB, Purdy GE, Balagaddé FK (2015) Confinement-Induced Drug-Tolerance in Mycobacteria Mediated by an Efflux Mechanism. PLoS ONE 10(8): e0136231. doi:10.1371/journal.pone.0136231

Editor: Jérôme Nigou, Centre National de la Recherche Scientifique—Université de Toulouse, FRANCE

Received: April 23, 2015

Accepted: July 30, 2015

Published: August 21, 2015

Data Availability Statement: All relevant data are within the paper and its Supporting Information files.

Funding: This work was supported by the Howard Hughes Medical Institute (http://www.hhmi.org/) and the University of KwaZulu-Natal College of Health Sciences.

Competing Interests: The authors have declared that no competing interests exist.

Abstract

Tuberculosis (TB) is the world's deadliest curable disease, responsible for an estimated 1.5 million deaths annually. A considerable challenge in controlling this disease is the prolonged multidrug chemotherapy (6 to 9 months) required to overcome drug-tolerant mycobacteria that persist in human tissues, although the same drugs can sterilize genetically identical mycobacteria growing in axenic culture within days. An essential component of TB infection involves intracellular *Mycobacterium tuberculosis* bacteria that multiply within macrophages and are significantly more tolerant to antibiotics compared to extracellular mycobacteria. To investigate this aspect of human TB, we created a physical cell culture system that mimics confinement of replicating mycobacteria, such as in a macrophage during infection. Using this system, we uncovered an epigenetic drug-tolerance phenotype that appears when mycobacteria are cultured in space-confined bioreactors and disappears in larger volume growth contexts. Efflux mechanisms that are induced in space-confined growth environments contribute to this drug-tolerance phenotype. Therefore, macrophage-induced drug tolerance by mycobacteria may be an effect of confined growth among other macrophage-specific mechanisms.

Introduction

Tuberculosis, caused by infection with *Mycobacterium tuberculosis* (*Mtb*) remains one of the world's deadliest diseases, killing an estimated 1.5 million people annually [1]. Whereas drug-susceptible forms of the disease are in principle curable, the duration of treatment courses is at least 6 months and may last years [2]. Multidrug resistant TB (MDR-TB) and extensively drug resistant TB (XDR-TB) have poorer and less certain outcomes [2–4]. It is expected that shortened antituberculosis treatment regimens will improve patient adherence to treatment, and thereby foster better case management and disease control and minimize the risk of drug resistance [5, 6]. An interesting aspect of long-term chemotherapy in TB is that, whereas more than 95% of the tubercle bacilli population detectable in a patient's sputum can be cleared in the first few days of treatment, prolonged treatment is required to eradicate the residual minority

population (<5%) [7, 8] using drugs that are rapidly potent in vitro [9–11]. Overcoming this bacterial persistence is central to shortening TB treatment [12]. The transient nature of persistence—an epigenetic drug-tolerance phenotype—has pushed research in this area toward miniaturization and chip-based control using time-lapse microscopy to study the phenotypic heterogeneity within bacterial populations in situ [13–15]. Whereas these efforts have thus far investigated persistence in an extracellular context, recent studies have shown that the intracellular (or intramacrophage) mycobacterial sub-population, which makes up an essential component of human TB infection [16, 17], is significantly more tolerant to antibiotics [18, 19]. Separate studies have shown that the dimensions and diffusional characteristics of the growth environment can influence bacterial gene expression [20–22]. To investigate persistence, we characterized the growth and drug susceptibility of mycobacteria replicating in space-confined microfabricated cell culture environments (or microdialysers) to mimic the confinement experienced by mycobacteria replicating within macrophages.

We focused our experiments on *Mycobacterium smegmatis*, an experimentally tractable surrogate for *M. tuberculosis* with respect to rifampicin—a frontline drug in TB treatment [23]. The microdialyser has a micro-sized cell culture chamber that is 200 picoliters (pL) in volume to approximate the ~5pL volume of the membrane-bound compartment of human macrophages [24]. Thus upon inoculation of a microdialyser culture chamber with ~5 mycobacteria, the cell density immediately exceeds 10^7 cells/ml and verges toward the effective cell density of an intra-macrophage mycobacterium, ~10^8 cells/ml [24].

Materials and Methods

Microfluidic device design and fabrication

The microdialyser chip was fabricated out of the silicone elastomer polydimethylsiloxane (PDMS) (General Electric RTV 615) using multi-layer soft lithography, as described previously [25]. Up to 120 microdialyser units can run in parallel on each chip.

The microdialyser reader

Mycobacteria were cultivated in growth chambers within the microdialyser chip (S1 Fig) which was positioned for live-cell imaging on an Olympus IX81 inverted microscope furnished with a PRIOR Scientific XYZ motorized stage system (Wirsam Scientific Precision Equipment (Pty) Ltd., Pinetown, South Africa). The motorized stage system enabled documentation of multiple simultaneous microdialyser cultures on a single chip. Imaging was done using a Plan Fluor 40X 0.6NA objective. Digital images were captured by a Hamamatsu digital CCD ORCA-R2 camera (Wirsam Scientific Precision Equipment (Pty) Ltd., Pinetown, South Africa). LabVIEW software was used to control the synchronized operation of these components and chip valve actuation.

Media, strains and growth conditions

M. smegmatis strain mc^2155 was received from Bill Jacobs (Albert Einstein College of Medicine). *M. smegmatis* Δ*ftsEX*—gift from Eric Rubin (Harvard University) comprised of an *M. smegmatis* mc^2155 strain with the *ftsEX* gene deleted and were hypersensitive to the RNA polymerase inhibitor, rifampicin, with a minimum inhibitory concentration of 1μg/ml [26]. *E. coli* Top10F' cells were purchased from Invitrogen. Conventional cell cultures were performed with 10 ml of 7H9 broth in tissue culture flasks at 37°C with shaking at 100 rpm and growth was determined by measuring the turbidity of the cultures at 600 nm (OD_{600}) twice daily unless otherwise stated. *M. smegmatis* cells in the microdialyser were grown in 7H9 broth at 37°C. The *M. smegmatis mmpL11* mutant was described previously [27].

M. smegmatis precultures were prepared by inoculating a 10ml medium (7H9 broth) sample with cells from a frozen stock and culturing at 37°C with shaking at 100 rpm until an OD_{600} reading of 0.8 was reached. The cell culture was centrifuged at 2500 rpm for one minute to cause the large cell clusters to gather towards the bottom of the tube. To load the cells into the microdialyser chip, first ~500μL of the supernatant cell suspension was aspirated into a piece of tygon tubing (0.02 OD X 0.06 ID, Cole Parmer) by suction using a 1 ml syringe. Next, the free end of the tygon tubing was connected to a cell input port on the microdialyser chip (see S1 Fig), using a stainless steel pin as an adaptor between the chip and the tygon tubing. The cells were introduced into each growth chamber by flowing the cell suspension from the tygon tubing through each chamber: in via an open inlet and out via an open outlet. Accordingly, cells were trapped in each growth chamber once the inlet and outlet of the chamber was subsequently closed, by actuating the appropriate valves on the chip. On average, cells were trapped in each chamber at a uniform cell density of $\sim 2\times10^7$ cells/ml. Thus, on average, the starting number of cells per growth chamber in the 200, 500, 1200 and 1700pL growth chambers was 5, 12, 30 and 42 cells respectively. Upon microdialyser inoculation, cells were incubated in the microdialyser growth chambers by maintaining the chip at 37°C using a Solent Scientific microscope incubation chamber heating system (Wirsam Scientific Precision Equipment (Pty) Ltd., Pinetown, South Africa).

The microdialyser operation process

The microdialyser uses a microdialysis scheme to periodically introduce fresh nutrients and remove waste from a captive population of mycobacteria through diffusive exchange, mimicking the passive bidirectional exchange of pro- and anti-mycobacterial factors across the macrophage membrane (Fig 1). The 200pL mycobacterial growth chamber of the microdialyser is connected via one or more link valves to an adjacent conditioning chamber that stores fresh medium (Fig 1A). Periodically (typically, hourly), the link-valves are opened for 60 seconds to allow small molecules to freely diffuse between the two chambers down their respective concentration gradients: fresh nutrients diffuse into the growth chamber while mycobacterial metabolic waste products diffuse into the conditioning chamber (Fig 1B). The relatively large size and non-motility deter the mycobacterial cells from exiting the growth chamber when the link valves are opened. Next, the conditioning chamber is refilled with fresh medium and awaits the next microdialysis step. We calibrated the diffusive exchange functionality of the microdialyser using colorimetric assays and demonstrated that on average, the microdialyser replaced the growth chamber fluid within six microdialysis steps (Fig 1C).

Colorimetric assays

The food dye used in the colorimetric microdialyser characterization assay was obtained from McCormick & Co., Hunt Valley, MD. The dye concentration in the microdialyser was determined based on the average pixel value of optical micrographs of a region within the growth chamber or the conditioning chamber during a series of microdialysis steps. The camera pixel value (**P**) is linear with respect to transmission (**T**), which is the anti-log of the negative of the optical density (**OD**) [28], as depicted in the equations below.

$$\mathbf{OD} = -log_{10}(\mathbf{T})$$

$$\mathbf{OD} \cong -log_{10}(\mathbf{P})$$

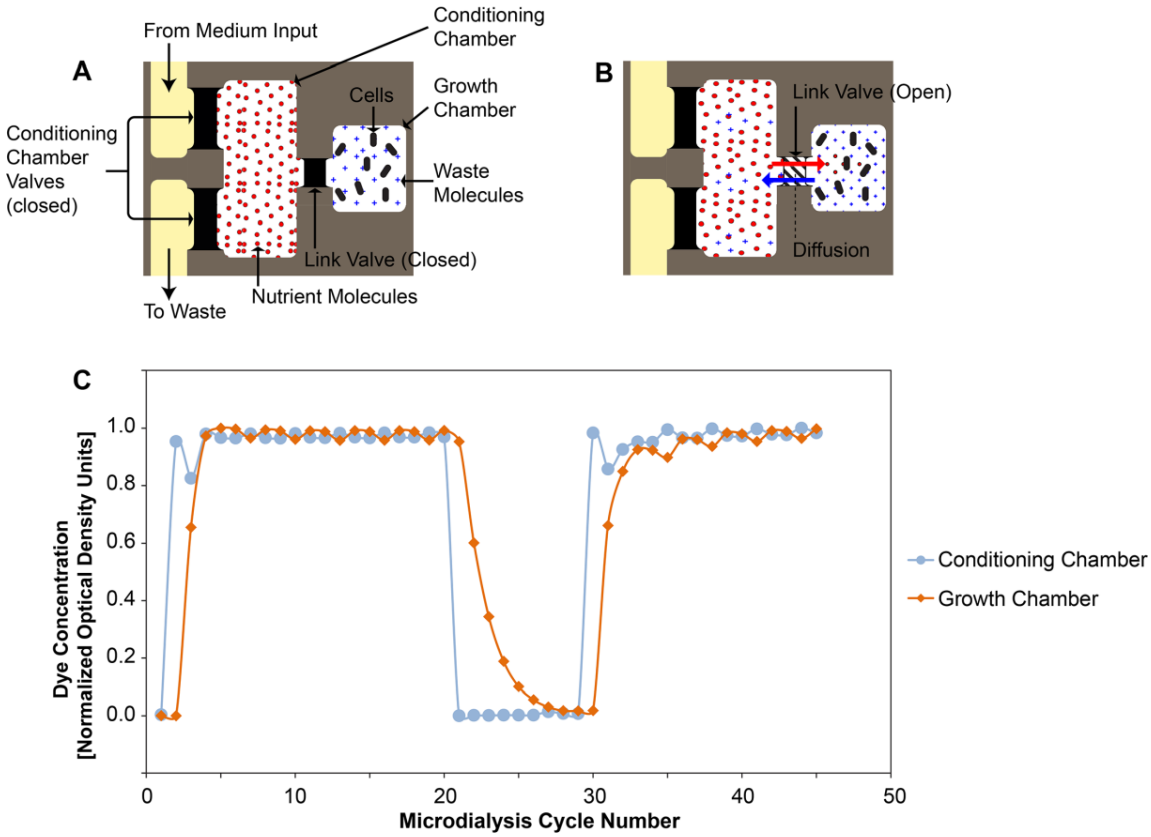

Fig 1. The microdialyser system. (A) Schematic diagram of a microdialyser unit with elements such as the growth and conditioning chambers, separated by a link valve labelled. **(B)** Once the link valve is open, passive diffusive exchange occurs between the growth and conditioning chambers: nutrient molecules (represented by red dots) diffuse into the growth chamber while mycobacterial metabolic waste products (blue crosses) diffuse into the conditioning chamber. **(C)** Functional illustration of diffusive exchange in the microdialyser showing the dye concentration in the growth chamber (orange diamonds) and the conditioning chamber (light blue circles). The fluid in the conditioning chamber is cycled between DYE (cycles 2–20 and 30–45) and WATER (cycles 1; 21–29). The dye concentration in the growth chamber depends on the concentration in the conditioning chamber. This result was reproduced over 160 times in 9 different chips.

doi:10.1371/journal.pone.0136231.g001

Microscopic cell surface density

The microdialyser architecture is such that all the cells dwell in a chamber $\leq$10 μm high, equivalent to the focal depth of the Plan Fluor 40X 0.6NA objective. We assessed bacterial growth in the microdialyser by enumerating the fraction of pixels occupied by *M. smegmatis* cells in images of microdialyser culture chambers (or cell surface density—a dimensionless quantity with a maximum value of 1), at different time points. We developed image-processing algorithms written in Matlab to determine the cell surface density in each picture. The motorized stage system enabled documentation of multiple simultaneous microdialyser experiments on a single chip.

Results and Discussion

At full operational capacity, the microdialyser chip can support 120 microdialyser culture units that operate independently, with each culture monitored in situ by optical microscopy to provide automated, real-time, non-invasive measurement of cell density. Mycobacterial growth was assessed from microscopic images of each growth chamber by enumerating the fraction of pixels occupied by bacterial cells (or cell surface density—a dimensionless quantity with a maximum possible value of 1) at different time points. Microdialyser growth curves followed the trend of typical mycobacterial growth: upon inoculation, a typical culture began with a lag period, followed by an exponential growth phase that gave way to a stationary phase. To functionally validate the effectiveness of the microdialyser in modulating the growth environment of its captive mycobacterial population, we demonstrated the ability to speed up or slow down the mycobacterial growth by switching the growth chamber medium from nutrient-poor to nutrient-rich and vice versa (Fig 2).

Conventional liquid phase cultures of *M. smegmatis* mc^2155 cells were treated with a series of antimycobacterial drugs, including rifampicin (35μg/ml), isoniazid (40μg/ml), ofloxacin (100 μg/ml) and hygromycin (100μg/ml). Growth was inhibited in conventional cultures by these drugs at the indicated concentrations (Fig 3A). Growth in microdialyser cultures was inhibited by the drugs with the exception of rifampicin, which had minimal growth inhibitory effect even at 350 μg/ml—which is 10× the concentration that inhibited growth in the conventional liquid phase cultures, ~40× the minimum inhibitory concentration (MIC) and ~10× the minimum bactericidal concentration (MBC) of rifampicin for mc^2155 cells [29, 30] (Fig 3B). For comparison, rifampicin at 350 μg/ml inhibited growth of *Escherichia coli* cells in microdialyser cultures and maintained its antibiotic potency for more than 200 hours, demonstrating that there was sufficient penetrance of the rifampicin into the microdialyser reactors (S2 Fig). This result also indicated that the rifampicin tolerance phenotype was specific to *M. smegmatis* and absent in *E. coli*. Given the small number of *M. smegmatis* cells present in the growth chamber (not exceeding 20) at the time the rifampicin resistance first appeared, a simple mutation rate versus population size argument excludes the possibility of a mutational cause of resistance to rifampicin. Because rifampicin is a front line drug in TB treatment, we sought to better characterize and further elucidate mechanisms underlying the rifampicin tolerance phenotype.

To investigate the role of confinement in the rifampicin resistance of microdialyser cell populations, we fabricated a new chip with growth chambers of various sizes: 200pL, 500pL, 1200pL and 1700pL (S1 Fig). Colorimetric assays ascertained that the diffusive penetrance of the microdialyser process was similar across all growth chamber sizes (S5 Fig). In addition, we obtained an Δ*ftsEX* mutant of *M. smegmatis* that is particularly hypersensitive to rifampicin with a MIC of 1μg/ml [26]. *M. smegmatis* Δ*ftsEX* cells grew similarly well in the various growth chamber sizes in drug-free medium. However, although *M. smegmatis* Δ*ftsEX* demonstrated resistance to rifampicin at 350 μg/ml in the 200pL cultures, the drug inhibited growth in the larger (500pL, 1200pL and 1700pL) cultures (Fig 4). Thus, the rifampicin resistance phenotype was dependent on the size of the growth chamber: appearing when the mycobacteria were cultured in the smallest (200pL) growth chambers and disappearing in the bigger reactor volumes. Wild type mc^2155 *M. smegmatis* cells growing in various sized growth chambers had a similar pattern of drug tolerance behavior when exposed to 350μg/ml of rifampicin (S4 Fig).

One potential cause of volume-dependent rifampicin tolerance may be due to increased bacterial density in space-confined environments through quorum sensing. In the generic model of quorum sensing [31, 32], bacterial cells secrete signaling molecules called autoinducers whose concentration in the surrounding medium increases with cell density. At low cell density, the autoinducer molecules produced at a basal level diffuse out of the cell, and are

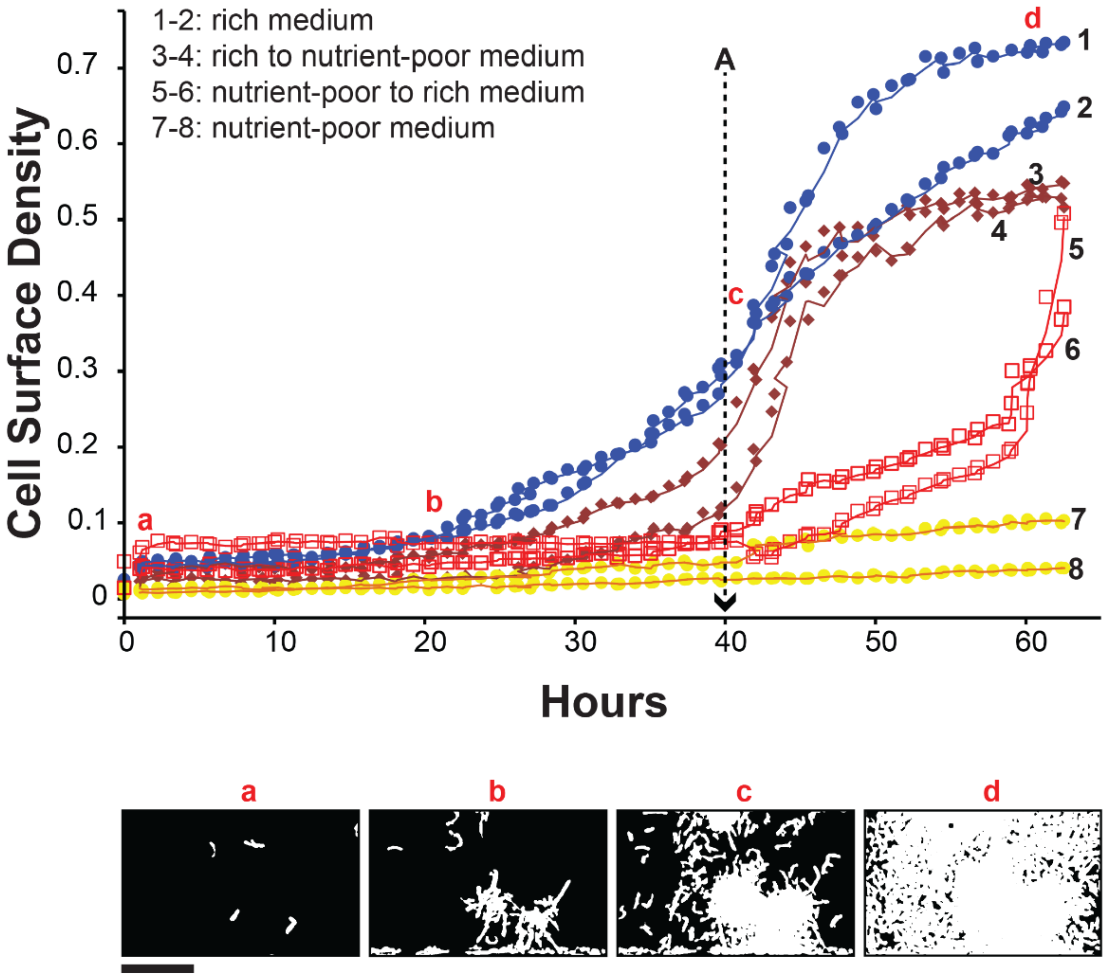

Fig 2. Functional validation of the microdialyser system. Typical growth curves of *M. smegmatis* mc^{2}155 cells in a microdialyser (growth chamber volume, 200pL) with the medium switching from nutrient-poor to nutrient-rich and vice versa. Initially, cultures 1 to 4 are grown in rich medium (7H9), and 5 to 8 in nutrient-poor medium (spent 7H9 medium harvested from *M. smegmatis* cell cultures that have reached stationary phase). At 40 hours (point A), the rich medium in cultures 3 and 4 was replaced with nutrient-poor medium using microdialysis, which slowed down growth in these cultures relative cultures 1 and 2 that remained rich. Conversely, at point A, the nutrient-poor medium in cultures 5 and 6 was replaced with rich medium, resulting in faster growth in these cultures relative cultures 7 and 8 that remained nutrient-poor. Cultures 1 to 8 were cultivated simultaneously on the same chip at 37°C. Each condition was demonstrated in at least three cultures. Bottom panels (a to d) show typical area maps of the cells in the growth chamber of microdialyser 1 at the corresponding points from which the cell surface density is determined. Scale bar, 50μm.

doi:10.1371/journal.pone.0136231.g002

ultimately lost to the environment. As the cell density increases, the autoinducer concentration reaches a threshold concentration and triggers a transcriptional response that results in increased expression of virulence determinants [33, 34], upregulation of biofilm formation [35–37] or entry into stationary phase [38, 39]—that is unattainable with low cell density. Large volume cultures require a proportionately large cell population to elicit quorum sensing

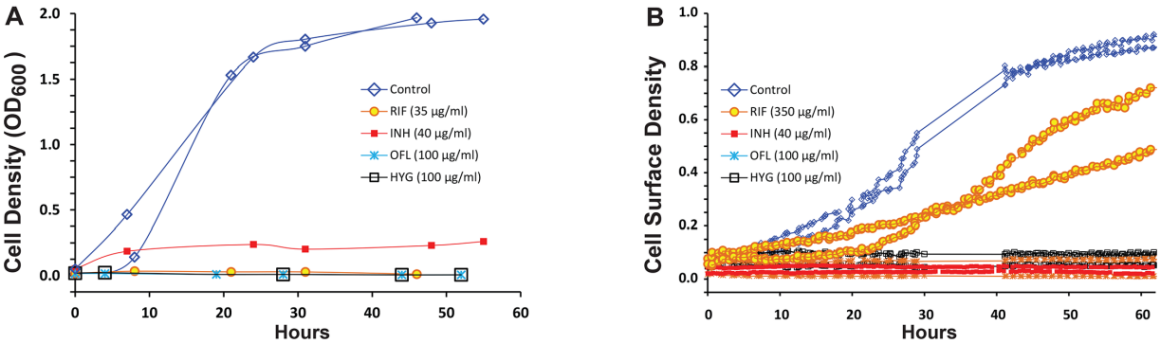

Fig 3. Drug susceptibility of *M. smegmatis* mc^{2}155 cells ON- and OFF-chip. (A) mc^{2}155 tissue culture flask growth curves illustrating the growth-inhibitory effect of rifampicin (35µg/ml), isoniazid (40µg/ml), ofloxacin (100 µg/ml) and hygromycin (100µg/ml). All measurements were performed in duplicate. **(B)** Microdialyser drug susceptibility of mc^{2}155 cells growing with rifampicin (350µg/ml), isoniazid (40µg/ml), ofloxacin (100 µg/ml) and hygromycin (100µg/ml) in 200 picoliter growth chambers. All the drugs except rifampicin had a strong growth-inhibitory effect at the concentrations indicated in the microdialyser. Over 10 control cultures performed exhibited positive growth. Hygromycin and ofloxacin inhibited growth in 5 distinct cultures per drug. Isoniazid inhibited growth in 8 of 11 cultures. Two of the isoniazid cultures had minimal growth and in one growth was more significant (S3 Fig). Rifampicin cultures had significant growth in 11 of 12 cultures (S4 Fig).

doi:10.1371/journal.pone.0136231.g003

behavior. However, in a sufficiently small growth environment, a few cells can elicit quorum sensing behavior more efficiently because the autoinducer molecules produced are kept in

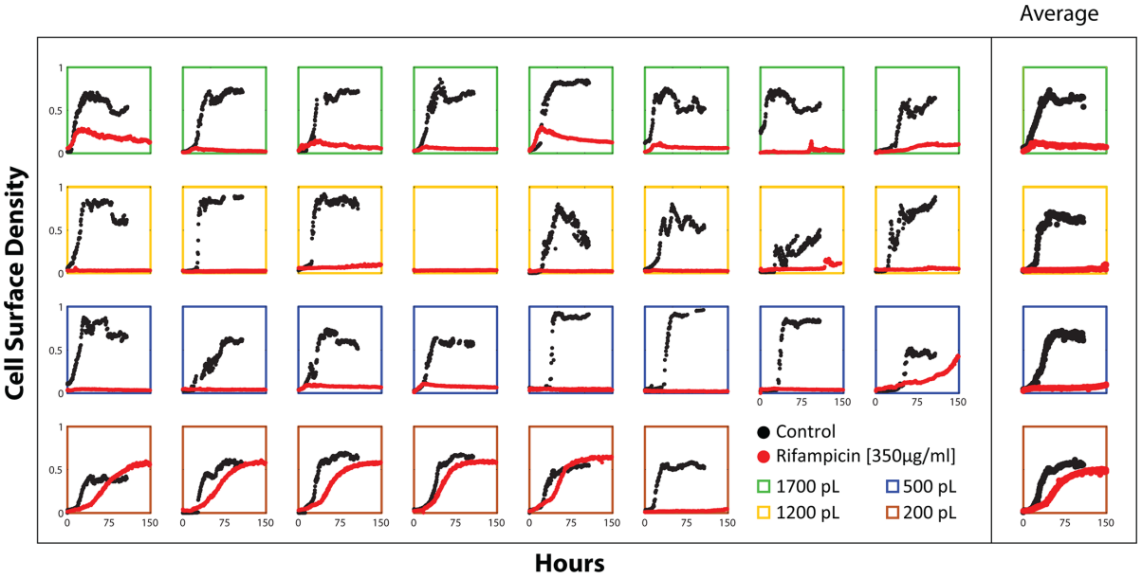

Fig 4. Growth dynamics of *M. smegmatis ΔftsEX* cells with or without rifampicin (350 µg/ml) across the various microdialyser growth chambers sizes: 1700pL (green boxes), 1200pL (yellow boxes), 500pL (blue boxes) and 200pL (brown boxes). The growth curves in the right-most column represent the average cell density of the individual reactors shown on the left. In drug-free medium, the cells exhibited positive growth across all the growth chamber volumes as indicated (black growth curves). With rifampicin, growth in five of six of the 200pL reactors was only slightly affected with the exception of one of the growth chambers in which the cells did not grow. Growth in the larger reactors (eight 1700pL, eight 1200pL and seven 500pL) was inhibited (red curves), except in one of the 500pL growth chambers. The cultures under each drug condition were cultivated simultaneously on the same chip at 37°C.

doi:10.1371/journal.pone.0136231.g004

close proximity by the boundaries of the confined growth compartment and can therefore accumulate faster [40–42]. In a pattern consistent with quorum sensing control, when the time interval between consecutive microdialysis steps was doubled to two hours, the larger microdialyser cultures became more tolerant to rifampicin in a volume-dependent fashion, whereby the fraction of cultures with positive growth increased as the culture volume decreased (Fig 5). Notably, an inevitable consequence of the slower dilution rate was a reduced cellular growth rate due to the proportionately less frequent infusion of fresh nutrients. Bacteria growing with slower growth rates may be more tolerant to rifampicin, and therefore these cells experiencing a slower dilution rate may have a higher frequency of recovery. We measured the bacterial growth rates in the various growth chamber sizes in drug-free medium and found them to be similar (S6 Fig). Therefore, whereas slower growth rate may be a probable cause of the higher recovery frequency at the slower dilution rate, it does not explain the differential drug tolerance in the various growth chamber sizes. This pattern of expression is consistent with quorum sensing and may allow us to further study this system in mycobacteria.

Studies show that microbial efflux pumps can confer epigenetic resistance to antibiotics by enabling bacterial cells to extrude the drug molecules intended to kill them [18, 43–46]. We explored efflux activity as a potential underlying mechanism for rifampicin tolerance in the 200pL using the efflux inhibitor approach, which is widely used to indicate efflux activity [18, 47–49]. *M. smegmatis ΔftsEX* cells were cultured with rifampicin in the presence of verapamil —a mycobacterial efflux inhibitor [50]. As per the efflux inhibitor approach, dramatically reduced growth of the cells in the presence of verapamil suggested that confinement-induced drug tolerance was mediated by efflux mechanisms (Fig 6).

The discrepancy in drug sensitivity between the small and large volume microdialyser cultures can be exploited to investigate the genetic markers underlying confinement-induced drug tolerance. As a proof of principle, we investigated MmpL11, a cell wall lipid transport protein that contributes to biofilm formation in *M. smegmatis* [51]. In drug-free 200pL cultures, an *M. smegmatis* mutant lacking *mmpL11* functionality grew in all 12 reactors (Fig 7). However, only 11 of 16 mutant cultures registered growth in rifampicin medium, notwithstanding that the growth rate was slower in these cultures. Loss of MmpL11 function reduced resistance to rifampicin in the 200pL cultures, suggesting that MmpL11 protein contributes to confinement-induced rifampicin tolerance. It should be noted that there is no difference in rifampicin MIC between the wild-type *M. smegmatis* and *mmpL11* mutant during typical axenic culture. While bacteria cultured in the microdialysers are not forming biofilms per se, these results suggest that similar changes in the mycobacterial cell wall lipid composition occur in the confined space of a micro reactor as in a biofilm that result in a drug-tolerant phenotype. In the absence of MmpL11, *M. smegmatis* is unable to establish this drug-resistant state.

Unlike bactericidal antibiotics, bacteriostatic drugs ultimately depend upon the immune system for sterilization, and are therefore poor treatment options where the immune system is compromised [52]. Distinguishing between bacteriostatic and bactericidal action of antimicrobial drugs can be cumbersome using conventional drug susceptibility testing but the microdialyser can rapidly resolve this distinction for antimicrobial agents. Using the microdialyser process, we substituted the rifampicin-containing medium with drug-free medium without otherwise perturbing the cells in the non-growing cultures. Upon withdrawal of rifampicin via microdialysis, growth resumed in all the larger reactors (Fig 8), suggesting that the growth-inhibitory effect of rifampicin was of the bacteriostatic kind. It is worth noting that some conventional studies have indicated that rifampicin is bactericidal to *M. smegmatis* cells at 32 μg/ml [30].

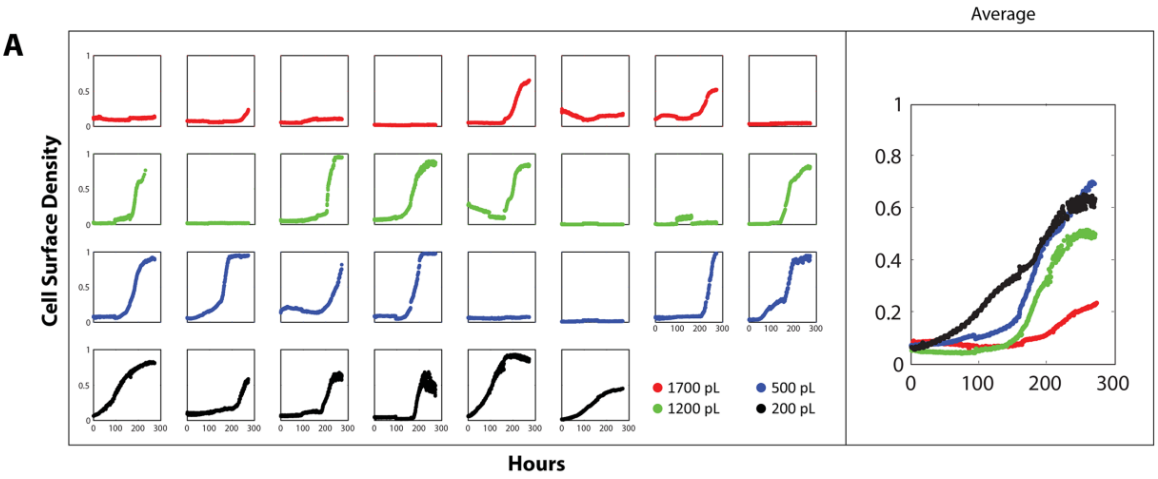

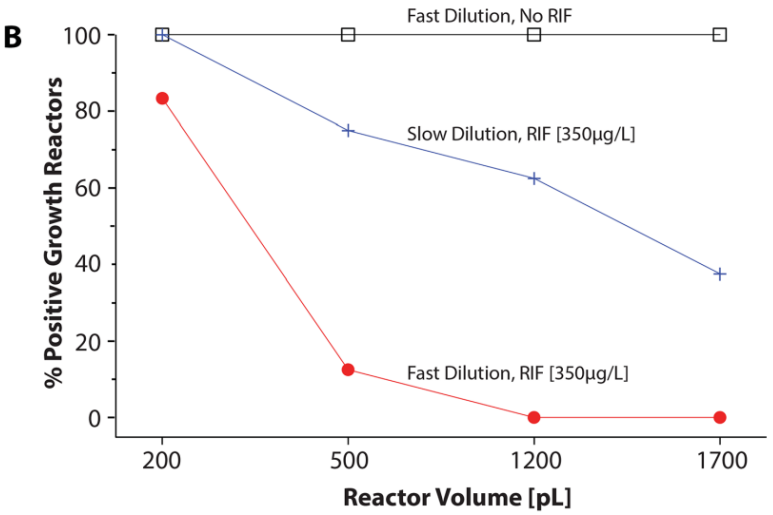

Fig 5. (A) Growth of *M. smegmatis ΔFtsEX* cells with rifampicin [350 µg/ml] with the time interval between consecutive microdialysis steps doubled to 2 hours—across the various microdialyser growth chambers sizes—1700pL (red curves), 1200pL (green), 500pL (blue) and 200pL (black). The growth curves on the right represent the average cell density of the individual reactors shown on the left. With the slower dilution rate, the cell populations in the larger reactors become more tolerant to rifampicin in accordance to the reactor volume: the fraction of reactors with growth decreases as the volume increases. All cultures were cultivated simultaneously on the same chip at 37°C. (B) The percentage of microdialyser cultures with positive growth at different dilution rates with rifampicin (350µg/ml) or in drug-free medium. At a dilution (microdialysis) interval of one hour, all drug-free cultures (black boxes) reactors registered positive growth independent of culture volume. Five of six 200pL cultures and among the larger cultures, only one of the eight 500pL cultures tolerated rifampicin (red circles). With the dilution interval doubled to two hours, the yield of the drug-containing cultures (blue crosses) increased albeit in a volume-dependent fashion, whereby the fraction of cultures with positive growth decreased as the culture volume increased. The cultures were cultivated at 37°C.

doi:10.1371/journal.pone.0136231.g005

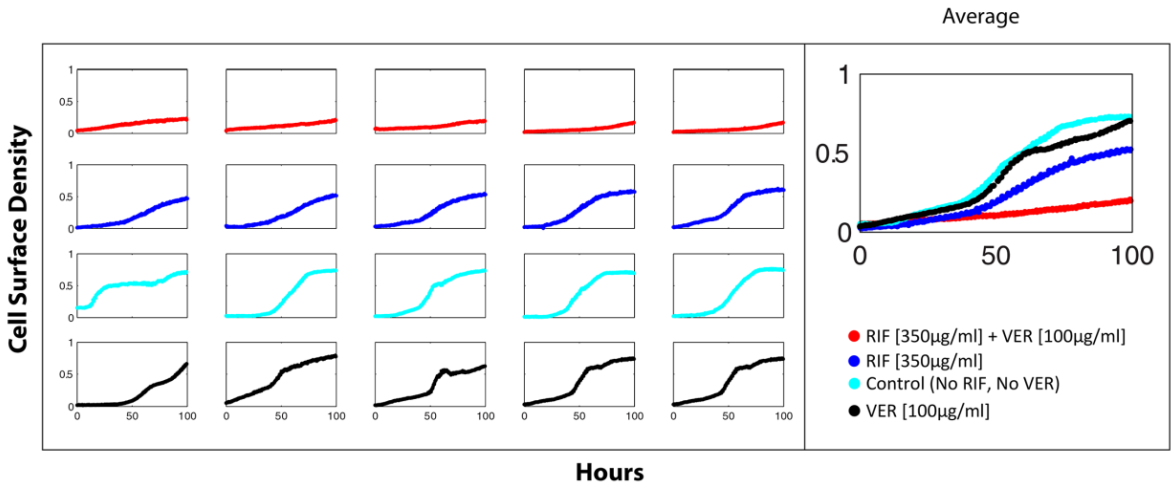

Fig 6. Efflux inhibition reduces drug tolerance. Effect of verapamil (100µg/ml) on 200pL ΔFtsEX cultures with or without rifampicin (350 µg/ml). The right-most growth curves represent the average cell density of the individual reactors shown in each row on the left. The control (cyan growth curves), rifampicin only (blue) and verapamil only (black) cultures registered positive growth. Rifampicin tolerance was dramatically reduced in cultures that also contained verapamil (red). All cultures were cultivated simultaneously on the same chip at 37°C.

doi:10.1371/journal.pone.0136231.g006

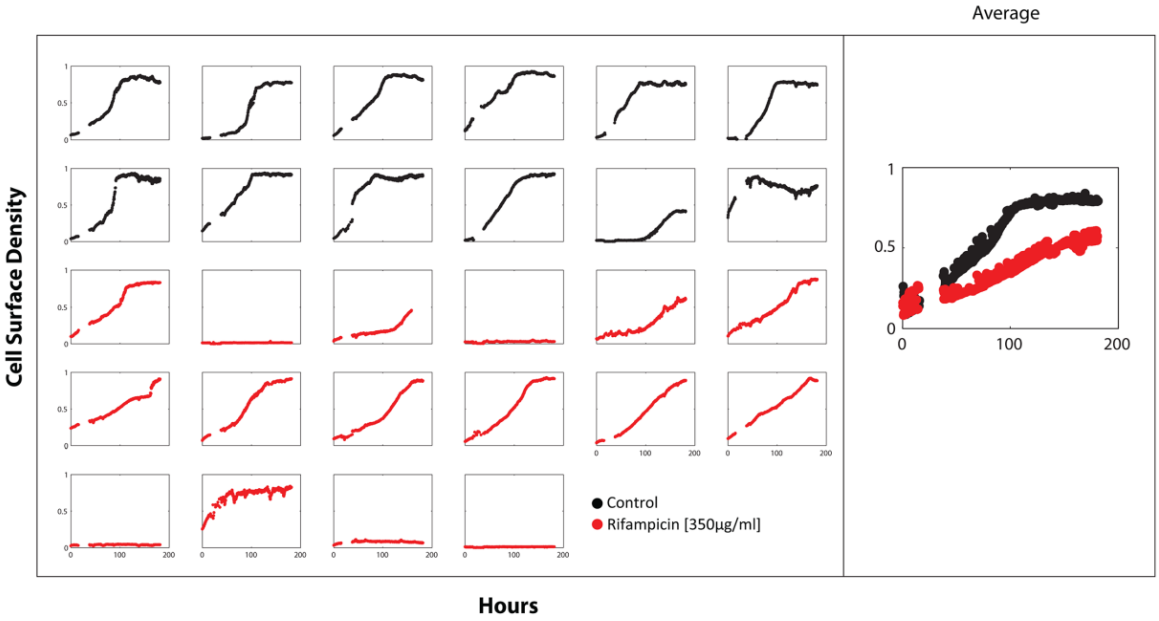

Fig 7. Loss of MmpL11 function reduced resistance to rifampicin in the 200pL cultures. Effect of rifampicin (350 µg/ml) on the growth of *M. smegmatis mmpL11* mutants in 200pL cultures. The growth curves in the right-most column represent the average cell density of the individual reactors shown on the left. All 12 (100%) mutant drug-free cultures grew (black growth curves). However, only 11 of 16 (69%) mutant cultures grew in rifampicin medium and growth in these cultures was generally slower. All cultures were cultivated simultaneously on the same chip at 37°C.

doi:10.1371/journal.pone.0136231.g007

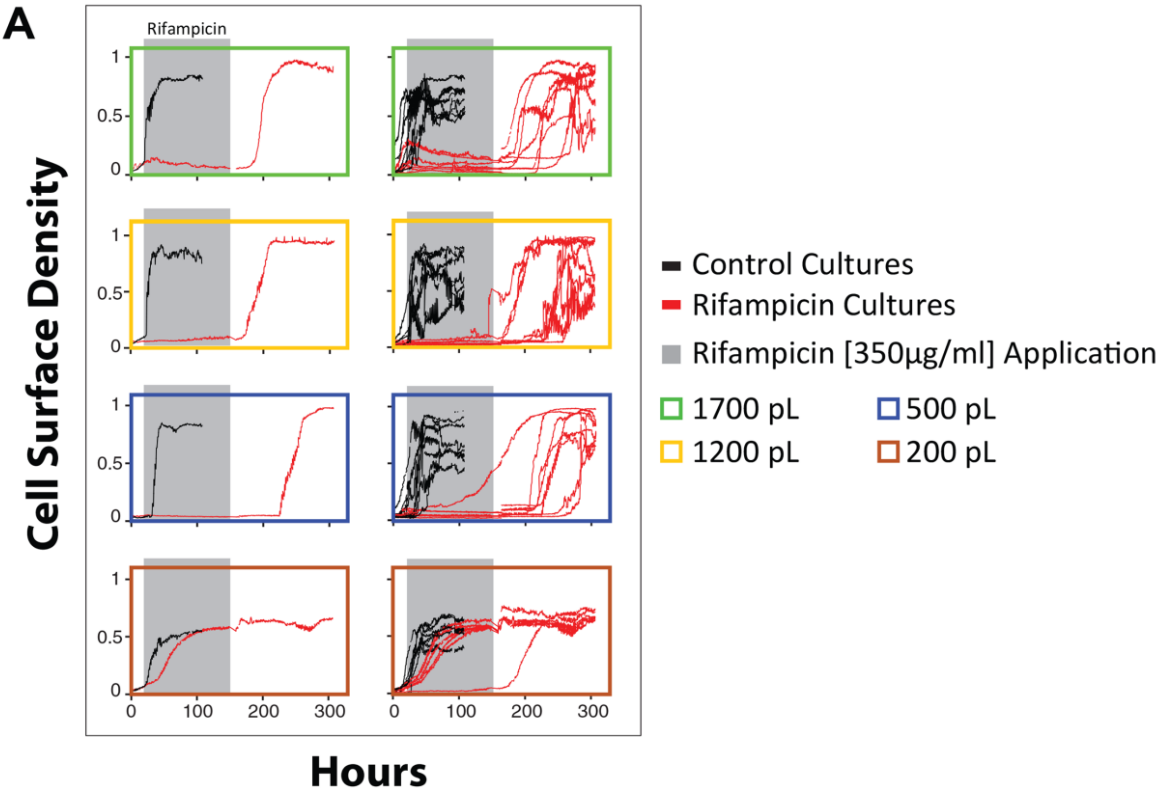
A
Rifampicin
Cell Surface Density
Hours
Control Cultures
Rifampicin Cultures
Rifampicin [350µg/ml] Application
1700 pL
500 pL
1200 pL
200 pL

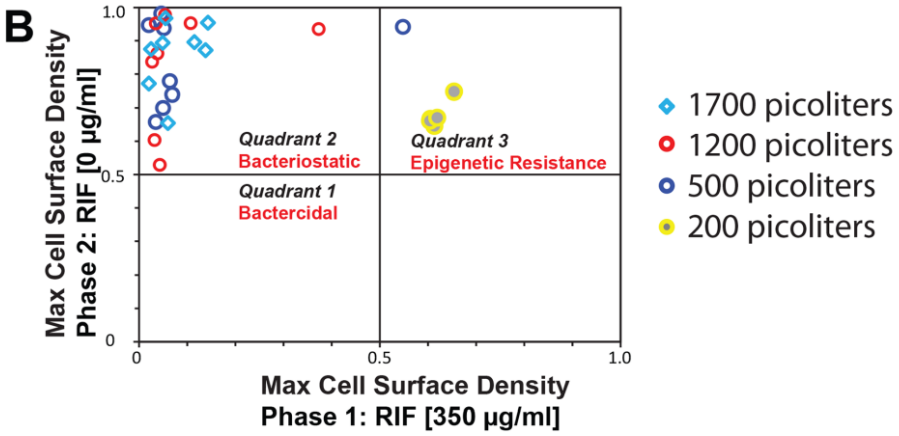
B
Max Cell Surface Density
Phase 2: RIF [0 µg/ml]
Max Cell Surface Density
Phase 1: RIF [350 µg/ml]
Quadrant 2
Bacteriostatic
Quadrant 3
Epigenetic Resistance
Quadrant 1
Bactercidal
1700 picoliters
1200 picoliters
500 picoliters
200 picoliters

Fig 8. (A) Use of the microdialyser system to resolve the bacteriostatic/bactericidal credentials of antimicrobial drugs. The graphs in the left column represent a typical growth curves for each growth chamber size and those in the right column represent a set of growth curves for the same growth chamber volume. The cultures represented by the red curves were first cultured in drug-free medium for 15 hours. Using the microdialysis process, at 15 hours, rifampicin (350 μg/ml) was introduced to these cultures and then withdrawn at 150 hours. Although microbial growth in the bigger volume reactors—seven 500, eight 1200 and eight 1700pL—was effectively suppressed when rifampicin was applied, cell growth resumed when the drug was withdrawn, suggesting that rifampicin was bacteriostatic under these conditions. The cells in one of the eight 500pL maintained slow growth in the presence of the drug. Microbial growth in five of six small (200pL) growth chambers was only slightly decreased by the drug and suppressed in one of the reactors in which the drug was bacteriostatic. Control cultures are depicted by black curves demonstrating consistently positive growth in drug-free medium across all growth chamber sizes. (B) A system for distinguishing the bacteriostatic/bactericidal credentials of antimicrobial drugs. The X-axis represents the cell density reached by ΔFtsEX cells in the reactors shown above (Fig 8A) after culturing for 150 hours in medium with rifampicin (350 μg/ml) during the first phase of culture. The Y-axis represents the new cell density attained in the same reactors after 150 additional hours of culturing in medium without rifampicin. Accordingly, data points in quadrants 1, 2 and 3 represent reactors in which the cells are dead, static or resistant respectively. In general *M. smegmatis* Δ*ftsEX* cells were resistant to rifampicin in the 200pL reactors and static in the rest.

doi:10.1371/journal.pone.0136231.g008

Conclusions

A physical cell culture system that mimics confinement of mycobacteria such as in a macrophage during infection enabled us to investigate confinement-induced drug tolerance in *M. smegmatis* cells. We uncovered an epigenetic rifampicin-resistance phenotype that was dependent on the size of the growth chamber: appearing when the mycobacteria were cultured in the small (200pL) growth chambers and disappearing in the bigger reactor volumes (500pL, 1200pL and 1700pL). The drug-tolerant phenotype was mediated in large part by efflux mechanisms, which were induced in confined growth environment. The confinement-induced drug tolerance observed in the microdialyser has similarities with the macrophage-induced tolerance that others have reported in intramacrophage mycobacterial species [18]. To the degree that confinement is a significant common factor for mycobacteria replicating in small microdialyser reactors or macrophages, macrophage-induced drug tolerance may be an effect of confined growth in addition to other macrophage specific mechanisms.

In vitro drug susceptibility tests performed using conventional cell culture systems, which are the basis for drug prescriptions, are notoriously poor predictors of treatment outcomes in human TB [53, 54]. Our results suggest that the volume difference between the in vitro and in vivo (intramacrophage) growth compartments for *M. tuberculosis*, together with its implications for epigenetic drug resistance, may be a contributor to the apparent incongruity between drug susceptibility tests and treatment outcomes. Indeed, unlike the mycobacteria freshly inoculated into a conventional culture vessel, intramacrophage mycobacteria, which comprise a significant portion of TB infection [16], experience a space-confined growth environment that our experiments suggest can induce drug tolerance. Confinement-induced drug tolerance in *M. tuberculosis* may contribute to persistence in tuberculosis patients, where drugs that are rapidly potent in vitro require prolonged administration to achieve comparable effects. The microdialyser may thus provide an appropriate paradigm for research on therapeutic interventions aimed at rapidly neutralizing the drug-tolerant mycobacteria that currently prolong treatment in human TB.

Supporting Information

S1 Fig. Design and operation of the microdialyser with multiple volume reactors. (A) Optical micrograph of the microdialyser chip showing a single module. Scale bar, 0.5mm. The module features 8 medium input ports, 5 cell input ports, 10 output ports and 30 individually addressable microdialyser culture units: six 200-, eight 500-, eight 1200 and eight 1700-picoliter cell culture chambers. The blue rectangular box indicates the region depicted in B, C and D. **(B)** Optical micrograph showing three microdialysers in a row to illustrate the main aspects of the microdialysis scheme. Elements such as the growth chamber, conditioning chamber and

link valves are labelled (see Fig 1). With the link valve closed, the conditioning chamber of the middle microdialyser unit is filled with blue dye (representing fresh medium). Scale bar, 0.3mm. **(C)** Once the link valve is open, diffusive exchange between the growth and conditioning chambers occurs. **(D)** After a series of (typically six) microdialysis steps, the growth chamber fluid is completely replaced with the fluid introduced via the conditioning chamber.
(PNG)

S2 Fig. *E. coli* cells are susceptible to rifampicin in 200pL microdialyser reactors. Growth of *E. coli* Top10 F' cells in 200pL microdialyser reactors with switching between medium with and without rifampicin. The red curves represent microdialyser *E. coli* cultures that were initially drug-free (0 to 110hrs). Addition of rifampicin (350 μg/ml) at 110hrs (point A) resulted in a dramatic decrease in the cell population. The blue curves represent *E. coli* cultures that initially contained 350 μg/ml of rifampicin (0 to 110hrs). Removal of the drug at point A led to growth recovery in 2 of 12 cultures. All cultures were cultivated on the same chip in LB medium at 37°C.
(EPS)

S3 Fig. Isoniazid susceptibility of *M. smegmatis* mc^{2}155 cells in microdialysor reactors. Microdialyser drug susceptibility of mc^{2}155 cells growing with isoniazid (40μg/ml) in 200pL growth chambers. Isoniazid inhibited growth in 8 of 11 cultures incubated in two chips. Two of the isoniazid cultures had minimal growth (reaching a cell surface density of 0.2) and in one growth was more significant (reaching a cell surface density of 0.4).
(EPS)

S4 Fig. Growth dynamics of *M. smegmatis* mc^{2}155 cells with or without rifampicin (350 μg/ml) across the various microdialyser growth chambers sizes. In drug-free medium (black curves), the cells exhibited positive growth across all the growth chamber volumes as indicated—1700pL, growth in 8 of 8 cultures; 1200pL, growth in 8 of 8 cultures; 500pL, growth in 7 of 7 cultures; and 200pL, growth in 6 of 6 cultures. With rifampicin (red curves), growth in the larger reactors was inhibited—1700pL, growth in 0 of 8 cultures; 1200pL, growth in 0 of 8 cultures; and 500pL, growth in 0 of 8 cultures. In the 200pL cultures with rifampicin, there was significant growth in 11 of 12 growth chambers.
(EPS)

S5 Fig. Functional illustration of diffusive exchange in the multi-volume microdialyser showing the dye concentration in the various growth chamber volumes and the conditioning chamber. The formulation in the conditioning chambers is cycled between DYE (cycles 2–7 and 13–19) and WATER (cycles 1; 8–12). The dye concentration in the various growth chambers is determined by the formulation in the conditioning chamber. The chamber-to-chamber variations in dye concentration are attributable to minor height differences in the growth chambers.
(EPS)

S6 Fig. Exponential growth rates for *M. smegmatis ΔFtsEX* cells growing in various growth chamber sizes in drug-free medium. Various growth rates were measured for bacteria growing in the drug-free microdialyser cultures depicted in Fig 4, however there was no significant difference in growth rates across the various growth chamber sizes.
(EPS)

Acknowledgments

We thank W. Jacobs for *M. smegmatis* mc^2155 cells, E. Rubin and M. Marakalala for *M. smegmatis* Δ*ftsEX* cells. We also thank D. Mckearin, D. Irvine, B. Bloom, A. Pym, V. Mizrahi, J. Green, E. Barlow, J. Rogich and E. Aiken for helpful discussions.

Author Contributions

Conceived and designed the experiments: BL FB. Performed the experiments: BL FB. Analyzed the data: BL FB. Contributed reagents/materials/analysis tools: BL GP FB. Wrote the paper: BL GP FB.

References

1. Global tuberculosis report 2014. Geneva (Switzerland): World Health Organization, 2014 Contract No.: WHO/HTM/TB/2014.08.
2. Dye C, Lonnroth K, Jaramillo E, Williams BG, Raviglione M. Trends in tuberculosis incidence and their determinants in 134 countries. Bulletin of the World Health Organization. 2009; 87(9):683–91. Epub 2009/09/29. PMID: 19784448; PubMed Central PMCID: PMCPMC2739916.
3. Matteelli A, Roggi A, Carvalho AC. Extensively drug-resistant tuberculosis: epidemiology and management. Clinical epidemiology. 2014; 6:111. doi: 10.2147/CLEP.S35839 PMID: 24729727
4. Günther G. Multidrug-resistant and extensively drug-resistant tuberculosis: a review of current concepts and future challenges. Clinical Medicine. 2014; 14(3):279–85. doi: 10.7861/clinmedicine.14-3-279 PMID: 24889573
5. Ma Z, Lienhardt C, McIlleron H, Nunn AJ, Wang X. Global tuberculosis drug development pipeline: the need and the reality. The Lancet. 2010; 375(9731):2100–9.
6. Gospodarevskaya E, Tulloch O, Bunga C, Ferdous S, Jonas A, Islam S, et al. Patient costs during tuberculosis treatment in Bangladesh and Tanzania: the potential of shorter regimens. The International Journal of Tuberculosis and Lung Disease. 2014; 18(7):810–7. doi: 10.5588/ijtld.13.0391 PMID: 24902557
7. Mitchison D, Davies G. The chemotherapy of tuberculosis: past, present and future. The international journal of tuberculosis and lung disease: the official journal of the International Union against Tuberculosis and Lung Disease. 2012; 16(6):724–32. Epub 2012/05/23. doi: 10.5588/ijtld.12.0083 PMID: 22613684; PubMed Central PMCID: PMCPMC3736084.
8. Jindani A, Dore CJ, Mitchison DA. Bactericidal and sterilizing activities of antituberculosis drugs during the first 14 days. American journal of respiratory and critical care medicine. 2003; 167(10):1348–54. Epub 2003/01/10. doi: 10.1164/rccm.200210-1125OC PMID: 12519740.
9. Gomez JE, McKinney JD. M. tuberculosis persistence, latency, and drug tolerance. Tuberculosis (Edinburgh, Scotland). 2004; 84(1–2):29–44. Epub 2003/12/13. PMID: 14670344.
10. Hingley-Wilson SM, Sambandamurthy VK, Jacobs WR Jr. Survival perspectives from the world's most successful pathogen, Mycobacterium tuberculosis. Nature immunology. 2003; 4(10):949–55. Epub 2003/09/30. doi: 10.1038/ni981 PMID: 14515128.
11. de Steenwinkel JE, de Knegt GJ, Marian T, van Belkum A, Verbrugh HA, Kremer K, et al. Time–kill kinetics of anti-tuberculosis drugs, and emergence of resistance, in relation to metabolic activity of Mycobacterium tuberculosis. Journal of antimicrobial chemotherapy. 2010:dkq374.
12. Connolly LE, Edelstein PH, Ramakrishnan L. Why is long-term therapy required to cure tuberculosis? PLoS medicine. 2007; 4(3):e120. Epub 2007/03/29. doi: 10.1371/journal.pmed.0040120 PMID: 17388672; PubMed Central PMCID: PMCPMC1831743.
13. Aldridge BB, Fernandez-Suarez M, Heller D, Ambravaneswaran V, Irimia D, Toner M, et al. Asymmetry and aging of mycobacterial cells lead to variable growth and antibiotic susceptibility. Science (New York, NY). 2012; 335(6064):100–4. Epub 2011/12/17. doi: 10.1126/science.1216166 PMID: 22174129; PubMed Central PMCID: PMCPMC3397429.
14. Wakamoto Y, Dhar N, Chait R, Schneider K, Signorino-Gelo F, Leibler S, et al. Dynamic persistence of antibiotic-stressed mycobacteria. Science (New York, NY). 2013; 339(6115):91–5. Epub 2013/01/05. doi: 10.1126/science.1229858 PMID: 23288538.
15. Golchin SA, Stratford J, Curry RJ, McFadden J. A microfluidic system for long-term time-lapse microscopy studies of mycobacteria. Tuberculosis (Edinburgh, Scotland). 2012; 92(6):489–96. Epub 2012/09/08. doi: 10.1016/j.tube.2012.06.006 PMID: 22954584.

16. Viveiros M, Martins M, Couto I, Rodrigues L, Machado D, Portugal I, et al. Molecular tools for rapid identification and novel effective therapy against MDRTB/XDRTB infections. Expert review of anti-infective therapy. 2010.
17. Schlesinger L. Lung Macrophages and Dendritic Cells in Health and Disease. 1997.
18. Adams KN, Takaki K, Connolly LE, Wiedenhoft H, Winglee K, Humbert O, et al. Drug tolerance in replicating mycobacteria mediated by a macrophage-induced efflux mechanism. Cell. 2011; 145(1):39–53. Epub 2011/03/08. doi: 10.1016/j.cell.2011.02.022 PMID: 21376383; PubMed Central PMCID: PMCPMC3117281.
19. Hartkoorn RC, Chandler B, Owen A, Ward SA, Bertel Squire S, Back DJ, et al. Differential drug susceptibility of intracellular and extracellular tuberculosis, and the impact of P-glycoprotein. Tuberculosis (Edinburgh, Scotland). 2007; 87(3):248–55. Epub 2007/01/30. doi: 10.1016/j.tube.2006.12.001 PMID: 17258938.
20. Carnes EC, Lopez DM, Donegan NP, Cheung A, Gresham H, Timmins GS, et al. Confinement-induced quorum sensing of individual Staphylococcus aureus bacteria. Nature chemical biology. 2010; 6(1):41–5. Epub 2009/11/26. doi: 10.1038/nchembio.264 PMID: 19935660.
21. Horswill AR, Stoodley P, Stewart PS, Parsek MR. The effect of the chemical, biological, and physical environment on quorum sensing in structured microbial communities. Analytical and bioanalytical chemistry. 2007; 387(2):371–80. PMID: 17047948
22. Connell JL, Wessel AK, Parsek MR, Ellington AD, Whiteley M, Shear JB. Probing prokaryotic social behaviors with bacterial "lobster traps". MBio. 2010; 1(4):e00202–10. doi: 10.1128/mBio.00202-10 PMID: 21060734
23. Chaturvedi V, Dwivedi N, Tripathi RP, Sinha S. Evaluation of Mycobacterium smegmatis as a possible surrogate screen for selecting molecules active against multi-drug resistant Mycobacterium tuberculosis. The Journal of general and applied microbiology. 2007; 53(6):333–7. Epub 2008/01/12. PMID: 18187888.
24. Krombach F, Munzing S, Allmeling AM, Gerlach JT, Behr J, Dorger M. Cell size of alveolar macrophages: an interspecies comparison. Environmental health perspectives. 1997; 105 Suppl 5:1261–3. Epub 1997/12/24. PMID: 9400735; PubMed Central PMCID: PMCPMC1470168.
25. Thorsen T, Maerkl SJ, Quake SR. Microfluidic large-scale integration. Science (New York, NY). 2002; 298(5593):580–4.
26. Mavrici D, Marakalala MJ, Holton JM, Prigozhin DM, Gee CL, Zhang YJ, et al. Mycobacterium tuberculosis FtsX extracellular domain activates the peptidoglycan hydrolase, RipC. Proceedings of the National Academy of Sciences of the United States of America. 2014; 111(22):8037–42. Epub 2014/05/21. doi: 10.1073/pnas.1321812111 PMID: 24843173; PubMed Central PMCID: PMCPMC4050617.
27. Purdy GE, Niederweis M, Russell DG. Decreased outer membrane permeability protects mycobacteria from killing by ubiquitin-derived peptides. Molecular microbiology. 2009; 73(5):844–57. doi: 10.1111/j.1365-2958.2009.06801.x PMID: 19682257
28. Vivino M. NIH Image Engineering (Scientific and image processing technical notes related to NIH Image) [cited 2015 July 11]. Available: http://rsb.info.nih.gov/nih-image/more-docs/Engineering/ImgEngr.html.
29. Li X, Tao J, Han J, Hu X, Chen Y, Deng H, et al. The gain of hydrogen peroxide resistance benefits growth fitness in mycobacteria under stress. Protein & cell. 2014; 5(3):182.
30. Barbassa L, Mamizuka EM, Carmona-Ribeiro AM. Supramolecular assemblies of rifampicin and cationic bilayers: preparation, characterization and micobactericidal activity. BMC biotechnology. 2011; 11 (1):40.
31. Waters CM, Bassler BL. Quorum sensing: cell-to-cell communication in bacteria. Annu Rev Cell Dev Biol. 2005; 21:319–46. PMID: 16212498
32. Miller MB, Bassler BL. Quorum sensing in bacteria. Annual Reviews in Microbiology. 2001; 55(1):165–99.
33. Hentzer M, Wu H, Andersen JB, Riedel K, Rasmussen TB, Bagge N, et al. Attenuation of Pseudomonas aeruginosa virulence by quorum sensing inhibitors. The EMBO journal. 2003; 22(15):3803–15. PMID: 12881415
34. Zhu J, Miller MB, Vance RE, Dziejman M, Bassler BL, Mekalanos JJ. Quorum-sensing regulators control virulence gene expression in Vibrio cholerae. Proceedings of the National Academy of Sciences. 2002; 99(5):3129–34.
35. Hammer BK, Bassler BL. Quorum sensing controls biofilm formation in Vibrio cholerae. Molecular microbiology. 2003; 50(1):101–4. PMID: 14507367

36. De Kievit TR, Gillis R, Marx S, Brown C, Iglewski BH. Quorum-sensing genes in Pseudomonas aeruginosa biofilms: their role and expression patterns. Applied and environmental microbiology. 2001; 67 (4):1865–73. PMID: 11282644

37. Kong K-F, Vuong C, Otto M. *Staphylococcus* quorum sensing in biofilm formation and infection. International Journal of Medical Microbiology. 2006; 296(2):133–9.

38. Lazazzera BA. Quorum sensing and starvation: signals for entry into stationary phase. Current opinion in microbiology. 2000; 3(2):177–82. PMID: 10744996

39. Ren D, Bedzyk LA, Rick WY, Thomas SM, Wood TK. Stationary-phase quorum-sensing signals affect autoinducer-2 and gene expression in Escherichia coli. Applied and environmental microbiology. 2004; 70(4):2038–43. PMID: 15066794

40. Redfield RJ. Is quorum sensing a side effect of diffusion sensing? Trends in microbiology. 2002; 10 (8):365–70. PMID: 12160634

41. Hense BA, Kuttler C, Muller J, Rothballer M, Hartmann A, Kreft JU. Does efficiency sensing unify diffusion and quorum sensing? Nature reviews Microbiology. 2007; 5(3):230–9. Epub 2007/02/17. doi: 10.1038/nrmicro1600 PMID: 17304251.

42. Boedicker JQ, Vincent ME, Ismagilov RF. Microfluidic confinement of single cells of bacteria in small volumes initiates high-density behavior of quorum sensing and growth and reveals its variability. Angewandte Chemie (International ed in English). 2009; 48(32):5908–11. Epub 2009/07/01. doi: 10.1002/anie.200901550 PMID: 19565587; PubMed Central PMCID: PMCPMC2748941.

43. De Rossi E, Ainsa JA, Riccardi G. Role of mycobacterial efflux transporters in drug resistance: an unresolved question. FEMS microbiology reviews. 2006; 30(1):36–52. Epub 2006/01/28. doi: 10.1111/j.1574-6976.2005.00002.x PMID: 16438679.

44. De Rossi E, Arrigo P, Bellinzoni M, Silva PA, Martin C, Ainsa JA, et al. The multidrug transporters belonging to major facilitator superfamily in Mycobacterium tuberculosis. Molecular medicine (Cambridge, Mass). 2002; 8(11):714–24. Epub 2003/01/10. PMID: 12520088; PubMed Central PMCID: PMCPmc2039957.

45. Louw GE, Warren RM, Gey van Pittius NC, Leon R, Jimenez A, Hernandez-Pando R, et al. Rifampicin reduces susceptibility to ofloxacin in rifampicin-resistant Mycobacterium tuberculosis through efflux. American journal of respiratory and critical care medicine. 2011; 184(2):269–76. Epub 2011/04/23. doi: 10.1164/rccm.201011-1924OC PMID: 21512166; PubMed Central PMCID: PMCPmc3698754.

46. Louw GE, Warren RM, Gey van Pittius NC, McEvoy CR, Van Helden PD, Victor TC. A balancing act: efflux/influx in mycobacterial drug resistance. Antimicrobial agents and chemotherapy. 2009; 53 (8):3181–9. Epub 2009/05/20. doi: 10.1128/aac.01577-08 PMID: 19451293; PubMed Central PMCID: PMCPmc2715638.

47. Adams KN, Szumowski JD, Ramakrishnan L. Verapamil, and its metabolite norverapamil, inhibit macrophage-induced, bacterial efflux pump-mediated tolerance to multiple anti-tubercular drugs. Journal of Infectious Diseases. 2014; 210(3):456–66. doi: 10.1093/infdis/jiu095 PMID: 24532601

48. Balganesh M, Dinesh N, Sharma S, Kuruppath S, Nair AV, Sharma U. Efflux pumps of Mycobacterium tuberculosis play a significant role in antituberculosis activity of potential drug candidates. Antimicrobial agents and chemotherapy. 2012; 56(5):2643–51. doi: 10.1128/AAC.06003-11 PMID: 22314527

49. Gupta S, Cohen KA, Winglee K, Maiga M, Diarra B, Bishai WR. Efflux inhibition with verapamil potentiates bedaquiline in Mycobacterium tuberculosis. Antimicrobial agents and chemotherapy. 2014; 58 (1):574–6. doi: 10.1128/AAC.01462-13 PMID: 24126586

50. Li X-Z, Nikaido H. Efflux-mediated drug resistance in bacteria. Drugs. 2009; 69(12):1555–623. doi: 10.2165/11317030-000000000-00000 PMID: 19678712

51. Pacheco SA, Hsu F-F, Powers KM, Purdy GE. MmpL11 protein transports mycolic acid-containing lipids to the mycobacterial cell wall and contributes to biofilm formation in Mycobacterium smegmatis. Journal of Biological Chemistry. 2013; 288(33):24213–22. doi: 10.1074/jbc.M113.473371 PMID: 23836904

52. Stratton CW. Dead bugs don't mutate: susceptibility issues in the emergence of bacterial resistance. Emerging infectious diseases. 2003; 9(1):10–6. Epub 2003/01/21. doi: 10.3201/eid0901.020172 PMID: 12533275; PubMed Central PMCID: PMCPMC2873758.

53. Heginbothom ML. The relationship between the in vitro drug susceptibility of opportunist mycobacteria and their in vivo response to treatment. The international journal of tuberculosis and lung disease: the official journal of the International Union against Tuberculosis and Lung Disease. 2001; 5(6):539–45. Epub 2001/06/21. PMID: 11409581.

54. Bottger EC. The ins and outs of Mycobacterium tuberculosis drug susceptibility testing. Clinical microbiology and infection: the official publication of the European Society of Clinical Microbiology and Infectious Diseases. 2011; 17(8):1128–34. Epub 2011/06/03. doi: 10.1111/j.1469-0691.2011.03551.x PMID: 21631641.

Supplementary Material

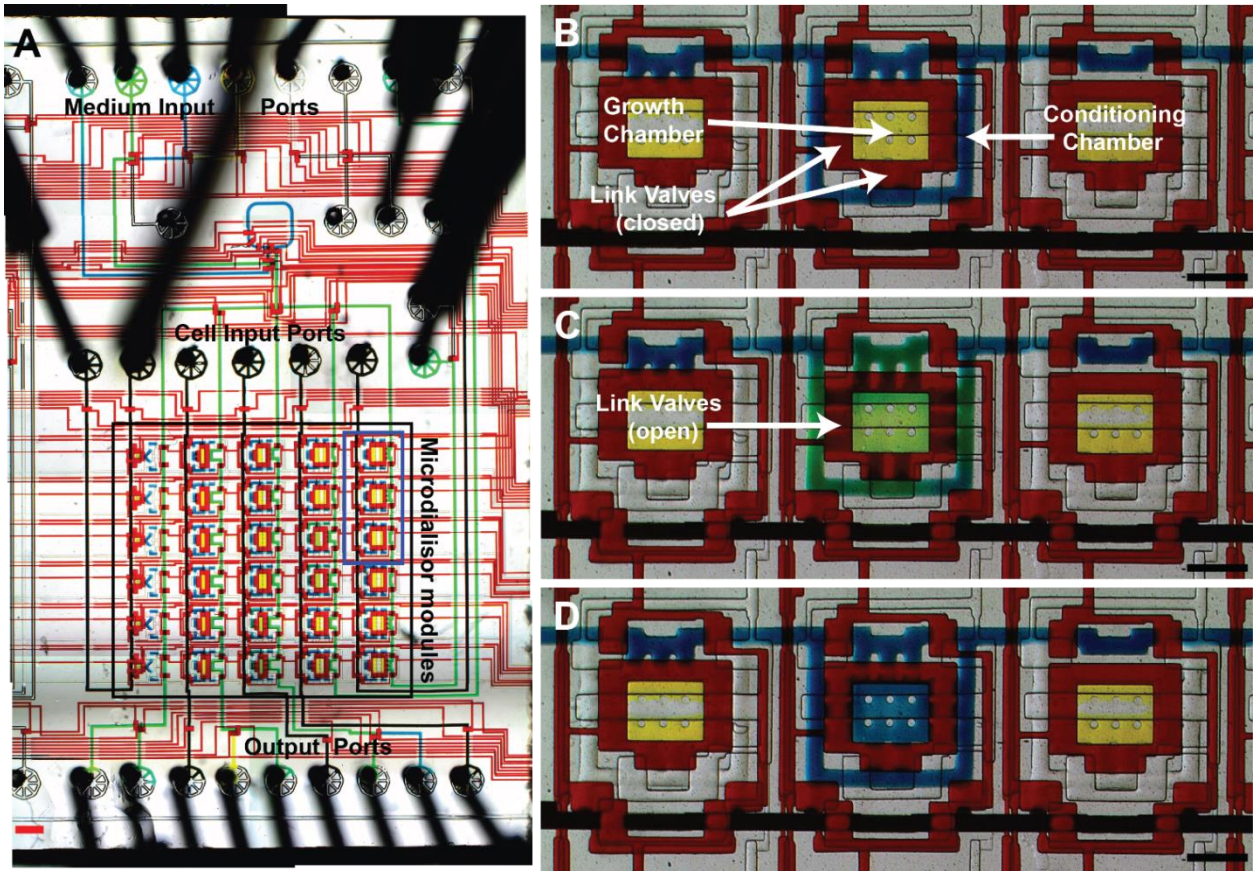

S1 Fig. Design and operation of the microdialysor with multiple volume reactors. (A) Optical micrograph of the microdialyser chip showing a single module. Scale bar, 0.5mm. The module features 8 medium input ports, 5 cell input ports, 15 output ports and 30 individually addressable microdialyser culture units: six 200-, eight 500-, eight 1200 and eight 1700-picoliter cell culture chambers. The blue rectangular box indicates the region depicted in B, C and D. **(B)** Optical micrograph showing three microdialysers in a row to illustrate the main aspects of the microdialysis scheme. Elements such as the growth chamber, conditioning chamber and link valves are labelled. With the link valve closed, the conditioning chamber of the middle microdialyser unit is filled with blue dye (representing fresh medium). Scale bar, 0.3mm. **(C)** Once the link valve is open, diffusive exchange between the growth and conditioning chambers occurs. **(D)** After a series of (typically six) microdialysis steps, the growth chamber fluid is completely replaced with the fluid introduced via the conditioning chamber.

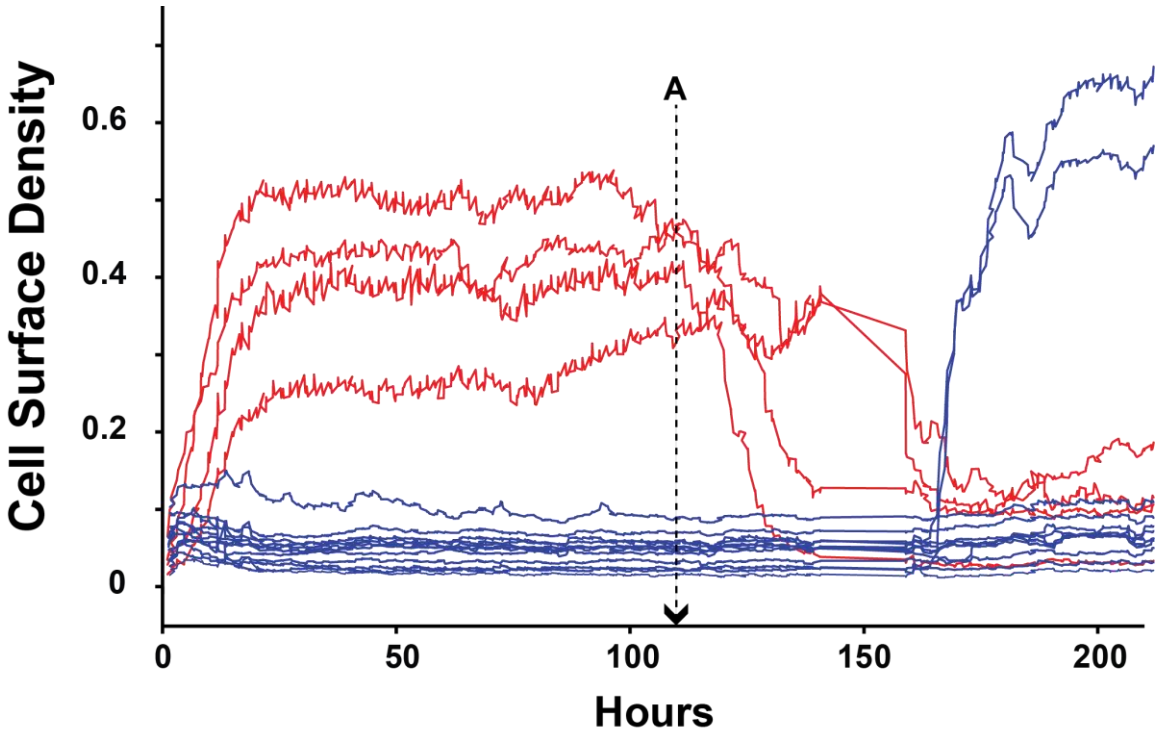

S2 Fig. *E. coli* cells are susceptible to rifampicin in 200pL microdialysor reactors. Growth of *E. coli* Top10 F' cells in 200 pL microdialyser reactors with switching between medium with and without rifampicin. The red curves represent microdialyser *E. coli* cultures that were initially drug-free (0 to 110hrs). Addition of rifampicin (350 µg/ml) at 110hrs (point **A**) resulted in a dramatic decrease in the cell population. The blue curves represent *E. coli* cultures that initially contained 350 µg/ml of rifampicin (0 to 110hrs). Removal of the drug at point A led to growth recovery in 2 of 12 cultures. All cultures were cultivated on the same chip in LB medium at 37°C.

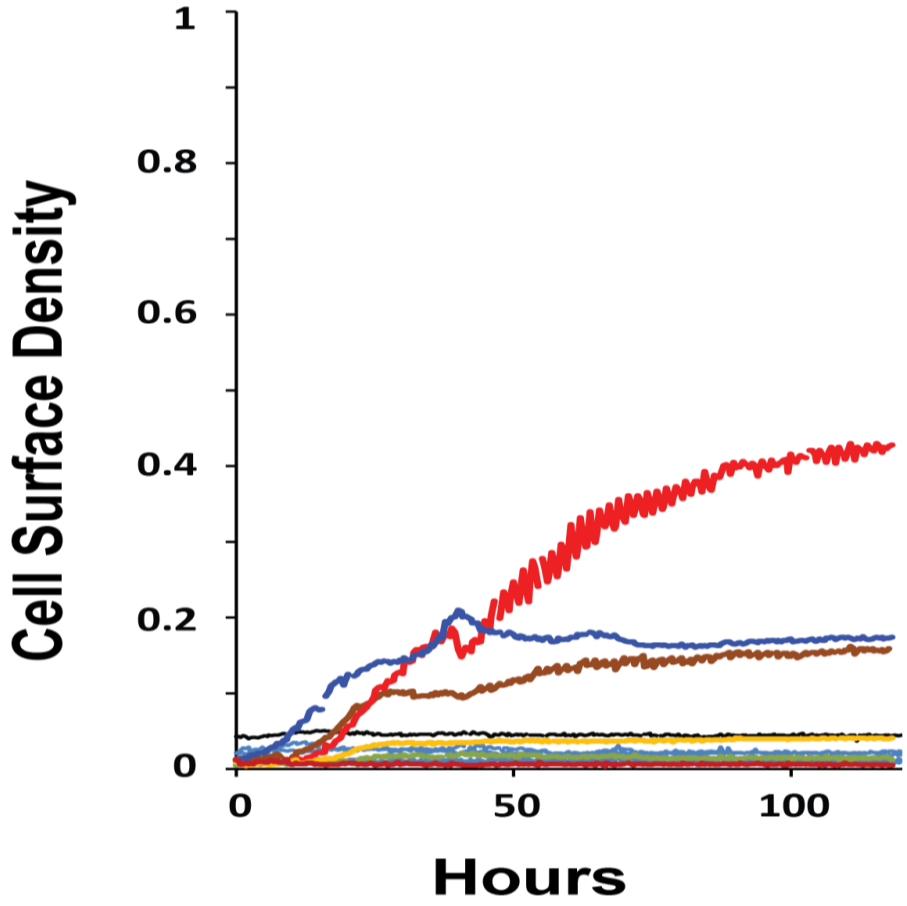

S3 Fig. Isoniazid susceptibility of *M. smegmatis* mc^{2}155 cells in microdialyser reactors. Microdialyser drug susceptibility of mc^{2}155 cells growing with isoniazid (40 ug/ml) in 200 pL growth chambers. Isoniazid inhibited growth in 8 of 11 cultures incubated in two chips. Two of the isoniazid cultures had minimal growth (reaching a cell surface density of 0.2) and in one growth was more significant (reaching a cell surface density of 0.4)

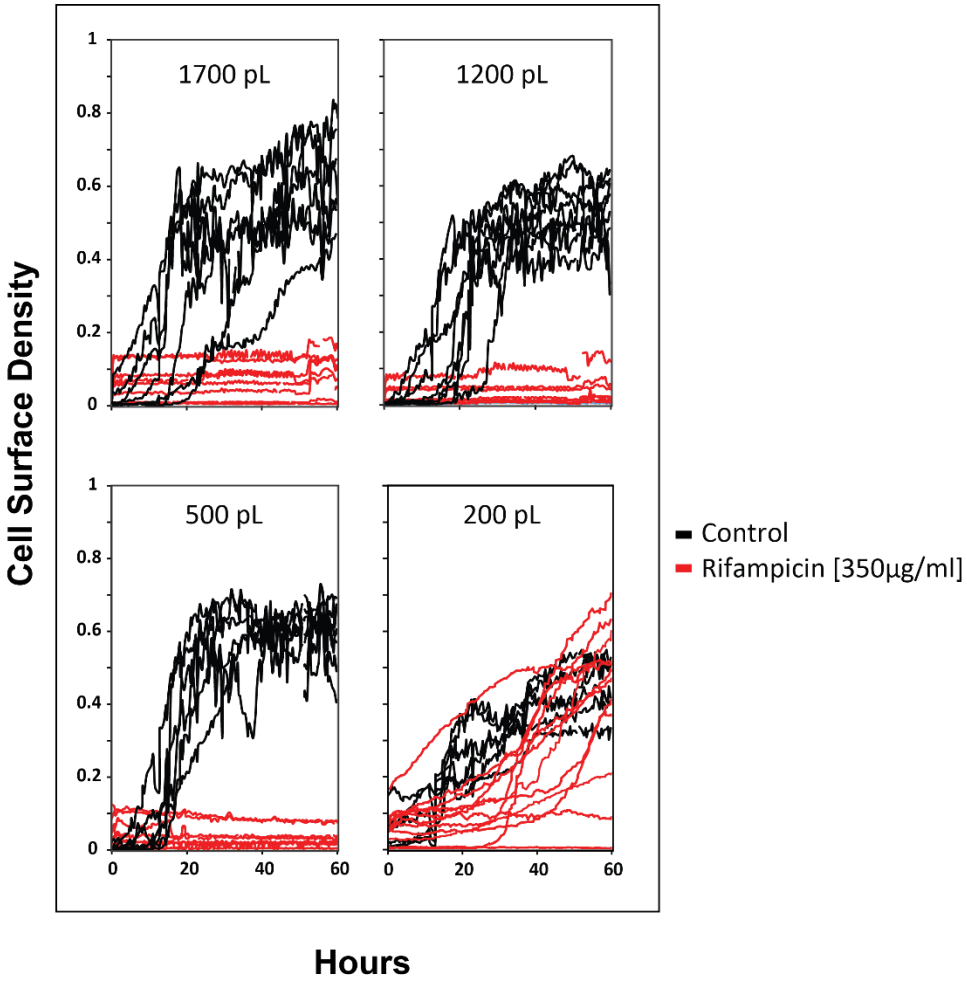

S4 Fig. Growth dynamics of *M. smegmatis* mc^{2}155 cells with or without rifampicin (350 ug/ml) across the various microdialyser growth chambers sizes. In drug-free medium (black curves), the cells exhibited positive growth across all the growth chamber volumes as indicated—1700 pL, growth in 8 of 8 cultures; 1200 pL, growth in 8 of 8 cultures; 500 pl, growth in 7 of 7 cultures; and 200 pL, growth in 6 of 6 cultures. With rifampicin (red curves), growth in larger reactors was inhibited—1700 pL, growth in 0 of 8 cultures; 1200 pL, growth in 0 of 8 cultures; and 500 pL, growth in 0 of 8 cultures. In the 200 pL cultures with rifampicin, there was significant growth in 11 of 12 growth chambers.

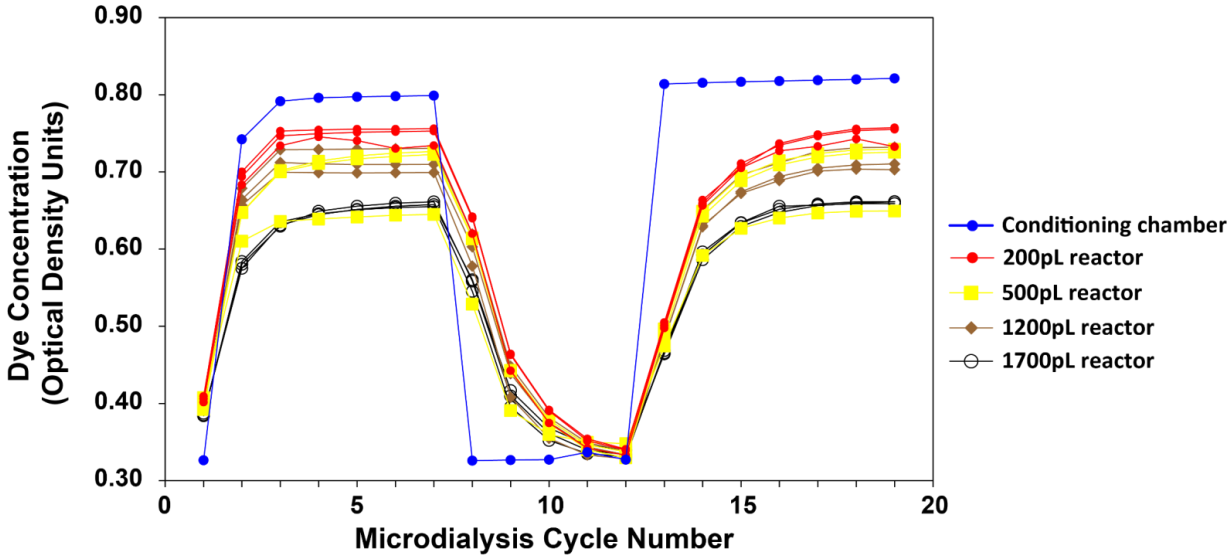

S5 Fig. Functional illustration of diffusive exchange in the multi-volume microdialyser showing the dye concentration in the various growth chamber volumes and the conditioning chamber. The formulation in the conditioning chambers is cycled between DYE (cycles 2-7 and 13-19) and WATER (cycles 1; 8-12). The dye concentration in the various growth chambers is determined by the formulation in the conditioning chamber. The chamber-to-chamber variations in dye concentration are attributable to minor height differences in the growth chambers.

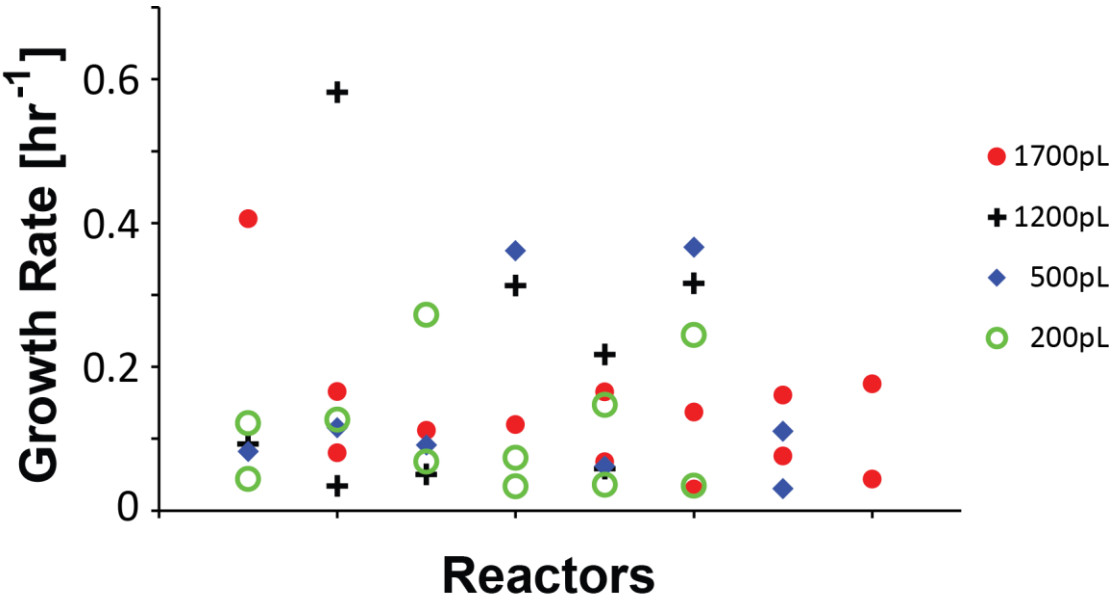

S6 Fig. Exponential growth rates for *M. smegmatis* ΔFtsEX cells growing in various growth chamber sizes in drug-free medium. Various growth rates were measured for bacteria growing in the drug-free microdialyser cultures depicted in Fig 4, however there was no significant difference in growth rates across the various growth chamber sizes.

Supporting Information

The Fluidic Design and Fabrication

The chip schematic design was developed on AutoCAD software. The microdiayser chip was fabricated out of the silicone elastomer polyethylsiloxane (PDMS) (General Electric RTV 615) using multi-layer soft lithography, as described previously. Up to 120 microdialyser units can run in parallel on each chip.

Calorimetric Assays

The food dye used in the calorimetric microdialyser characterization assays was obtained from McCormick & Co., Hunt Valley, MD. The dye concentration in the microdialyser was determined by averaging the pixel values of optical micrographs of a region within the growth chamber of the growth chamber, conditioning chamber during a series of microdialysis steps or formulation mixing.

Microfluidics Based DST

Rifampicin stock solution 2 mg/ml in ethanol, Sigma Aldrich, 97% HPLC was added to sterile 7H9 Broth medium to a final concentration of 350 µg/ml, corresponding to approximately 10X MIC of mc^2155. Hygromycin, isoniazid and ofloxacin dissolved in 7H9 Broth medium to create 2 mg/ml stock solution, which was further diluted to a final concentration of 100 µg/ml, 40 µg/ml and 100 µg/ml, respectively.

Before the on chip experiments, bacteria from the frozen stock were inoculated in 7H9 broth medium at 37°C with shaking at 100 rpm. The bacteria were grown to exponential phase OD_{600} = 0.8. Approximately 150 µL of bacterial suspension was flown into the chip were 5 to 10 cells were trapped in each reactor. After cells have settled on chip, they were exposed to 7H9 Broth medium containing an antibiotic for 60 seconds every hour unless stated otherwise. In all on chip experiment, the chip was incubated at 37°C throughout the experiment.

Fabrication Protocol: The Microdialyser Device

3'' silicon wafer substrate

Mold Fabrication

1. Push up hybrid control molds
   Spin SU8 2010: 2500rpm x 1 min /130 second ramp up
   Film thickness = 11 microns
   Pre-exposure Bake: contact bake hotplate

1 min x 65°C / 2 min x 95°C

Expose wafer: 3 s at 7 Mw/ cm^2

Post-exposure Bake: 2 min x 65°C / 5 min x 95°C

Develop: 100% Shipley SU8 Nanodeveloper

Rinse with developer

Dry under nitrogen

Hard Bake: 3 hours 200°C

Spin SU8 2015: 1500rpm x 1 min /270 second ramp up

Film thickness = 24 microns

Pre-exposure Bake: contact bake hotplate

3 min x 65°C / 5 min x 95°C

Expose wafer: 3.5 s at 7 Mw/ cm^2

Post-exposure Bake: 5 min x 65°C / 15 min x 95°C

Develop: 100% Shipley SU8 Nanodeveloper

Rinse with developer

Dry under nitrogen

2. Push-down control molds

   Spin SU8 2015: 1500rpm x 1 min /270 second ramp up

   Film thickness = 24 microns

   Pre-exposure Bake: contact bake hotplate

   3 min x 65°C / 5 min x 95°C

   Expose wafer: 3.5 s at 7 Mw/ cm^2

   Post-exposure Bake: 5 min x 65°C / 15 min x 95°C

   Develop: 100% Shipley SU8 Nanodeveloper

   Rinse with developer

   Dry under nitrogen

3. Flow hybid mold

   Spin SU9 2005: 2500 rpm x 1 min / 270 seconds ramp up

   Film thickness = 5 microns

   Pre-Exposure Bake: contact bake hotplate

   1 min x 65°C / 2min x 95°C

   Expose wafer: 5 s at 7 Mw/ cm^2

   Develop: 100% Shipley SU8 Nanodeveloper

Rinse with fresh developer

Dry under nitrogen

Hard bake 3 hours

Spin SU8 2010: 2500rpm x 1 min /130 second ramp up

Film thickness = 11 microns

Pre-exposure Bake: contact bake hotplate

1 min x 65°C / 2 min x 95°C

Expose wafer: 3 s at 7 Mw/ cm^2

Post-exposure Bake: 2 min x 65°C / 5 min x 95°C

Develop: 100% Shipley SU8 Nanodeveloper

Rinse with developer

Priming: HDMS vapour 2 min in tuperware container

Spin ma-p1275 positive tone resist: 1000 rpm x 1 min / 133 sec ramp up

Film thickness = 10 microns

Soft bake: contact bake hotplate

90 sec x 95°C

Expose wafer: 15 s at 7Mw / cm^2

Develop:100% ma-D 531 developer

Rinse with DI H_20

Dry under nitrogen

Reflow: contact hotplate

65°C x 3 min / 115°C x 15 min

4. MSL Fabrication

Priming: all molds

TMCS vapor 3 min in tuperware container (STP)

Cast Think Layer: combine 5:1 GE 615 TRV (80 g A: 16 g B)

Mix in hybrid mixer: 5 min mix / 5 min degas

82 g onto flow mold (petri dish lined with Al foil)

Spin flow layer 1: combine 20:1 GE 615 RTV (20 g A: 1 g B)

Mix hybrid mixer: 5 min mix / 5 min degas

Dispense 5 mL on flow layer

2300 rpm x 60 s / 15 s ramp

1st Cure Thick Layer: convention oven

80° C for 45 min

Punching push down control input holes: peel thick layer from mold

Punch flow input holes

Align to spin-coated and cured flow layer mold

Bake in convention oven

80°C x 45 min

Spin push-up control layer: combine 20:1 GE 615 RTV (20 g A: 1 g B)

Mix hybrid mixer: 5 min mix / 2 min degas

Dispense 5 Ml on flow layer

1800 rpm x 60 sec / 15 s ramp

1st cure push-up control Layer: convection oven

80°C x 45 min

Control/flow/control bonding: peel thick / flow bonded layer from

Take care to not rip membranes

Punch flow input and output port holes

Align to spin-coated and cured push-up control layer

Ensure no air bubbles under membranes

Ensure to collapse no valves

Bake in convection oven

80°C x 45 min

Spin blank layer: combine 30:1 GE 615 RTV (30 g A: 1 g B)

Mix hybrid mixer: 5 min mix / 5 min degas

Dispense 5 Ml clean glass substrate

1800 rpm x 60 s / 15 s ramp

1st cure blank layer: convection oven

80°C x 60 min

Control / flow / control / blank bonding: peel control 1 / flow / control / control 2 bonded layer from mold

Take care to not rip membranes

Punch control 2 (push-up) input port holes

Align to spin-coated and cured blank mold

Ensure no air bubbles under membranes

Ensure no collapsed valves

Bake in convection oven

80°C x 8 hours

Matlab Image Processing script

```
%%%%% Bonisile Luthuli
%%%%  28 October 2013
%%%%  GROWTH CURVES
close all; clear all;
tic;
format long;

source_dir = 'I:\users\bonisile\shots\D30Oct2014_12_05\R1C1'
excel_name = 'reactor 1.xls';

%%% READING ALL IMAGES IN A DIRECTORY
all_images = 'PH_Raw*.lvm';
lvm_image_file_path = strcat(source_dir,'\',all_images);
my_source_lvm_files_struct = dir(lvm_image_file_path);
item_size = size(my_source_lvm_files_struct);
fsize = item_size(1);


%%%% Loop

% im11 = 10; %1
% im22 = 62; %fsize

im11 = 1; %1  9... 59
im22 = 217; %fsize

%%%% Change 1
thresh = 0.6; %%%%0.6
thrash = 0.45; %0.6;

%%%% Adjustments
bgndThresh = 8;
```

```
bgndMultFactor = 15;  %%%%15
FilterAve = 8;  %%%8
AdjustThresh = 0.0018;  %%%0.0018
bwSize = 250; %%300


for rois = 1:1
   for image = im11:im22  %1:fsize  39
      display_str = strcat('image ',num2str(image))

      filename = my_source_lvm_files_struct(image).name;
      filename_path = strcat(source_dir,'\', filename);
      LV_Image_All = dlmread(filename_path, '\t');
      %Temp_LV_Image_pre = imcrop(immultiply(LV_Image_All, 0.0001),positionF);%0.00030
      %Temp_LV_Image_pre = imcrop(imadjust(immultiply(LV_Image_All,
0.0001)),positionF);%0.00030

      Temp_LV_Image_pre1 = imadjust(immultiply(LV_Image_All, 0.0001));%0.00010


      if(image == im11)

         %% read one image

         figure, imshow(Temp_LV_Image_pre1 );

         piece = imrect;
         positionF1 = wait(piece);

         piece2 = imrect;
         positionF2 = wait(piece2);

      end

      Temp_LV_Image_pre2 = Temp_LV_Image_pre1;
      size_new = size(Temp_LV_Image_pre2);
      sx = size_new(1);
```

```
sy = size_new(2);

for xit = 1:sx
   for yit = 1:sy
      if(Temp_LV_Image_pre2(xit,yit) > thresh)
         Temp_LV_Image_pre2(xit,yit) = thrash;
      end
   end
end


Temp_LV_Image_pre = Temp_LV_Image_pre2;%0.00030

complement_image = immultiply(imcomplement(Temp_LV_Image_pre),1); %0.5

% %%%% REMOVE BACKGROUND
%%%% Change 2: (complement_image,strel('disk',Change)): 4 to 12
background = imopen(complement_image,strel('disk',bgndThresh));%8, 12

%%% change 3
subtract_background = immultiply((complement_image-background),bgndMultFactor); %15, 50

%%%% Change 4
H = filter2(fspecial('average', FilterAve),subtract_background)/255; %8

%%%% Change 5
J = imadjust(H, [AdjustThresh 1], [0 1]);  %0.2 0.01, 0.0001
K=graythresh(J);
L = im2bw(J,K);

%%%% Change 6
Lbw = bwareaopen(L, bwSize); %150

Lbw1 = imcrop(Lbw, positionF1);
Lbw2 = imcrop(Lbw, positionF2);

Or1 = imcrop(Temp_LV_Image_pre1, positionF1);
```

```
Or2 = imcrop(Temp_LV_Image_pre1, positionF2);

filename_path1 = strcat(source_dir,'\Proc_Im_', num2str(image),'_1.png');
filename_path2 = strcat(source_dir,'\Proc_Im_', num2str(image),'_2.png');

filename_path3 = strcat(source_dir,'\Proc_Im_', num2str(image),'_Or_1.png');
filename_path4 = strcat(source_dir,'\Proc_Im_', num2str(image),'_Or_2.png');

imwrite(Or1,filename_path3);
imwrite(Or2,filename_path4);

imwrite(Lbw1,filename_path1);
imwrite(Lbw2,filename_path2);



my_data(image) = sum(sum(Lbw1)) + sum(sum(Lbw2));



%%%% Get Image Date Info
my_strng = my_source_lvm_files_struct(image).date; %%%'25-Oct-2013 17:40:14';
day1 = strtok(my_strng,'-');
day = str2num(day1);
[token,remain] = strtok(my_strng,'-');
mystrng2 = [remain];
mnth = strtok(mystrng2,'-');
month = str2num(mnth);
[token,remain] = strtok(mystrng2,'-');
mystrng3 = [remain];
yr1 = strtok(mystrng3,' ');
yr =strrep(yr1,'-','');
year = str2num(yr);
[token,remain] = strtok(mystrng3,' ');
mystrng4 = [remain];
hr = strtok(mystrng4,':');
hour = str2num(hr);
```

```
[token,remain] = strtok(mystrng4,':');
mystrng5 = [remain];
mins = strtok(mystrng5,':');
minutes = str2num(mins);
[token,remain] = strtok(mystrng5,':');
seconds1 = [remain];
u = strrep(seconds1,':',");
seconds = str2num(u);

% month ='Jan'

switch mnth
   case 'Jan'
      month_num = 1;
      month_days = 31;
   case 'Feb'
      month_num = 2;
      month_days = 28;
   case 'Mar'
      month_num = 3;
      month_days = 31;
   case 'Apr'
      month_num = 4;
      month_days = 30;
   case 'May'
      month_num = 5;
      month_days = 31
   case 'Jun'
      month_num = 6;
      month_days = 30;
   case 'Jul'
      month_num = 7;
      month_days = 31;
   case 'Aug'
      month_num = 8;
      month_days = 31;
   case 'Sep'
```

```
            month_num = 9;
            month_days = 30
        case 'Oct'
            month_num = 10;
            month_days = 31;
        case 'Nov'
            month_num = 11;
            month_days = 30;
        case 'Dec'
            month_num = 12;
            month_days = 31
    end

    %month_num
    y = year*24*month_days*12;
    m = month_num*24*month_days;
    d = day*24;
    h = hour;
    m = minutes/60;
    s = seconds/3600;
    date_number = y+m+d+h+m+s;

    %%  End of Image Date
    my_time(image) = date_number;
  end
end

for t = im11:im22    %1:fsize
  my_time_zero(t) = my_time(t) - my_time(1);
end

%%%% write to excel%%%%%

excel_file = strcat(source_dir,'\',excel_name);

FID = fopen(excel_file,'w');
```

```
fprintf(FID,'Count \t my_time_zero(t) \t bw data \t log bw data \n');

for it= im11:im22 %1:fsize
    fprintf(FID,'%g \t',it);
    fprintf(FID,'%g \t',my_time_zero(it));

    to_data1 = my_data(it);
    fprintf(FID,'%g \t',to_data1);

    log_data1 = log(to_data1);
    fprintf(FID,'%g \n',log_data1);

end
fclose(FID);




close all;



figure, imshow(Temp_LV_Image_pre1);
figure, imshow(Temp_LV_Image_pre2);
figure, imshow(complement_image);
figure,imshow(background);
figure,imshow(subtract_background);
figure, imshow(L);
figure, imshow(Lbw);
figure, imshow(Lbw1);
figure, imshow(Lbw2);



toc
```

Chapter 4

CONCLUDING REMARKS

Here we successfully created the microdialyser chip, a culture-based drug susceptibility test for tuberculosis. The purpose of this design was to grow mycobacterial cells in different micro-reactors and study the effects of antibiotics through time lapse microscopy. We used *M. smegmatis* as a surrogate for *M. tuberculosis*. The microdialyser enabled mycobacterial culturing whose growth was observed via time lapsed microscopy. We further exposed trapped mycobacterial in miniaturized bioreactors of the microdialyser chip to a series of antibiotics where we observed antibiotic-induced cell death and tolerance in real time using this device.

Interestingly we repeatedly observed rifampicin tolerance to mycobacteria growing in space confined bioreactors (200 pL), but disappeared in larger contexts. Interestingly this drug tolerant phenomenon has been observed in mycobacteria growing inside the macrophage suggesting that the microenvironment created in the microdialyser mimics that observed *in vivo*. We then tested a number of hypothesis which suggested that an active efflux pump mediates rifampicin tolerance in mycobacteria cultured in miniaturised bioreactors. Although some studies have mentioned that efflux mechanism may be induced by macrophages, our results suggest that the size in which the mycobacterial cells are growing in, induces drug tolerance. We now know that more than one active pump is involved in expulsion of rifampicin from mycobacterial cells because efflux pump inhibitors reduced tolerance. In addition, MmpL11—a membrane protein involved in lipid transport seems to contribute.

Our data suggest that confinement induced rifampicin tolerance in the 200 pL growth chamber was mediated by an efflux mechanism which expelled rifampicin from the mycobacterial cells. Because drug tolerance was not observed in the case of drugs such as ofloxacin and hygromycin, it is plausible that the efflux pump responsible for rifampicin tolerance is specific to expulsion of rifampicin from the mycobacterial cell and not the other antibiotics in this case hygromycin and ofloxacin. From the current experimental data, this is our best explanation for the growth inhibitory effect of hygromycin and ofloxacin in the 200 pL growth chambers. Although there are efflux pumps that extrude a variety of structurally diverse antibiotics called multiple drug resistant pumps which might not have been induced by confinement.

I did not plate the mycobacteria from the 200 pL due to the limitations of the current chip that prevent retrieval of the microbial cells from the chip. However, I, performed an experiment in which I switched the medium feed from rifampicin containing medium to drug free medium in the bigger growth chambers. We observed that although growth was suppressed by medium containing rifampicin, growth resumed when the medium was replaced with drug-free medium revealing the bacteriostatic nature of rifampicin. The only experiment related to this was first culturing mycobacteria in the growth chamber 200 pL for 60 hours, when the mycobacteria had reached exponential phase, about 5 bacteria from the 200 pL were then moved to seed the adjacent conditioning chamber which is bigger (800 pL) than the growth chamber. And from this experiment we observed suppressed growth suggesting that mycobacteria produce different phenotypes in different environments. Our experiments do not dispute the plausibility that hygromycin and ofloxacin are bacteriostatic since the above experiment was not performed on these drugs.

The microdialyser chip should be further investigated as possible alternative to a more authentic DST that better test mimics the in vivo environment encountered by the tubercle bacilli in lungs, compared to conventional cell culture methods. This is especially important given that conventional cultures performed on plates and liquid medium are poor predictors of in vivo drug efficacy.

Our experiments suggest a quorum sensing mechanism involved in activation of the efflux pumps. Quorum sensing molecules are expected to be highly concentrated in a space confined environment and may play a role in induction of rifampicin tolerance—one of the major first-line anti-TB drugs. Since quorum sensing has been involved in critical mechanisms of microorganisms such as pathogenesis, virulence and development of biofilms it is highly possible that they can also be one of the microbial defence mechanisms aimed at neutralizing the effect of antibiotics.

Future Direction

To further investigate the effect of quorum sensing on mycobacteria, the idea would be to improve the current chip design to enable recovery of medium from the growth chamber for chemical analysis. This would enable us to perform experiments to measure the proposed quorum sensing molecules release by mycobacteria responsible for drug tolerance. We could also add generic quorum quenchers to the cell cultures to observe their effect on mycobacteria drug tolerance in the small growth chambers. The chip would also enable recovery of cells from the growth chamber to perform single cell transcriptomics to look for different gene expression profiles in the susceptible versus non-susceptible populations and adapt this system to TB susceptibility testing.

Further clinical applicability of our system will depend upon validation with various strains of *M. tuberculosis*. The next phase will be to culture *M. tuberculosis* isolates in the microdialyser system. The microdialyser would be an ideal drug susceptibility testing system for tuberculosis, since it is

fully automated, protective to the user from infectious strains of *M. tuberculosis*. This system will be relatively faster than current drug susceptibility testing methods by culture by minimizing the time required for colony forming units (CFU). We will also operationalise the formulator ring for automated combinatorial drug mixing, which will shield the user away from preparing multiple drug solutions.

This system would be more useful in resource-limited settings where point-of-care diagnostic tools are needed the most. Resource-limited settings are mostly situated I remote areas with one clinic serving large geographical areas, far away from diagnostics laboratories. A more portable (point-of-care) diagnostic test for TB would make the results easily accessible in every clinic within the community, and eliminate the need for sample transportation.

References

1 Iseman, M. D. *A clinician's guide to tuberculosis*. (Lippincott Williams & Wikins, 2000).

2 Kadner, R. J. *Bacteria*, <http://www.britannica.com/EBchecked/topic/48203/bacteria/272364/Growth-of-bacterial-populations> (2014).

3 Klann, A. G., Belanger, A. E., Abanes-De Mello, A., Lee, J. Y. & Hatfull, G. F. Characterization of the dnaG locus in Mycobacterium smegmatis reveals linkage of DNA replication and cell division. *Journal of bacteriology* **180**, 65-72 (1998).

4 Wayne, L. G. & Sramek, H. A. Agents of newly recognized or infrequently encountered mycobacterial diseases. *Clinical Microbiology Reviews* **5**, 1-25 (1992).

5 Boyd, S., Gutierrez, A. M. & McCulley, J. P. *Atlas and Text of Corneal Pathology and Surgery*. (Jaypee - Highlights Medical Publishers, Inc., 2011).

6 Davis, G. L. *et al.* Molecular assays for determining Mycobacterium laprae viability in tissues of experimentally infected mice. *PLOS Neglected Tropical Diseases* **7**, 1-9 (2013).

7 Mailaender, C. *et al.* The MspA porin promotes growth and increases antibiotic susceptibility of both Mycobacterium bovis BCG and Mycobacterium tuberculosis. *Microbiology* **150**, 853-864 (2004).

8 Goodfellow, M. & Magee, J. G. in *Mycobacteria* Vol. 1 *Basic aspects* (eds P.R.J. Gandadharam & P.A. Jenkins) 1-75 (Chapman & Hall medical microbiology series, 1998).

9 Stahl, D. A. & Urbance, J. W. The division between fast- and slow-growing species corresponds to natural relationships among the mycobacteria. *Journal of bacteriology* **172**, 116-124 (1990).

10 Hett, E. C. & Rubin, E. J. Bacterail growth and cell division: a Mycobacterial Perspective. *Microbiology and Molecular Biology* **72**, 126-156 (2008).

11 Brennan, P. J. Structure, function, and biogenesis of the cell wall of Mycobacterium tuberculosis. *Tuberculosis* **83**, 91-97 (2003).

12 Hett, E. C. & Rubin, E. J. Bacterial growth and cell division: a Mycobacterial perspective. *Microbiology and Molecular Biology* **72**, 126-156 (2008).

13 Alderwick, L. J., Birch, H. L., Mishra, A. K., Eggeling, L. & Bresra, G. S. Structure, function and biosynthesis of Mycobacterium tuberculosis cell wall: Arabinogalactan and lipoarabinomannan assembly with a view to discovering new drug targets. *Biochemical Society Transactions* **35**, 1325-1328 (2007).

14 Gengenbacher, M. & Kaufmann, S. H. E. Mycobacterium tuberculosis: Success through dormancy. *FEMS Microbiology Review* **36**, 514-532 (2012).

15 Richter, E., Rusch-Gerdes, S. & Hillemann, D. Drug susceptibility testing in TB: current status and future prospects. *Expert Reviews of Respiratory Medicine* **3**, 497-510 (2009).

16 Alcaide, F. *et al.* Usefulness of a new mycobacteriophge-based technique for rapid diagnosis of pulmonary tuberculosis. *Journal of Clinical Microbiology* **41**, 2867-2871 (2003).

17 Hartkoorn, R. C. *et al.* Differential drug susceptibility of intracellular and extracellular tuberculosis, and the impact of P-glycoprotein. *Tuberculosis* **87**, 248-255 (2007).

18 Gomez, J. E. & McKinneys, J. D. *M. tuberculosis* persistence, latency, and drug tolerance. *Tuberculosis* **84**, 29-44 (2004).

19 World Health Organisation Report 2009. (2009a).

20 Orgsnisation, W. H. Global Tuberculosis Report. *Geneva, Seitzerland: World Health Organization* (2014).

21 Global Tuberculosis Control: Epidemiology Strategy and Financing. WHO Report 2009. (2009b).

22 CDC. *Transmission and pathogenesis of tuberculosis*, <http://www.cdc.gov/tb/education/corecurr/pdf/chapter2.pdf> (

23 Flynn, J. L. & Chan, J. Tuberculosis: latency and reactivation. *infection and immunity* **69**, 4195-4201 (2001).

24 Selwyn, P. A. *et al.* Clinical manifestations and predictors of disease progression in drug users with human immunodeficiency virus infection. *New English Journal of Medicine* **327**, 1697-1703 (1992).

25 Hauck, F. R., Neese, B. H., Panchal, A. S. & El-Amin, W. Identification and management of latent tuberculosis infection. *American Family Physician* **79**, 879-886 (2009).

26 Tiwari, N., Adhikari, C., Tewari, A. & Kandpal, V. Investigation of geo-spatial hotspots for the occurrence of tuberculosis in Almora district, India, using GIS and spatial scan statistic. *International Journal of Health Geographics* **5** (2006).

27 Sudre, P., ten Dam, G. & Kochi, A. Tuberculosis: aglobal overview of the situation today. *Bulletin of the World Health Organisation* **70**, 149-159 (1992).

28 What iS DOTS? Aguide to the WHO-recommended TB control strategy known as DOTS. (1999).

29 Davies, P. D. The role of DOTS in tuberculosis treatment and control. *American Journal of Respiratory Medicine* **2**, 203-209 (2003).

30 World Health Organisation Report 2013. (2013).

31 WHO's 2013 global report on tuberculosis: successe, threats, and opportunities. (2013).

32 Churchyard, G. J. *et al.* Tuberculosis control in South Africa: Success, challenges and recommendations. *South African Medical Journal* **104**, 244-248 (2014).

33 Bergstrand, N. *Tuberculosis in Prisons: a growing public health challenge*, <http://www.usaid.gov/sites/default/files/documents/1864/USAID-TB-Brochure.pdf> (

34 Abdool Karim, S. S., Churchyard, G. J., Abdool Karim, Q. & Lawn, S. D. HIV and tuberculosis in South Africa: an urgent need to escalate the public health response. *The Lancet* **374**, 921-933 (2009).

35 *TB in South Africa: The 1960 to the present*, <http://www.tbfacts.org/tb-south-africa.html> (2013).

36 Naidoo, S., Taylor, M. & Jinabhai, C. C. Critical risk factors driving the tuberculosis epidemic in KwaZulu-Natal, South Africa. *The Southern African Journal of Epidemiology and Infection* **22**, 45-49 (2007).

37 Sekatane, C. S. & Goldstein, S. J. Patients' beliefs: do they affect tuberculosis control? *International Journal of Tuberculosis and Lung Diseases* **6**, 1075-1082 (2002).

38 Organization, W. H. World Health Organization. Global Tuberculosis Control 2009. Epidemiology, Strategy, Financing. *World Health Organization, Geneva*. (2009).

39 De Cock, K. M. & Chaisson, R. E. Will DOTS do it? A reappraisal of tuberculosis control in countries with high rates of HIV infection. *International Journal of Lung Diseases* **3**, 457-465 (1999).

40 Mofenson, L. M. & Laughon, B. E. Human Immunodeficienct Virus, Mycobacterium Tuberculosis, and Pregnancy: A deadly combination. *Clinical Infectious Diseases* **45**, 250-253 (2007).

41 Whalen, C. C. Failure of directly observed treatment for tuberculosis in Africa: A call for new approaches. *Clinical Infectious Diseases* **42**, 1048-1050 (2006).

42 Council, M. R. Streptomycin treatment of pulmonary tuberculosis. *Journal of Molecular Biology* **2**, 769–782 (1948).

43 Saltini, C. Chemotherapy and diagnosis of tuberculosis. *Respiratoy Medicine* **100**, 2085-2097 (2006).

44 Espinal, M. A. *et al.* Global trends in resistance to antituberculosis drugs. *The New England Journal of Medicine* **344**, 1294-1303 (2001).

45 Robitzek, E. H. & Selikoff, I. J. Hydrazine derivatives of isonicotinic acid (rimifon marsilid) in the treatment of active progressive caseous-pneumonic tuberculosis; a preliminaty report. *American Review of Tuberculosis* **65**, 402-428 (1952).

46 Zhang, Y., Heyme, B., Allen, B., Young, D. & Cole, S. The catalase-peroxidase gene and isoniazid resistance of *Mycobacterium tuberculosis*. *Nature* **358**, 591-593 (1992).

47 Rozwarski, D. A., Grant, G. A., Barton, D. H., W.R., J. J. & Sacchettini, J. C. Modification of the NADH of the isoniazid target (InhA) from *Mycobacterium tuberculosis*. *Science* **279**, 98-102 (1998).

48 Rawat, R., Whitty, A. & Tongue, P. J. The isoniazid-NAD adduct is a slow, tight-binding inhibitor of InhA, the *Mycobacterium tuberculosis* enoyl reductase: adduct affinity and drug resistance. *Proceedings of the National Academy of Sciences* **100**, 13881–13886 (2003).

49 Mokrousov, I. *et al.* Detection of isoniazid-resistant *Mycobacterium tuberculosis* strains by multiplex allele-specific PCR assay targeting *katG* codon 315 variation. *Journal Clinical Microbiology* **40**, 2509-2512 (2002).

50 Ramaswamy, S. & Musser, J. M. Molecular genetic basis of antimicrobial agent resistance in Mycobacterium tuberculosis: 1998 update. *Tubercle and Lung Disease* **79**, 3-29 (1998).

51 Blachard, J. S. Molecular mechanisms of drug resistance in Mycobacterium tuberculosis. *Annual Review of Biochemistry* **65**, 215-239 (1996).

52 Mitchison, D. A. Basic mechanisms of chemotherapy. *Chest* **76**, 771-781 (1979).

53 Organization, W. H. *Toman's tuberculosis case detection, treatment, and monitoring: questions and answers*. (World Health Organization Geneva, 2004).

54 Telenti, A., Imboden, P. & Marchesi, F. Direct, automated detection of rifampicin-resistant Mycobacterium tuberculosis by polymerase chain reaction and single-strand conformation polymorphism analysis. *Antimicrobial Agents and Chemotherapy* **37**, 2054-2058 (1993).

55 Caws, M. *et al.* Mutations prevalent among rifampicin- and isoniazid- resistant Mycobacterium tuberculosis isolates from a hospital in Vietnam. *Journal of Clinical Microbiology* **44**, 2333-2337 (2006).

56 Organization, W. H. Policy guidance on drug-susceptibility testing (DST) of second-line antituberculosis drugs. *Geneva, Seitzerland: World Health Organization* (2008).

57 Arentz, M., Sorensen, B., Horne, D. J. & Walson, J. L. Systematic review of the performance of rapid rifampicin resistance testing fordrug-resistant tuberculosis. *PLOS one*, doi:10.1371/journal.pone.0076533 (2013).

58 Yue, J. *et al.* Mutations in the rpoB gene of Miltidrug-resistant Mycobacterium tuberculosis isolates from China. *Journal of Clinical Microbiology* **41**, 2209-2212 (2003).

59 Shi, W. *et al.* Pyrazinamide inhibits *trans*-translation in Mycobacterium tuberculosis: a potential mechanism for shortening the duration of tuberculosis chemotherapy. *Science* **333**, 1630-1632 (2011).

60 Scorpio, A. & Zhang, Y. Mutations in pncA, a gene encoding pyrazinamidase/nicotinamidase, cause resistance to the antituberculous drug pyrazinamidase in tubercle bacillus. *Nature Medicine* **2**, 662-667 (1996).

61 Scorpio, A. *et al.* Characterization of pncA mutations in pyrazinamide-resistant *Mycobacterium tuberculosis*. *Antimicrobial Agents and Chemotherapy* **41**, 540-543 (1997).

62 Yang, J. *et al.* Structural basis for targeting the ribosomal protein S1 of Mycobacterium tuberculosis by pyrazinamide. *Molecular Microbiology* **95**, 791-803 (2015).

63 Mikusova, K., Slayden, R. A., Besra, G. S. & Brennan, P. J. Biogenesis of the mycobacterial wall and the site of action of ethambutol. *Antimicrobial Agents and Chemotherapy* **39**, 2484-2489 (1995).

64 Wolucka, B., McNeil, M., de Hoffmann, E., Chojnacki, T. & Brennan, P. J. Recognition of the lipid intermediate for arabinogalactan/arabinomannan biosynthesis and its relation to the mode of action of ethambutol on mycobacteria. *Journal of Biological Chemisty* **269**, 23328-23335 (1994).

65 Takayama, K. & Kilburn, J. O. Inhibition of synthesis of arabinogalactan by ethambutol in *Mycobacterium smegmatis*. *Antimicrobial Agents and Chemotherapy* **33**, 1493-1499 (1989).

66 Belanger, A. E. *et al.* The embAB genes of Mycobacterium avium encode an arabinosyl transferase involved in cell wall arabinan biosynthesis that is the target for the antimycobacterial drug ethambutol. *Proceedings of the National Academy of Sciences* **93**, 11919-11924 (1996).

67 Telenti, A. *et al.* The *emb* operon, a gene cluster of Mycobacterium tuberculosis involved in resistance to ethambutol. *Nature Medicine* **3**, 567-570 (1997).

68 Alcaide, F., Pfyffer, G. E. & Telenti, A. Role of embB in natural and acquired resistance to ethambutol in mycobacteria. *Antimicrobial Agents and Chemotherapy* **41**, 2270-2273 (1997).

69 America, A. t. s. C. f. D. C. a. P. i. d. s. o. Treatment of tuberculosis. *American Journal of Respiratory and Critical Care Medicine* **167**, 603-662 (2003).

70 Assistance, T. C. f. T. international standards for tuberculosis care. (2006).

71 TB DOTS Strategy Coordination, N. D. o. H. National Tuberculosis Management Guidelines. *National Department of Health, South Africa* (2014).

72 Organisation, W. H. World Health Organisation Treatment of tuberculosis: guidelines- 4th ed. *WHO, Geneva* (2009).

73 Hughes, J. & Osman, M. Diagnosis and management of drug-resistant tuberculosis in South African adults. *South African Medical Journal* **104**, doi:10.7196/SAMJ.9097 (2014).

74 Organisation, W. H. Multidrug- resistant Tuberculosis (MDR-TB) 2014 Update. (2014).

75 Weyer, K., Brand, J., Lancaster, J., Levin, J. & van der Walt, M. Determinants of multidrug-resistant tuberculosis in South Africa. *South African Medical Journal* **97**, 1120-1128 (2007).

76 Glaziou, P., Falzon, D., Floyd, K. & Raviglione, M. Global epidemiology of tuberculosis. *Seminars in Respiratory and Critical Care Medicine* **34**, 3-16 (2013).

77 Klopper, M. *et al.* Emergence and Spread of Extensively and Totally Drug-Resistant Tuberculosis, South Africa. *Emerging Infectious Diseases* **19** (2013).

78 Gandhi, N. R. *et al.* Extensively drug-resistant tuberculosis as a cause of death in patients co-infected with tuberculosis and HIV in a rural area of South Africa. *Lancet* **368**, 1575-1580 (2006).

79 Kvasnovsky, C. L. *et al.* Extensively drug-resistant TB in Eastern Cape, South Africa. *Journal of Acquired Immuno Deficiency Syndrome* **57**, 146-157 (2011).

80 Falzon, D., Gandhi, N. & Migliori, G. B. Resistance to fluoroquinolones and second-line injectable drugs: impact on MDR-TB outcomes. *European Respiratory Journal* **42**, 156-168 (2013).

81 The use of delamanid in the treatment of multidrug=resistant tuberculosis. *Geneva, Seitzerland: World Health Organization*, 1-47 (2014).

82 The use of bedaquiline in the treatment of multidrug-resistant tuberculosis. *Geneva, Seitzerland: World Health Organization*, 1-64 (2013).

83 Jugheli, L. *et al.* High level of cross-resitance between kanamycin, amikacin, and capreomycin among *Mycobacterium tuberculosis* isolates from Georgia and a close relation with mutations in the *rrs* gene. *Antimicrobial Agents and Chemotherapy* **53**, 5064-5068 (2009).

84 Organization, W. H. Companion handbook to the WHO guidlines for the programmatic management of drug-resistant tuberculosis. *WHO, Geneva* (2014).

85 Wang, F. *et al.* Mechanism of thioamide drug action against tuberculosis and leprosy. *Journal of Experimental Medicine* **204**, 73-78 (2007).

86 DeBarber, A. E., Mdluli, K., Bosman, M., Bekker, L. G. & Barry, C. E. Ethioamide activation and sensitivity in multidrug-resistant *Mycobacterium tuberculosis*. *Proceedings of the National Academy of Sciences* **97**, 9677-9882 (2000).

87 Morlock, G. P., Metchock, B., Sikes, D., Crawford, J. T. & Cooksey, R. C. ethA, inhA, and katG of ethionamide-resistant clinical Mycobacterium tuberculosis isolates. *Antimicrobial Agents and Chemotherapy* **47**, 3799-3805 (2003).

88 Zheng, J. *et al.* Para-aminosalicyclic acid is a prodrug targeting dihydrofolate reductase in Mycobacterium tuberculosis. *The Journal of Biological Chemistry* (2013).

89 Caminero, J. A., Sotgiu, G., Zumla, A. & Migliori, G. B. Best drug treatment for multidrug-resistant and extensively drug resistant tuberculosis. *Lancet Infectious Diseases* **10**, 621-629 (2010).

90 Feng, Z. & Barletta, R. G. Roles of Mycobacterium smegmatis D-alanine:D-alanine ligase and D-alnine racemase in the mechanism of action of resistance to the peptidoglycan inhibitor D-cycloserine. *Antimicrobial Agents and Chemotherapy* **47**, 283-291 (2003).

91 Dooley, K. E. *et al.* World Health Organization Group 5 drugs for the treatment of dru-resistant tuberculosis: unclear efficacy or untapped potential? *Journal of Infectious Diseases* **207**, 1352-1358 (2013).

92 Hugonnet, J. E. & Blanchard, J. S. Irreversible inhibition of the Mycobacterium tuberculosis beta-lactamase by clavulanate. *Biochemistry* **46**, 11998-12004 (2007).

93 Koul, A. *et al.* Diarylquinolines are bactericidal for dormant mycobacteria as a result of disturbed ATP homeostasis. *Journal of Biological Chemisty* **283**, 25273-25280 (2008).

94 Walker, J. R. & Tadena, N. J. Tuberculosis drug gets fast-track clearance. *The Wall Street Journal* (2013).

95 Cholo, M. C., Steel, H. C., Fourie, P. B., Germishuizen, W. A. & Anderson, R. Clofazimine: current status and future prospects. *Journal of Antimicrobial Chemotherapy*, doi:doi:10.1093/jac/dkr444 (2011).

96 Xavier, A. S. & Lakshmanan, M. Delamanid: a new armor in combating drug-resistant tuberculosis. *Journal of Pharmacology and Phamarcotherapeutics* **5**, 222-224 (2014).

97 McKenna, L., Zhang, A. & Lessem, E. An activist's guide to tuberculosis drugs. *Treatment action group* (2014).

98 Livermore, D. A. Linezolid *in vitro*: mechanism and antibacterial spectrum. *Journal of Antimicrobial Chemotherapy* **51**, doi:DOI: 10.1093/jac/dkg249 (2003).

99 Otu, A. *et al.* Drug resistance among pulmonary tuberculosis patients in Calabar, Nigeria. *Pulmonary Medicine* (2013).

100 Desikan, P. Sputum smear microscopy in tuberculosis: Is it still relevant. *The Indian Journal of Medical Research* **137**, 442-444 (2013).

101 Nelson, K. E. & Williams, C. R. *Infectious disease epidemiology theory and practice*. socond edition edn, (Jones and Bartlett Publishers, 2007).

102 Gazi, A., Islam, R., Kilbria, M. G. & Mahmud, Z. General advanced diagnostic tools to detect Mycobacterium tuberculosis and their drug susceptibility: review. *European Journal of Clinical Microbiology and Infectious Diseases*, doi:10.1007/s10096-014-2306-5 (2015).

103 Costa Filho, C. F. F. & Costa, M. G. F. Sputum smear microscopy for tuberculosis: evaluation of autofocus functions and automatic identification of tuberculosis mycobacterium. *Understanding Tuberculosis-global experiences and innovative approached to the dianosis* (2012).

104 Waitt, C. J. *et al.* The effect of a tuberculosis chest X-rays image reference set on non-expert reader performance. *European Radiology* **23**, 2459-2468 (2013).

105 Standards, U. S. f. t. N. C. f. C. L. (NCCLS, Wayne).

106 Canetti, G. *et al.* Advances in techniques of testing mycobacterial drug sensitivity, and the use of sensitivity tests in tuberculosis control programmes. *Bulletin of the World Health Organization* **41**, 21-43 (1969).

107 Division, T. C. T. Revised National TB Control Programme training manual for *Mycobacterium tuberculosis* culture & drug susceptibility testing. (2009).

108 Research, I. C. o. M. What is new in the diagnosis of tuberculosis. *Indian Council of Medical Research Bulletin* **32** (2002).

109 Fonseca, L., Moore, D. & Durier, N. Inventory of methods for mycobacterial culture and phenotypic drug susceptibility testing (DST). *The culture and phenotypic DST sub-group of the STOP TB Partnership New Diagnostics working group* (2011).

110 Tortoli, E., Benedetti, M., Fontanelli, A. & Simonettin, M. Evaluation of automated BACTEC MGIT 960 system for testing susceptibility of Mycobacterium tuberculosis to four major antituberculous drugs: comparison with the radiometric BACTEC 460TB method and the agar plate method of proportion. *Journal Clinical Microbiology* **40**, 607-610 (2002).

111 Williams-Bouyer, N., Yorke, R., Lee, H. I. & Woods, G. L. Comparisin of the BACTEC MGIT 960 and ESP Culture system II for growth and detection of mycobacteria. *Journal Clinical Microbiology* **38**, 4167-4170 (2000).

112 Stella, E. J., Franceschelli, J. J., Tasselli, S. E. & Morbidoni, H. R. Analysis of novel mycobacteriophages indicates the existence of different strategies for phage inheritance in mycobacteria. *PLOS one*, doi:DOI: 10.1371/journal.pone.0056384 (2013).

113 Caroli, G. & Avio, C. M. Isolation of mycobacteriophages from surface water. *Annali Sclavo* **17**, 568 (1975).

114 Palomino, J. C. Nonconventional and new methods in the diagnosis of tuberculosis: feasibility and applicability in the field. *European Respiratory Journal* **26**, 339-350 (2005).

115 McNerney, R., Mallard, K., Urassa, H. M., Lemma, E. & Donoghue, H. D. Colorimetric phage-based assay for detection of rifampin-resistant *Mycobacterium tuberculosis*. *Clinical Microbiology* **45**, 1330-1332 (2007).

116 Minion, J. & Pai, M. Bacteriophage assays for rifampicin resistance detection in *Mycobacterium tuberculosis*: updated meta-analysis. *International Journal of Tuberculosis and Lung Diseases* **14**, 941-951 (2010).

117 Ling, D. I., Zwerling, A. A. & Pai, M. GenoType MTBDR assays for the diagnosis of multidrug-resistant tuberculosis: a meta-analysis. *European Respiratory Journal* **32**, 1156-1174 (2008).

118 Brossier, F., Veziris, N., Jarlier, V. & Sougakoff, W. Performance of MTBDR plus for detecting high/ low levels of *Mycobacterium tuberculosis* resistance to Isoniazid. *International Journal of Tuberculosis and Lung Diseases* **13**, 260-265 (2009).

119 Kalokhe, A. S. Multidrug-resistant tuberculosis drug susceptibility and molecular diagnostic testing: a review of the literature. *American Journal of Respiratory and Critical Care Medicine* **345**, 143-148 (2013).

120 Blakemore, R., Story, E. & Helb, D. Evaluation of the analytical performance of the Xpert(R) MTB/RIF assay. *Journal Clinical Microbiology* **48**, 2495-2501 (2010).

121 Boehmec, C. C., Nabeta, P. & Hillemann, D. Rapid molecular detection of tuberculosis and rifampic resistance. *New England Journal of Medicine* **363**, 1005-1015 (2010).

122 El-Hajj, H. H., Marras, S. A., Tyagi, S., Kramer, F. R. & Alland, D. Detection of rifampicin resistance in *Mycobacterium tuberculosis* in a single tube with molecular beacons. *Journal Clinical Microbiology* **39**, 4131-4137 (2001).

123 Van Rie, A., Page-Shipp, L. & Scott, L. Xpert(R) MTB/RIF for point-of-care diagnosis of TB in high-HIV burden, resource-limited countries: hype or hope? *Expert Review of Molecular Diagnostics* **10**, 937-946 (2010).

124 Whitesides, G. M. The origins and the future of microfluidics. *Nature* **442**, doi:doi:10.1038/nature05058 (2006).

125 Unger, M. A., Chou, H. P., Thorsen, T., Scherer, A. & Quake, S. R. Monolithic microfabricated valves and pumps by multilayer soft lithography. *Science* **288**, 113-116 (2000).

126 Thorsen, T., Maerkl, S. J. & Quake, S. R. Microfluidic large-scale intergration. *Science* **298**, 580-584 (2002).

127 Hong, J. W., Studer, V., Hang, G., Anderson, W. F. & Quake, S. R. Anonoliter-scale nucleic acid processor with parallel architecture. *Nature Biotechnology* **22**, 435-439 (2004).

128 Ohashi, T., Mawatari, K., Sato, K., Tokeshi, M. & Kitamori, M. A micro-ELISA system for the rapid and sensitive measurement of total and specific immunoglobulin E and clinical application to allergy diagnosis. *Lab on Chip* **9**, 991-995 (2009).

129 Balagadde, F. K., You, L., Hansen, C. L., Arnold, F. H. & Quake, S. R. Long-term monitoring of bacterial undergoinig programmed population control in a micochemostat. *Science* **309**, 137-140 (2005).

130 Aldridge, B. B. *et al.* Asymmetry and aging of mycobacterial cells leads to variable growth and antibiotic susceptibility. *Science* **335**, 100-104 (2012).

131 Chen, C. H. *et al.* Rapid antimicrobial susceptibility testing using high surface-to-volume ratio microchannels. *Analytical Chemistry* **82**, 1012-1019 (2010).

132 Ormerod, L. P. Multidrug-resistanttuberculosis (MDR-TB): epidemiology, prevention and treatment. *British Medical Bulletin* **73-74**, 17-24 (2005).

133 Dheka, K., Warren, R. M., Zumla, A. & Grobusch, M. P. Extensively drug-resistant tuberculosis: Epidemiology and management challenges. *Infectious Disease Clinics of North America* **24**, 705-725 (2010).

134 Colman, R. E. *et al.* Dection of Low-Level Mixed-Population Drug Resistance in Mycobacterium tuberculosis Using High Fidelity Amplicon Sequencing. *PLOS one* **10**, doi:10.1371/journal.pone.0126626 (2015).

135 Pholwat, S. *et al.* Integrated Microfluidic card with TaqMan Probes and High-Resolution Melt Analysis to Detect Tuberculosis Drug Resistance Mutations across 10 Genes. *mBio* **6**, doi:10.1128/mBio.02273-14 (2015).

136 Hartkoorn, R. C. *et al.* Differential drug susceptibility of intracellular and extracellular tuberculosis, and the impact of P-glycoprotein. *Tuberculosis* **87**, 248-255 (2007).

137 Adams, K. N. *et al.* Drug tolerance in replicating mycobacteria mediated by a macrophage-induced efflux mechanism. *Cell* **145**, 39-53 (2011).